

Award Number: W81XWH-05-1-0545

TITLE: Inhibitors for Androgen Receptor Activation Surfaces

PRINCIPAL INVESTIGATOR: Robert J. Fletterick, Ph.D.

CONTRACTING ORGANIZATION: University of California, San Francisco

REPORT DATE: September 2006

TYPE OF REPORT: Annual

PREPARED FOR: U.S. Army Medical Research and Materiel Command  
Fort Detrick, Maryland 21702-5012

DISTRIBUTION STATEMENT: Approved for Public Release;  
Distribution Unlimited

The views, opinions and/or findings contained in this report are those of the author(s) and should not be construed as an official Department of the Army position, policy or decision unless so designated by other documentation.

# REPORT DOCUMENTATION PAGE

Form Approved  
OMB No. 0704-0188

Public reporting burden for this collection of information is estimated to average 1 hour per response, including the time for reviewing instructions, searching existing data sources, gathering and maintaining the data needed, and completing and reviewing this collection of information. Send comments regarding this burden estimate or any other aspect of this collection of information, including suggestions for reducing this burden to Department of Defense, Washington Headquarters Services, Directorate for Information Operations and Reports (0704-0188), 1215 Jefferson Davis Highway, Suite 1204, Arlington, VA 22202-4302. Respondents should be aware that notwithstanding any other provision of law, no person shall be subject to any penalty for failing to comply with a collection of information if it does not display a currently valid OMB control number. **PLEASE DO NOT RETURN YOUR FORM TO THE ABOVE ADDRESS.**

<b>1. REPORT DATE (DD-MM-YYYY)</b> 01-09-2006		<b>2. REPORT TYPE</b> Annual		<b>3. DATES COVERED (From - To)</b> 1 SEP 2005 - 31 AUG 2006	
<b>4. TITLE AND SUBTITLE</b> Inhibitors for Androgen Receptor Activation Surfaces				<b>5a. CONTRACT NUMBER</b>	
				<b>5b. GRANT NUMBER</b> W81XWH-05-1-0545	
				<b>5c. PROGRAM ELEMENT NUMBER</b>	
<b>6. AUTHOR(S)</b> Robert J. Fletterick, Ph.D.  E-Mail: <a href="mailto:flett@msg.ucsf.edu">flett@msg.ucsf.edu</a>				<b>5d. PROJECT NUMBER</b>	
				<b>5e. TASK NUMBER</b>	
				<b>5f. WORK UNIT NUMBER</b>	
<b>7. PERFORMING ORGANIZATION NAME(S) AND ADDRESS(ES)</b>  University of California, San Francisco San Francisco, CA 94143-0962				<b>8. PERFORMING ORGANIZATION REPORT NUMBER</b>	
<b>9. SPONSORING / MONITORING AGENCY NAME(S) AND ADDRESS(ES)</b> U.S. Army Medical Research and Materiel Command Fort Detrick, Maryland 21702-5012				<b>10. SPONSOR/MONITOR'S ACRONYM(S)</b>	
				<b>11. SPONSOR/MONITOR'S REPORT NUMBER(S)</b>	
<b>12. DISTRIBUTION / AVAILABILITY STATEMENT</b> Approved for Public Release; Distribution Unlimited					
<b>13. SUPPLEMENTARY NOTES:</b> Original contains colored plates: ALL DTIC reproductions will be in black and white.					
<b>14. ABSTRACT:</b> The androgen receptor (AR) is a proven therapeutic target for treating prostate cancer. Known therapeutics target the ligand binding domain (LBD) at the exact place where dihydrotestosterone (DHT) binds. Upon binding DHT, AR reorganizes to form new interaction surfaces such as the AF2 surface that attracts coregulators. AF2 has been proposed as a second therapeutic target as coactivator recruitment is a key step for AR function. We developed two screening methods to find compounds that bind to AF2. Our method has proved successful with the thyroid receptor. In solution, a competition assay reports coactivator displacement and 3D screening by X-ray crystallography visualizes the compounds on the receptor. Two classes of compounds have been identified that bind to AF2: the first class bind weakly and do not compete with coactivator binding (2-methylindole, and two protein kinase inhibitors), while the second class have micromolar affinity and compete with coactivator binding (TRIAC, and three aspirin derivatives). Screening revealed a significant and undiscovered cryptic surface site that we call binding function 3 (BF3), which might be implicated in AR regulation. These are the first compounds reported to block AR protein-protein interactions and might serve as starting templates for more selective and effective antiandrogens.					
<b>15. SUBJECT TERMS</b> X-ray crystallography, high throughput screening, medicinal chemistry					
<b>16. SECURITY CLASSIFICATION OF:</b>			<b>17. LIMITATION OF ABSTRACT</b>	<b>18. NUMBER OF PAGES</b>	<b>19a. NAME OF RESPONSIBLE PERSON</b>
<b>a. REPORT</b>	<b>b. ABSTRACT</b>	<b>c. THIS PAGE</b>			<b>USAMRMC</b>
U	U	U	UU	45	<b>19b. TELEPHONE NUMBER (include area code)</b>

## Table of Contents

Cover.....	
SF 298.....	2
Table of Contents.....	3
Introduction.....	4
Body.....	4
Key Research Accomplishments.....	7
Reportable Outcomes.....	8
Conclusions.....	8
References.....	9
Appendices.....	10

## INHIBITORS FOR ANDROGEN RECEPTOR ACTIVATION SURFACES

### INTRODUCTION

The androgen receptor (AR) is a proven therapeutic target for treating prostate cancer. Known therapeutics target the ligand binding domain (LBD) at the exact place where dihydrotestosterone (DHT) binds (Fig.1). Upon binding DHT, AR reorganizes to form new interaction surfaces such as the AF2 surface that attracts coregulators<sup>1,2</sup>. AF2 has been proposed as a second therapeutic target as coactivator recruitment is a key step for AR function. We have developed two screening methods to find compounds that bind to AF2. Our method has already been proven to be successful with the thyroid receptor<sup>3,4</sup>. In solution, a competition assay reports coactivator displacement and 3D screening by X-ray crystallography visualizes the compounds on the receptor. Two classes of compounds have been identified that bind to AF2: the first class bind weakly and do not compete with coactivator binding (2-methylindole, and two protein kinase inhibitors), while the second class have micromolar affinity and compete with coactivator binding (TRIAC, and three aspirin derivatives). Screening revealed a significant and undiscovered cryptic surface site that we call binding function 3 (BF3), which might be implicated in AR regulation. These are the first compounds reported to block AR protein-protein interactions and might serve as starting templates for more selective and effective antiandrogens.

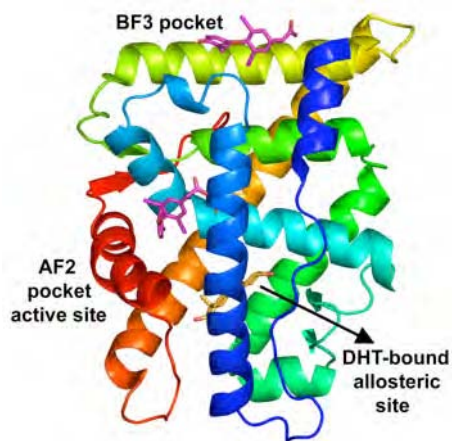
### RESEARCH ACCOMPLISHMENTS

#### Aim 1. Identify Reactive Fragments that Bind Interaction Sites on the AR-LBD Surface.

We screened several chemical libraries of compounds with two strategies to identify organic molecules that bind to the AR LBD surface.

The 3D screening approach identified six compounds that bind to the AR LBD in crystals (Figs. 1 and 2). Four compounds are bound to AF2 pocket: 2-methylindole (2MI), 1-tert-Butyl-3-(2,5-dimethyl-benzyl)-1H-pyrazolo[3,4-d]pyrimidin-4-ylamine (K10), 3-((1-tert-butyl-4-amino-1H-pyrazolo[3,4-d]pyrimidin-3-yl)methyl)phenol (RB1), and T3 hormone. The compound salicylaldehyde (SA) binds elsewhere on the surface of the receptor. The compounds 2MI, T3 hormone, indole-3-carboxylic acid (ICA) were visualized together with the compounds TRIAC and flufenamic acid (identified in the next screen, see below), at BF3.

**FIGURE 1.** Schematic of AR LBD showing the location of the coactivator binding site (active site AF2 pocket), binding function 3 (BF3) and DHT-bound allosteric site (DHT shown in orange stick model). Depicted in pink stick models are the TRIAC molecules bound to AF2 and BF3. The figure was generated with Pymol.



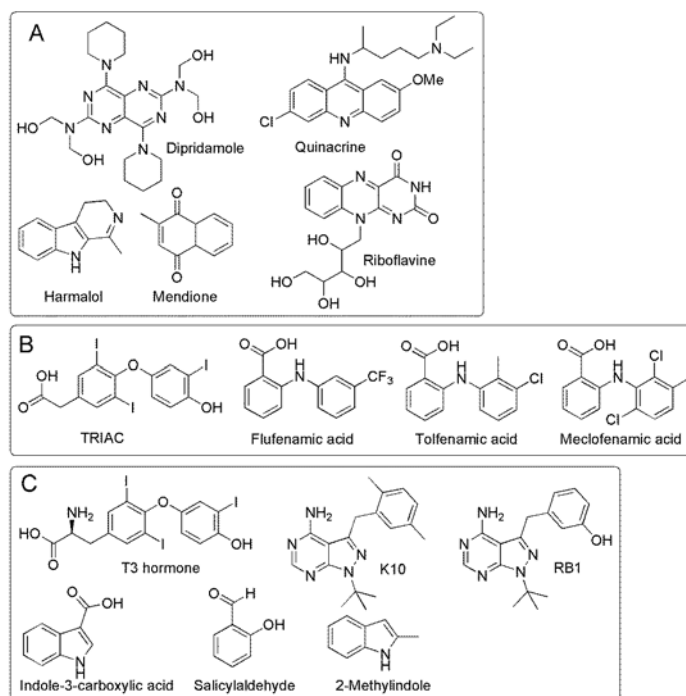


**FIGURE 2. Chemical formulas of small molecules capable of binding to the AR LBD surface.**

A: Compounds exceeding 40% inhibition of the interaction between AR LBD and labeled peptide with increased fluorescence intensity values; B: Compounds exceeding 40% inhibition of the interaction between AR LBD and labeled peptide without increased fluorescence intensity; C: Compounds identified by 3D X-ray crystallographic screen

## Aim 2. Identify Rationally Designed Compounds or FDA approved Drugs that Bind the AR Surface

In the past year, we have completed screens of several libraries of compounds in order to identify scaffolds that are capable of binding to pockets on the AR LBD surface. These studies have revealed several novel molecules that bind to both the AF-2 pocket and to a new, previously unappreciated, pocket we have named BF-3. Based upon these results, we have synthesized two libraries of compounds for follow-up. Initial characterization of these compound libraries indicates that a number of the targeted compounds bind to the AR and modulate AR function. We have been able to significantly increase potency in these series relative to the original screening hits and are currently pursuing co-crystallization in order to better understand the structure activity relationships and the mechanism of action for these compounds.

We found nine compounds inhibited the interaction between AR LBD and SRC2-3 (Fig. 2). The AF2-binding molecules share structural characteristics but not chemotype. The three non-steroidal non-inflammatory drugs (NSAIDs): flufenamic acid, tolfenamic acid and meclofenamic acid has aspirin-like character. Structural features are shared with TRIAC.

The drugs flufenamic acid, tolfenamic acid, meclofenamic acid, TRIAC and mendione had no effect on the interaction of TR·T3 with SRC2-2. They were therefore considered validated hits. These compounds were subject to a study of the dose to response of inhibition relationship over a range of concentrations of 0.14 to 300  $\mu\text{M}$  to allow the calculation of the  $\text{IC}_{50}$  values (Fig.3). Tolfenamic acid showed the highest potency with an  $\text{IC}_{50}$  value of 44  $\mu\text{M}$ . The other drugs showed slightly weaker potencies. The overall hit rate was 0.33%.

A cross-evaluation was carried out by testing six compounds, identified to bind to AR LBD by 3D crystallographic screening, in the competitive fluorescence polarization assay (Fig. 2C). The natural thyroid hormone T3 showed a weaker inhibition of the interaction between the labeled coactivator and AR LBD in comparison to its structural homologue. All other small molecules did not significantly inhibit the recruitment of the labeled coactivator.

Crystal structures of AR LBD crystals soaked with flufenamic acid, T3 hormone and TRIAC are shown in Figures 4 and 5. Conditions have not been found for the other NSAIDs compounds that yield crystals that diffract X-rays and allow structure determination. Figure 4 shows the structures in summary.

**FIGURE 3. Binding assays** (curves were obtained by fitting data to the following equation  $(y = \text{min} + (\text{max} - \text{min})/1 + (x/K_d)^{\text{Hill slope}})$ ). A: Direct binding assay of labeled SRC2-3 peptide to AR LBD. Competitive fluorescence polarization assay of TRIAC (Tiratricol), Flufenamic acid and Meclofenamic acid in the presence of AR LBD (1  $\mu\text{M}$ ) and fluorescently labeled SRC2-3 peptide (10 nM).

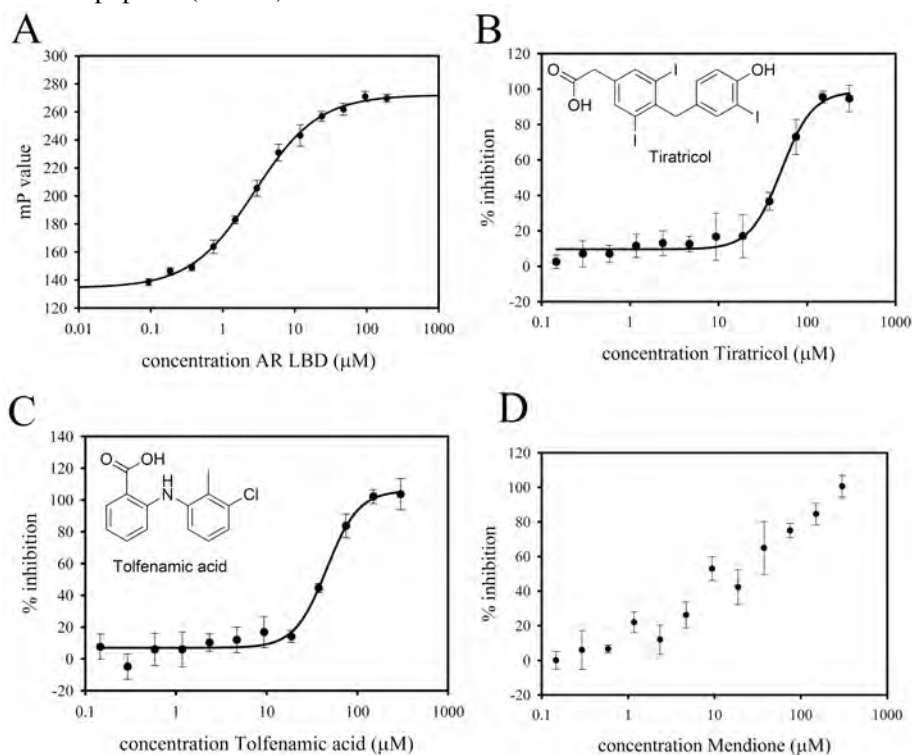
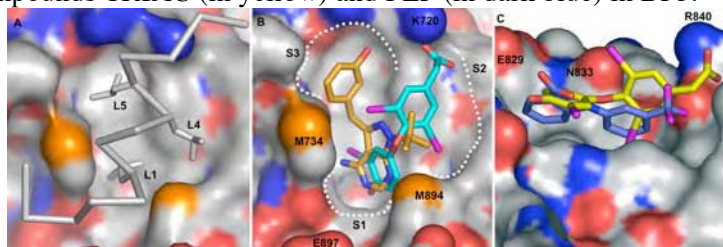


**FIGURE 4. Comparisons of the compounds bound to AR-LBD surface.**

A. Our previously published structure of coactivator SRC1-3 peptide bound to AF2 is shown here for comparison reasons. The leucine residues from the  $L_1XXL_4L_5$  motif are shown as stick models and the peptide backbone is shown in grey as an  $\alpha$ -trace.

B. Superimposition of the compounds RB1 (in orange) and TRIAC (in blue) in AF2. The molecule RB1 (as K10) interacts with the AF2 pocket S1 and S3 subsites. However, TRIAC positions itself in S1 and in between S2 and S3 subpockets.

C. Superimposition of the compounds TRIAC (in yellow) and FLF (in dark blue) in BF3.

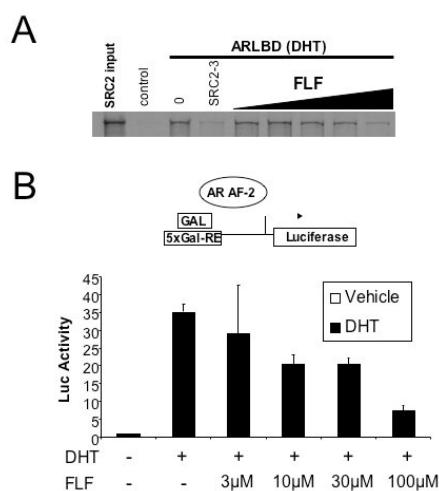


### Aim 3. The compound FLF Inhibits AR AF-2 Activity *in vivo*

To determine whether any of the compounds identified in the screen interfere with AR function, we examined their effects upon AR interactions with full length SRC2 *in vitro* and AR activity *in vivo*. The NSAID FLF inhibited interactions of bacterially expressed AR LBD with radiolabeled *in vitro*-translated full length

SRC2 in a dose-dependent fashion, and did so as efficaciously as an excess of SRC2-3 competitor peptide (Figure 3). High concentrations of TRIAC caused AR LBD to precipitate in these assays (not shown). FLF also inhibited activity of transfected AR LBD tethered to a reporter gene (GAL-LUC) with a heterologous GAL DNA binding function (Fig. 5). Significant inhibition of AR AF-2 activity was obtained with 10-30  $\mu\text{M}$  FLF, comparable to the values obtained in the FP assays. In parallel, similar concentrations of FLF failed to inhibit activity of thyroid hormone receptor AF-2 and an unrelated transcriptional activation function derived from the coactivator protein CBP (not shown). Modest inhibition of AR AF-2 activity was also obtained with 10-30  $\mu\text{M}$  TRIAC but this effect was not specific to AR (not shown). Thus, one of the compounds identified in the FP screen (FLF) also inhibits AR LBD interactions with a coactivator *in vitro* and AR AF-2 activity in cell culture.

**Figure 5. FLF Inhibits AR AF-2 activity.** (A) SDS-PAGE gel showing quantities of *in vitro* translated full length SRC2 retained in pulldown assays performed with bacterially expressed GST-AR-LBD/DHT complex (3  $\mu\text{g}$  per assay). Binding is shown in assays performed with vehicle (0), 10  $\mu\text{g}$  of SRC2-3 peptide (15-mer) or increasing concentrations of FLF (0.01-1mM). (B) Results of AR AF-2 transcriptional readout assay performed in HeLa cells. Transfected components are shown in schematic at the top. The panel shows results of luciferase assays (light units  $\times 10^4$ ) normalized to  $\beta$ -galactosidase activity. Error bars represent standard errors derived from triplicate points.



## KEY RESEARCH OUTCOMES

- A high-throughput crystallography method has been developed to discover novel antiandrogens to treat prostate cancer.
- Discovery of the first small molecules that bind to the androgen receptor surface able to modulate their transcriptional activity *in vitro* and *in vivo*.
- Discovery of a novel protein association site on the androgen receptor.

## REPORTABLE OUTCOMES

- (1) **Eva Estebanez-Perpina**, Leggy A. Alexander, Paul Webb, Phuong Nguyen, Ellena Mar, Raynard Bateman, Kevan M. Shokat, John D. Baxter, Kiplin R. Guy and Robert J. Fletterick. (2006) Inhibitors of Androgen Receptor-Coregulator Assembly. **Submitted to *PNAS***.
- (2) **Estébanez-Perpiñá, E.**, Jouravel, N., Arnold, L.A., Togashi, M., Mar, E., Sablin, E., Nguyen, P., R. Baxter, J.D., Webb, P., Guy, R. K. and Fletterick, R.J. First Small Molecule Inhibitor of Thyroid Hormone Receptor Coregulator binding. To be submitted to *PNAS*, September 2006.
- (3) **Estebanez-Perpina, E.**, Moore, J.M., Mar, E., Delgado-Rodrigues, E., Nguyen, P., Baxter, J.D., Buehrer, B.M., Webb, P., Fletterick, R.J., Guy, R.K. The molecular mechanisms of coactivator utilization in ligand-dependent transactivation by the androgen receptor. *J Biol Chem.* **2005**, *280*, 8060-8068.
- (4) Arnold, L. A., **Estebanez-Perpina, E.**, Togashi, M., Jouravel, N., Shelat, A., McReynolds, A.C., Mar, E., Nguyen, P., Baxter, J.D., Fletterick, R.J., Webb, P., Guy, R.K. Discovery of small molecule inhibitors of the interaction of thyroid hormone receptor with transcriptional coregulators. *J. Biol. Chem.* **2005** *280*(52), 43048-55.
- (5) Arnold, L. A., **Estebanez-Perpina, E.**, Togashi, M., Shelat, A., Ocasio, C.A., McReynolds, A.C., Nguyen, P., Baxter, J.D., Fletterick, R.J., Webb, P., Guy, R.K. A high-throughput screening method to identify small molecule inhibitors of thyroid hormone receptor coactivator binding. *Sci STKE* **2006**, *341*, 13.

## CONCLUSION

Using two complementary approaches, we have identified the first generation of small molecules that target the coactivator-binding pocket of AR. Our complementary assays identified the first generation of compounds that bind weakly to AR LBD coactivator binding pocket and that inhibit coactivator recruitment *in vitro*. These compounds might serve as starting chemical scaffolds to synthesize compounds that bind more tightly. Some of the lead compounds that we have identified are marketed drugs that are safe and bioavailable. Perhaps the second-generation analogs will be candidate drugs for further development. This class of inhibitors would likely have clinical value and should work synergistically with existing drugs, and may become a new class of drugs for treatment of prostate cancer and other syndromes.

Our studies have uncovered cryptic ligand binding sites on the AR molecule that seems to be acting as preferred sites recruiting several small molecules. The most surprising hydrophobic pocket hot-spot is the solvent accessible BF3 site, as it recruits four compounds. These findings are significant because the BF3 site is linked with AR function. The function of the BF3 site will be tested by biological profiling of the newly identified ligand and its analogues and mutagenesis of AR.

**REFERENCES**

- (1) Estebanez-Perpina, E., Moore, J.M., Mar, E., Delgado-Rodrigues, E., Nguyen, P., Baxter, J.D., Buehrer, B.M., Webb, P., Fletterick, R.J., Guy, R.K. The molecular mechanisms of coactivator utilization in ligand-dependent transactivation by the androgen receptor. *J Biol Chem.* **2005**, *280*, 8060-8068.
- (2) Hur, E.; Pfaff, S. J.; Sturgis, P. E.; Hanne, G.; Buehrer, B. M. et al. Recognition and Accommodation at the Androgen Receptor Coactivator Binding Interface. *PLoS* **2004**, *2*, 363.
- (3) Arnold, L. A., Estebanez-Perpina, E., Togashi, M., Jouravel, N., Shelat, A., McReynolds, A.C., Mar, E., Nguyen, P., Baxter, J.D., Fletterick, R.J., Webb, P., Guy, R.K. Discovery of small molecule inhibitors of the interaction of thyroid hormone receptor with transcriptional coregulators. *J. Biol. Chem.* **2005**.
- (4) Arnold, L. A., Estebanez-Perpina, E., Togashi, M., Shelat, A., Ocasio, C.A., McReynolds, A.C., Nguyen, P., Baxter, J.D., Fletterick, R.J., Webb, P., Guy, R.K. A high-throughput screening method to identify small molecule inhibitors of thyroid hormone receptor coactivator binding. *Sci STKE* **2006**, *341*, 13.

# A High-Throughput Screening Method to Identify Small Molecule Inhibitors of Thyroid Hormone Receptor Coactivator Binding

Leggy A. Arnold,<sup>1\*</sup> Eva Estébanez-Perpiñá,<sup>2</sup> Marie Togashi,<sup>3</sup> Anang Shelat,<sup>1</sup>  
Cory A. Ocasio,<sup>4</sup> Andrea C. McReynolds,<sup>5</sup> Phuong Nguyen,<sup>3</sup> John D. Baxter,<sup>3</sup>  
Robert J. Fletterick,<sup>2</sup> Paul Webb,<sup>3</sup> R. Kiplin Guy<sup>1</sup>

(Published 27 June 2006)

## INTRODUCTION

### MATERIALS

- Common Reagents and Chemicals
- SRC2-2 Labeling
- Protein-Expression and Purification of the Thyroid Receptor
- Protein-Binding Assay, High-Throughput Screen, and Dose-Response Analysis
- Glutathione-S-Transferase Pull-Down Assay
- Hormone Displacement Assay
- Transcription Assay

### EQUIPMENT

- Common Laboratory Equipment
- SRC2-2 Labeling
- Protein Expression and Purification of the Thyroid Receptor
- Protein-Binding Assay, High-Throughput Screen, and Dose-Response Analysis
- Glutathione-S-Transferase Pull-Down Assay
- Hormone Displacement Assay
- Transcription Assay

### RECIPES

- SRC2-2 Labeling
- Protein Expression and Purification of the Thyroid Receptor
- Protein-Binding Assay, High-Throughput Screen, and Dose-Response Analysis
- Glutathione-S-Transferase Pull-Down Assay
- Hormone Displacement Assay
- Transcription Assay

### INSTRUCTIONS

- SRC2-2 Labeling
- Protein Expression and Purification of the Thyroid Receptor
- Protein-Binding Assay, High-Throughput Screen, and Dose-Response Analysis
- Hit Validation by Glutathione-S-Transferase Pull-Down Assay
- Hormone Displacement Assay
- Transcription Assay

### RELATED TECHNIQUES

### NOTES AND REMARKS

### REFERENCES

---

<sup>1</sup>St. Jude Children's Research Hospital, Department of Chemical Biology and Therapeutics, 333 North Lauderdale Street, Memphis, TN 38105, USA.

<sup>2</sup>University of California San Francisco, Department Biochemistry and Biophysics, 600 Sixteenth Street, San Francisco, CA 94143, USA. <sup>3</sup>University of California San Francisco, Diabetes Center and Department of Medicine, HSW 1210, 513 Parnassus Avenue, San Francisco, CA 94122, USA.

<sup>4</sup>University of California, San Francisco, Department of Pharmaceutical Chemistry, 600 Sixteenth Street, San Francisco, CA 94143, USA. <sup>5</sup>University of California, San Francisco, Department of Pharmaceutical Chemistry, 1700 Fourth Street, Room 509, San Francisco, CA 94143, USA.

\*Address correspondence to: Alexander Arnold, St. Jude Children's Research Hospital, Department of Chemical Biology and Therapeutics, 332 N. Lauderdale St., Memphis, TN 38105-2794, USA. Telephone, (901) 495 5803; fax, (901) 495-5715; e-mail, alexander.arnold@stjude.org

## Abstract

To provide alternative methods for regulation of gene transcription initiated by the binding of thyroid hormone (T3) to the thyroid receptor (TR), we have developed a high-throughput method for discovering inhibitors of the interaction of TR with its transcriptional coactivators. The screening method is based on fluorescence polarization (FP), one of the most sensitive and robust high-throughput methods for the study of protein-protein interactions. A fluorescently labeled coactivator is excited by polarized light. The emitted polarized light is a function of the molecular properties of the labeled coactivator, especially Brownian molecular rotation, which is very sensitive to changes in the molecular mass of the labeled complex. Dissociation of hormone receptor from fluorescently labeled coactivator peptide in the presence of small molecules can be detected by this competition method, and the assay can be performed in a high-throughput screening format. Hit compounds identified by this method are evaluated by several secondary assay methods, including a dose-response analysis, a semiquantitative glutathione-S-transferase assay, and a hormone displacement assay. Subsequent *in vitro* transcription assays can detect inhibition of thyroid signaling at low micromolar concentrations of small molecules in the presence of T3.

## Introduction

The thyroid hormone receptor (TR) is part of the superfamily of nuclear hormone receptors (NRs) whose major transcriptional activity is controlled by the thyroid hormone 3,5,3'-triiodo-L-thyronine (T3) (1, 2). As a heterodimer with the retinoid X receptor (RXR), TR binds to specific thyroid response elements (TREs) on DNA (3). Gene regulation mediated by TR is especially important during growth and development, as well as general metabolism (4–6). Abnormal levels of T3 are responsible for medical conditions such as obesity, high plasma cholesterol levels, type II diabetes, high blood pressure, and increased risk of heart failure (7–11). The binding of T3 occurs at the ligand-binding pocket present in the ligand-binding domain (LBD) of the receptor (12). This binding event induces a conformational change of the TR to enable the formation of the solvent-exposed hydrophobic pocket that contains the transactivation function 2 (AF2) domain. The formation of a competent AF2 allows recruitment of coregulatory proteins that strongly influence transcriptional regulation, because they link the receptor to the transcriptional machinery. Several coactivators of the TR have been identified (13).

Modulation of the TR-stimulated transcription by small molecules has focused on the development of T3 analogs (14–19). Although some antagonists have now been reported, it remains unclear if such analogs can overcome the undesirable side effects on cardiac stimulation (20, 21). The interface formed by the TR AF2 domain and its coactivators offers the possibility to modulate TR-dependent gene transcription in the presence of its natural hormone.  $\alpha$ -helical proteomimetics have been reported to inhibit this interaction in competition binding assays but, to date, none of these inhibitors regulated NR signaling in cellular systems (22–25).

High-throughput screening (HTS) is frequently used to discover small molecules that inhibit protein-protein interactions, (26) although only a limited number of compounds have been reported that are active in cellular models. (27, 28). We applied the technique of fluorescence polarization (29) and developed a competitive NR coactivator binding assay to discover small molecules with the ability to bind to TR in the presence of T3 and block binding of coregulators (30). This method is very time efficient, and 140K small molecules were screened in 2 to 3 weeks using a semiautomated screening protocol. The hit verification by secondary assays is an important part of the protocol and identifies if this inhibition has biological relevance in cellular signal transduction by inhibiting the transcriptional activity of the TR in the presence of T3.

The process for developing and executing an HTS campaign required multiple sequential steps (Fig. 1). The procedure starts

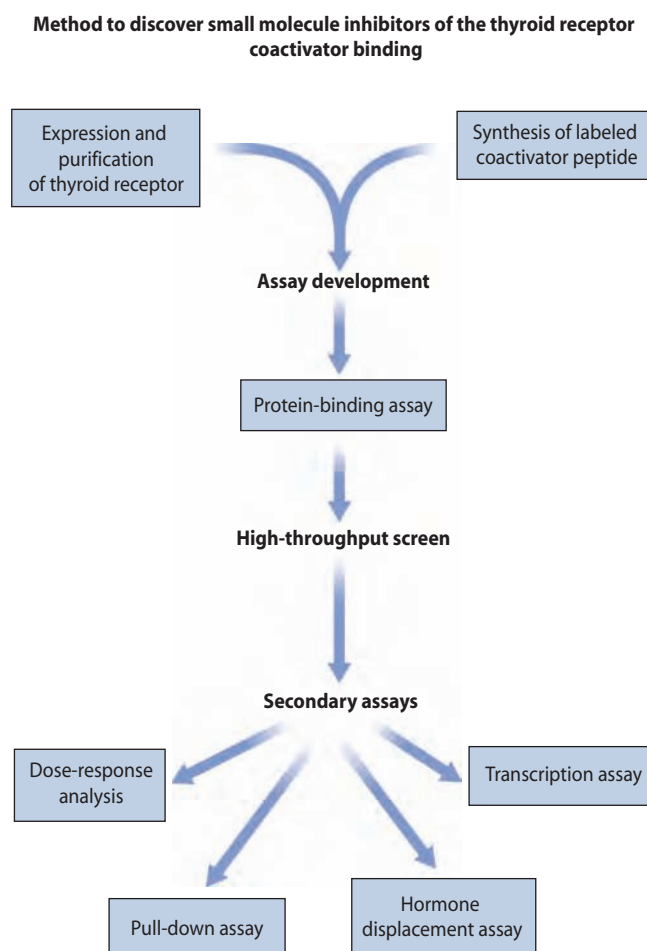


**Fig. 1.** The workflow of the high-throughput method includes assay development (synthesis of labeled coactivator peptide, protein expression and purification, and protein-binding assay), high-throughput screening, and the secondary assays (dose-response analysis, pull-down assay, hormone displacement assay, and transcription assay).

with the expression and purification of TR protein and the synthesis of fluorescently labeled coactivator peptide. The assay development phase included the measurement of the binding constant of TR for quality control (QC) and determination of the screening concentration (about  $2 \times K_d$ ). The HTS involved liquid handling (transfer of liquids by a laboratory automation workstation) and the measurement of fluorescence intensity (FI) and fluorescence polarization (FP). The FP values of the positive and negative controls determined 0% and 100% inhibition of coactivator recruitment. Compounds with inhibitory ability of  $>50\%$  and FI variations of less than 10% in comparison to the controls were identified as hit compounds. These hit compounds were validated in secondary assays. The dose response analysis using a competition coactivator binding assay determined the  $IC_{50}$  value of the compounds. The ability to inhibit the interaction between full length TR and coactivator was investigated by a glutathione-S-transferase (GST) pull-down assay. The hormone displacement assay ensures that the small molecule is competing with the coactivator and not with T3. Finally, the transcription assay determines if the small molecules are capable to penetrate the cell membrane and inhibit signal transduction in a cellular environment.

The following methods detail the steps for identifying and validating compounds that inhibit TR activity in the presence of the TR ligand T3. These methods can be adapted to screening for compounds that influence the activity of other NRs by using a labeled peptide that binds with high affinity to the NR under investigation or by screening for compounds that compete for co-repressor binding instead of coactivator binding to the NR.

## Materials

Many of the procedures rely on the same reagents and chemicals. A list of reagents and chemicals common to two or more procedures is listed first. Each individual subsection lists additional reagents specific to that procedure.

### Common Reagents and Chemicals

96-well opaque plate (Costar #3365)  
 Ampicillin (anhydrous basic, 96.0 to 100.5%; Sigma)  
 BCA assay (Pierce)  
 Dimethyl sulfoxide (DMSO; ACS grade, 99.9%; Aldrich)  
 Dithiothreitol (DTT; Aldrich)  
*E. coli* BL21 strain (Stratagene)  
 EDTA ethylenediaminetetraacetic acid disodium salt dihydrate (ACS reagent; Aldrich)  
 Glycerol (ACS reagent; Aldrich)  
 Isopropyl-beta-D-thiogalactopyranoside (IPTG; Sigma)  
 KCl, potassium chloride (Aldrich)  
 LB agar EZMix powder (Sigma)  
 LB broth EZMix powder (Sigma)  
 Liquid nitrogen  
 Lysozyme (from chicken egg white, lyophilized powder, 50,000 U/mg; Sigma)  
 Methanol (MeOH; for HPLC, 99.9%; Aldrich)  
 $MgCl_2$  (hexahydrate; Aldrich)  
 NaCl (Sigma)  
 NP-40 (Aldrich)  
 NuPAGE 10% bis-tris gel with MOPS (Invitrogen)  
 NuPAGE LDS sample loading buffer (Invitrogen)  
 Phosphate-buffered saline (PBS; Sigma)  
 Phenylmethylsulfonyl fluoride (PMSF; Sigma)  
 Poly-Prep Column (BioRad, #731-1550)  
 Thyroid hormone, 3,5,3'-triiodo-L-thyronine (T3; Sigma)

TNT T7 quick coupled transcription/translation system (Promega)  
Tris(hydroxymethyl)aminomethane, hydrochloride (Tris-HCl; Sigma)  
Tween 20 (Sigma)

### SRC2-2 Labeling

5-iodoacetamidofluorescein (Molecular Probes)  
Acetonitrile (for HPLC, 99.9%; Aldrich)  
Coactivator SRC2-2 peptide (CLKEKHKILHRLQLDSSSPV) (crude; BIO SYNTHESIS, Lewisville, TX)  
Dimethyl formamide (DMF; ACS grade, 98.8%; Aldrich)  
Ethaneethiol (Aldrich)  
Trifluoroacetic acid (TFA; spectrophotometric grade; Aldrich)

### Protein Expression and Purification of the Thyroid Receptor

Antipain (Sigma)  
*E. coli* strain BL21(DE3)pLysE (Invitrogen)  
hTR $\alpha$  LBD (His<sub>6</sub> E148-V410) cloned into the expression vector pET DUET-1 (Novagen)  
hTR $\beta$  LBD (His<sub>6</sub> T209-D461) cloned into the expression vector pET DUET-1 (Novagen)

*Note: Both constructs were cloned into the BamHI and HindIII restriction sites downstream of the hexahistidine tag of the expression vector pET DUET-1. The replacement of C309 for alanine (A) in the hTR $\beta$  LBD construct was performed with the QuickChange XL Site-Directed Mutagenesis Kit (Stratagene). The sequences of all constructs were verified by DNA sequencing and the plasmids are available upon request.*

Imidazole (Sigma)  
Leupeptin (Sigma)  
Pepstatin (Sigma)  
Talon protein purification column (Metal Affinity Chromatography; BD Biosciences)

### Protein-Binding Assay, High-Throughput Screen, and Dose-Response Analysis

384-well black plate (Costar, #3710)  
384-well opaque plate (Costar, #3702)  
Centrifugal filter units (Ultra-15, 10K NMWL; Amicon)  
Compounds 3 and 11 (10 mM in DMSO) were a gift from Tim Geistlinger (23)  
SRC2-2 peptide, labeled with fluorescein (see Instructions, below)  
TR $\beta$  LBD (see Instructions, below)

### Glutathione-S-Transferase Pull-Down Assay

<sup>35</sup>S-methionine (1000 MCi; Perkin Elmer)  
Acetic acid (ACS grade; Aldrich)  
Bovine serum albumin (BSA; Sigma, #A-2153)  
Glutathione Sepharose 4B (GE, #17-0756-01)  
GST-TR $\beta$  full length (available on request)  
4-(2-Hydroxyethyl)piperazine-1-ethanesulfonic acid (Hepes; Sigma)  
Plasmid SRC2 (available on request)  
Protease inhibitor cocktail (set II; Calbiochem)  
Triton X (Aldrich)

## Hormone Displacement Assay

<sup>125</sup>I-T<sub>3</sub>, 3,5,3'-triiodo-L-thyronine (2200 Ci/mmol; Perkin Elmer)  
Column rack and trough (Fisher)  
G25 Sephadex (Aldrich)  
Histone from calf thymus (Sigma)  
Microscintillation fluid (Beckman)  
Monothioglycerol (MTG; Aldrich)  
Phosphate, dibasic, hexahydrate (Aldrich)  
Plasmid, full-length TR $\beta$  containing a CMV promoter (available on request)  
Scintillation vials (7 ml; Fisher)

## Transcription Assay

96-well plate (white, flat bottom with lid, tissue culture-treated, Costar #3917)  
Bovine calf serum (defined; HyClone)  
Cell culture-treated PS dish, 150 mm (Corning)  
Dextran-coated charcoal (Sigma-Aldrich)  
Dual luciferase reporter assay kit (Promega)  
Dulbecco's Modified Eagle's Medium/Nutrient Mixture F-12 Ham with L-glutamine and 15 mM Hepes, without sodium bicarbonate and phenol red (DMEM/Ham's F12; powder; Sigma)  
Dulbecco's Modified Eagle's H-21 containing 4.5 g/liter glucose, 584 mg/liter glutamine, 3.7 g/liter sodium bicarbonate and phenol red (DMEM/H12; HyClone)  
Electroporation cuvette (4 mm gap; Eppendorf)  
Glucose 10% (HyClone)  
PBS buffer, without Mg<sup>2+</sup> and Ca<sup>2+</sup> ions (MediaTech)  
Penicillin-streptomycin 100 $\times$  (penicillin 6.37 g/liter, streptomycin 10 g/liter; HyClone)  
Plasmid hTR $\beta$  (available on request)  
pRL-CMV Vector (Promega)  
Reporter plasmid [synthetic TR response element (DR-4) containing two copies of a direct repeat spaced by four nucleotides (AGGTCA-cagg-AGGTCA) cloned immediately upstream of a minimal (-32 to +45) thymidine kinase promoter linked to luciferase coding sequence] (available on request)  
Sodium bicarbonate (NaHCO<sub>3</sub>; Aldrich)  
Trypsin 0.05%, versene 0.02%, in saline A (HyClone)  
U2OS cells (human bone osteosarcoma epithelial cells; ATCC, #HTB-96)

## Equipment

Many of the procedures rely on the same equipment. A list of equipment common to two or more procedures is listed first. Each individual subsection lists additional equipment specific to that procedure.

## Common Laboratory Equipment

2.8-liter Fernback flasks  
Biomate 3 spectrometer (Thermo)  
Centrifuge (Eppendorf 5810R)

Centrifuge, JLA-14 rotor (Avanti J-25; Beckman)  
Glass beads (0.5 mm diameter)  
Maxi Rotator (Barnstead)  
Petri dishes  
Plate reader (Analyst AD; LJI Biosystems)  
Shaker incubator (Innova 44; New Brunswick Scientific)  
Shaker, rotisserie (Thermolyne)  
SigmaPlot 8.0 (SPSS; Chicago, IL)  
Sonicator (Branson 250)  
Ultra-Centrifuge, VTi50 rotor (Optima L-90K; Beckman)  
Water bath

### **SRC2-2 Labeling**

Analytical HPLC-MS system (Alliance HT, Micromass ZQ 4000; Waters)  
HT-4X evaporator (Genevac)  
Preparative HPLC system (Delta 600; Waters)  
RP-C18 Xterra column 5  $\mu\text{m}$ , 19 mm  $\times$  50 mm (Waters)  
RP-C18 Xterra column 5  $\mu\text{m}$ , 6 mm  $\times$  50 mm (Waters)

### **Protein Expression and Purification of the Thyroid Receptor**

Incubator (Thermo)

### **Protein-Binding Assay, High-Throughput Screen, and Dose-Response Analysis**

Assay Explorer: In-house screening software written in Pipeline Pilot 4.5.1 (Scitegic)

*Note: This Web-based program automates the process of joining experimental data to compound information, flagging suspicious plates based on low Z-factors, extracting compounds with statistically significant activity, and annotating hits with additional information (for example, chemical similarity to known bioactive compounds, known genotoxic or cytotoxic molecules, or available compounds, and profiles from ADME models). Data are available online at [http://www.stjude.com/research/guy/AssayReporter/TR\\_SCREEN/](http://www.stjude.com/research/guy/AssayReporter/TR_SCREEN/)*

Multi-channel pipette (12 channels)

Multimek (Beckman)

*Note: This instrument is a laboratory automation workstation that performs liquid handling, including pipetting, diluting, and dispensing.*

Wellmate (Matrix)

*Note: This instrument can dispense liquids into 96-well and 384-well microplates with a tubing cartridge.*

### **Glutathione-S-Transferase Pull-Down Assay**

Centrifugal concentrator (CentriVap; Labconco)

PhosphorImager (Storm; GE)

### **Hormone Displacement Assay**

Equipment to work with radiolabeled compounds emitting gamma rays (lead protection)

Scintillation counter (Beckman)

## Transcription Assay

Cell culture hood  
 Genepulser (BioRad)  
 Hemocytometer  
 Incubator, 37°C, 5% CO<sub>2</sub> (MCO 36M; Sanyo)  
 Microscope

## Recipes

### SRC2-2 Labeling

#### **Recipe 1: TFA in Water**

Dissolve 2 ml of TFA in 4000 ml of deionized water.

*Note: TFA is a corrosive and volatile liquid and should be stored and handled in a well-ventilated place (fume hood).*

#### **Recipe 2: TFA in Acetonitrile**

Dissolve 2 ml of TFA in 4000 ml of acetonitrile.

#### **Recipe 3: TFA in MeOH**

Dissolve 2 ml of TFA in 4000 ml of methanol.

#### **Recipe 4: 20 mM Tris Buffer, pH 9.0**

Dissolve 3.15 g of Tris-HCl in 80 ml of deionized water, adjust pH to 9.0 with NaOH (aq), and adjust volume to 100 ml with deionized water.

### Protein Expression and Purification of the Thyroid Receptor

#### **Recipe 5: 1 M Tris Buffer, pH 7.0**

Dissolve 157.6 g of Tris-HCl in 800 ml of deionized water, adjust to pH 7.0 with NaOH (aq), and adjust volume to 1000 ml with deionized water.

#### **Recipe 6: 3 M NaCl**

Dissolve 174 g of NaCl in 1000 ml of deionized water.

#### **Recipe 7: 100 mM DTT**

Dissolve 154.2 mg of DTT in 10 ml of deionized water. Store in 1 ml aliquots at -20°C.

#### **Recipe 8: 100 mM PMSF**

Dissolve 174.2 mg of PMSF in 10 ml of ethanol. Store in 1 ml aliquots at -20°C.

#### **Recipe 9: 10 mM T3**

Dissolve 9.76 mg of T3 in 2 ml of DMSO; store at -20°C.

#### **Recipe 10: 10 mM Leupeptin**

Dissolve 49.3 mg of leupeptin in 10 ml of deionized water. Store in 0.5 ml aliquots at -20°C.

#### **Recipe 11: 10 mM Pepstatin**

Dissolve 8.5 mg of pepstatin in 10 ml of methanol. Store in 0.5 ml aliquots at -20°C.

#### **Recipe 12: 10 mM Antipain**

Dissolve 67.7 mg of antipain in 10 ml of DMSO. Store in 0.5 ml aliquots at -20°C.

#### **Recipe 13: Sonication Buffer**

<i>Stock solution</i>	<i>Volume</i>	<i>Final concentration</i>
1 M Tris Buffer, pH 7.0 (Recipe 5)	5 ml	50 mM
3 M NaCl (Recipe 6)	5 ml	150 mM
100 mM DTT (Recipe 7)	0.2 ml	0.2 mM
100 mM PMSF (Recipe 8)	0.1 ml	0.1 mM

## PROTOCOL

10 mM T3 (Recipe 9)	0.1 ml	0.01 mM
10 mM leupeptin (Recipe 10)	0.5 ml	0.05 mM
10 mM pepstatin (Recipe 11)	0.5 ml	0.05 mM
10 mM antipain (Recipe 12)	0.5 ml	0.05 mM
Glycerol	10 ml	10%

Add deionized water to 80 ml, adjust to pH 7.5 if necessary with NaOH (aq), and adjust volume to 100 ml with deionized water.

*Note: Protease inhibitor cocktail tablets (complete, EDTA-free) from Roche may be used instead of leupeptin, pepstatin, and antipain.*

### Recipe 14: 1 M Imidazole

Dissolve 6.8 g imidazole in 80 ml of deionized water, adjust to pH 7.5 with HCl (aq), and adjust volume to 100 ml with deionized water.

### Recipe 15: Talon Buffer 1

<i>Stock solution</i>	<i>Volume</i>	<i>Final concentration</i>
1 M Tris Buffer, pH 7.0 (Recipe 5)	5 ml	50 mM
3 M NaCl (Recipe 6)	10 ml	300 mM
Glycerol	10 ml	10%

Add deionized water to 80 ml, adjust to pH 7.5 if necessary with NaOH (aq), and adjust volume to 100 ml with deionized water.

### Recipe 16: Talon Buffer 2

<i>Stock solution</i>	<i>Volume</i>	<i>Final concentration</i>
1 M Tris Buffer, pH 7.0 (Recipe 5)	5 ml	50 mM
3 M NaCl (Recipe 6)	5 ml	150 mM
Glycerol	10 ml	10%
100 mM DTT (Recipe 7)	0.2 ml	0.2 mM
100 mM PMSF (Recipe 8)	0.1 ml	0.1 mM
10 mM T3 (Recipe 9)	0.1 ml	0.01 mM
1 M Imidazole (Recipe 14)	3 ml	30 mM

Add deionized water to 80 ml, adjust to pH 7.5 if necessary with NaOH (aq), and adjust volume to 100 ml with deionized water.

### Recipe 17: Talon Buffer 3

<i>Stock solution</i>	<i>Volume</i>	<i>Final concentration</i>
1 M Tris Buffer, pH 7.0 (Recipe 5)	5 ml	50 mM
3 M NaCl (Recipe 6)	5 ml	150 mM
Glycerol	10 ml	10%
1 M Imidazole (Recipe 14)	7.5 ml	75 mM

Add deionized water to 80 ml, adjust to pH 8.0 if necessary with NaOH (aq), and adjust volume to 100 ml with deionized water.

### Recipe 18: Talon Buffer 4

<i>Stock solution</i>	<i>Volume</i>	<i>Final concentration</i>
1 M Tris Buffer, pH 7.0 (Recipe 5)	1 ml	50 mM
3 M NaCl (Recipe 6)	1 ml	150 mM
Glycerol	2 ml	10%
1 M Imidazole (Recipe 14)	10 ml	500 mM

Adjust to pH 8.0 if necessary with NaOH (aq), and adjust volume to 20 ml with deionized water.

### Recipe 19: 1000 × Ampicillin

Dissolve 1 g of ampicillin in 10 ml of deionized water. Store in 1 ml aliquots at  $-20^{\circ}\text{C}$ .

### Recipe 20: 1 × LB Broth

Dissolve 20 g of LB powder in 1000 ml of deionized water. Autoclave and store at room temperature.

**Recipe 21: 2 × LB Broth**

Dissolve 40 g of LB powder in 1000 ml of deionized water. Autoclave and store at room temperature.

**Recipe 22: 0.5 M IPTG**

Dissolve 2.38 g of IPTG in 20 ml of deionized water. Sterilize through a 0.22- $\mu$ m filter and store at 4°C in 1 ml aliquots.

**Recipe 23: Assay Buffer**

Compound	Amount	Final concentration
NaCl	23.2 g	100 mM
Tris	12.5 g	20 mM
EDTA	1.48 g	1 mM
DTT	306 mg	1 mM

Dissolve in 3.5 l deionized water, adjust to pH 7.0 with NaOH (aq), adjust volume to 3.6 liters with deionized water, and add:

NP-40	0.4 ml	0.01%
Glycerol	400 ml	10%

**Protein-Binding Assay, High-Throughput Screen, and Dose-Response Analysis**

*Note: In addition to the following recipes, this procedure requires Assay Buffer (Recipe 23).*

**Recipe 24: Protein Cocktail**

- 1  $\mu$ M hTR $\beta$  LBD
  - 1  $\mu$ M T3
  - 0.025  $\mu$ M SRC2-2 labeled with fluorescein
- Prepare in Assay Buffer (Recipe 23).

*Note: The concentration of TR (1 mM) in the Protein Cocktail represents 2 $\times$  K<sub>d</sub>. The solution of labeled SRC2-2 (25 nM in buffer) should give a 100-fold increased fluorescence intensity signal compared to straight buffer. Because fluorescent molecules can degrade after several freeze-thaws and exposure to light, we advise checking the fluorescence intensity of the solution before starting the experiment.*

**Recipe 25: Positive Control**

Mix 1  $\mu$ l of 10 mM compound 3 (10  $\mu$ M) into 999  $\mu$ l Protein Cocktail (Recipe 24). Prepare just before use.

**Recipe 26: Negative Control**

Mix 1  $\mu$ l of 10 mM compound 11 (10  $\mu$ M) into 999  $\mu$ l Protein Cocktail (Recipe 24). Prepare just before use.

**Glutathione-S-Transferase Pull-Down Assay**

*Note: In addition to the following recipes, this procedure requires 1 M Tris Buffer, pH 7.0 (Recipe 5), 3 M NaCl (Recipe 6), 100 mM DTT (Recipe 7), and 100 mM PMSF (Recipe 8).*

**Recipe 27: TST Buffer**

Stock solution	Volume	Final concentration
1 M Tris Buffer, pH 7.0 (Recipe 5)	25 ml	50 mM
3 M NaCl (Recipe 6)	25 ml	150 mM

Add deionized water to 400 ml, adjust to pH 7.5 if necessary with NaOH (aq), adjust volume to 500 ml with deionized water, and add 0.25 ml of Tween 20 for a final concentration of 0.05%.

**Recipe 28: Protease Inhibitor Cocktail (1000 $\times$ )**

Dissolve protease inhibitor cocktail tablet in 1 ml of DMSO. Add 4 ml of deionized water to a final volume of 5 ml and store at -20°C in 1 ml fractions.

**Recipe 29: 0.5 M Hepes Buffer**

Dissolve 11.9 g of Hepes in 80 ml of deionized water, adjust to pH 7.9 with NaOH (aq), and adjust to final volume of 100 ml with deionized water.

**Recipe 30: 3 M KCl**

Dissolve 222 g of KCl in 1000 ml of deionized water.

**Recipe 31: 1 M MgCl<sub>2</sub>**

Dissolve 20.3 g of MgCl<sub>2</sub> in 100 ml of deionized water.

**Recipe 32: A-150**

<i>Stock solution</i>	<i>Volume</i>	<i>Final concentration</i>
0.5 M Hepes Buffer (Recipe 29)	20 ml	20 mM
3 M KCl (Recipe 30)	25 ml	150 mM
1 M MgCl <sub>2</sub> (Recipe 31)	5 ml	10 mM
Glycerol	5 ml	1%

Add deionized water to 400 ml, adjust to pH 8.0 with NaOH (aq), and adjust volume to 500 ml with deionized water.

**Recipe 33: IPAB Buffer**

<i>Stock solution</i>	<i>Volume</i>	<i>Final concentration</i>
100 mM DTT (Recipe 7)	0.2 ml	0.2 mM
100 mM PMSF (Recipe 8)	0.1 ml	0.1 mM
Protease Inhibitor Cocktail (Recipe 28)	0.1 ml	

Adjust to 100 ml with A-150 (Recipe 32).

**Recipe 34: PBB**

<i>Stock solution</i>	<i>Volume</i>	<i>Final concentration</i>
1% Triton-X in PBS	2 ml	
1% NP-40 in PBS	2 ml	
100 mM DTT (Recipe 7)	0.25 ml	1 mM
100 mM PMSF (Recipe 8)	0.12 ml	0.5 mM
Protease Inhibitor Cocktail (Recipe 28)	25 µl	
2 g/liter BSA	0.24 ml	0.016 g/l

Adjust to 25 ml with A-150 (Recipe 32).

*Note: 25 ml is enough for two or three gels. Prepare immediately before use and store on ice.*

**Recipe 35: 1.5 mM T3**

Dissolve 7.32 mg of T3 in 10 ml of DMSO and store at -20°C in 1 ml aliquots.

**Recipe 36: Gel Fixer**

60 ml acetic acid

100 ml MeOH

Adjust to 500 ml with deionized water.

**Hormone Displacement Assay**

*Note: In addition to the following recipes, this procedure requires 100 mM PMSF (Recipe 8).*

**Recipe 37: 1 mM T3**

Dissolve 9.76 mg of T3 in 20 ml of DMSO; store at -20°C.

**Recipe 38: Hormone Assay Buffer**

<i>Compound</i>	<i>Amount</i>	<i>Final concentration</i>
KCl	29.8 g	400 mM
Sodium phosphate (dibasic)	5.36 g	20 mM
EDTA	186 mg	0.5 mM
MgCl <sub>2</sub>	203 mg	1 mM

Dissolve in 700 ml of deionized water, adjust to pH 8.0 with NaOH (aq), adjust volume to 900 ml with deionized water, and add 100 ml of glycerol for a final concentration of 10%.

**Recipe 39: 5 mg/ml Histones**

Dissolve 5 mg of histones in 1 ml of deionized water. Prepare just before use.

**Recipe 40: 50% MTG**

Dissolve 1 g of MTG in 1 ml of deionized water. Prepare just before use.

**Recipe 41: Hormone Assay Cocktail**

Stock solution	Volume	Final concentration
100 mM PMSF (Recipe 8)	0.75 $\mu$ l	1 mM
5 mg/ml Histones (Recipe 39)	7.5 $\mu$ l	0.05 mg/ml
50% MTG (Recipe 40)	1.5 $\mu$ l	0.1%
TNT reaction (about 25 fM protein)	120 $\mu$ l	
<sup>125</sup> I-T3	34 $\mu$ l	

Adjust to 750  $\mu$ l with Hormone Assay Buffer (Recipe 38).

*Note: The volume of <sup>125</sup>I-T3 required will change with time. Upon delivery, the concentration is ~145 nM, but it will decay over time. Therefore, calculate the required amount based on the formula*

$$^{125}\text{I} \text{ to add} = \text{starting concentration} \times 1/2^{(\text{days since initial concentration measured}/60 \text{ days})}$$

**Transcription Assay**

**Recipe 42: Growth Medium**

- 500 ml DMEM/H21
- 50 ml newborn calf serum, heat-inactivated (see note) (10%)
- 5 ml penicillin-streptomycin 100x

*Note: To heat-inactivate newborn calf serum, thaw the serum slowly to 37°C and mix the contents of the bottle thoroughly. Place the bottle for 30 min in a water bath at 56°C and swirl every 10 min. Cool immediately in an ice bath and store at 4°C.*

**Recipe 43: Assay Medium**

- 1 package (for 1 liter) DMEM/Ham's F12 powder
- 1.338 g NaHCO<sub>3</sub> (16 mM)
- Adjust to 1000 ml with deionized water. Filter-sterilize, then add:
- 100 ml newborn calf serum, heat-inactivated, hormone-depleted (see note) (10%)
- 10 ml penicillin-streptomycin 100x

*Note: To deplete heat-inactivated newborn calf serum of hormones, treat 500 ml of heat-inactivated newborn calf serum for 2 hours with 5 g of dextran-coated charcoal at 25°C in the dark. Centrifuge for 10 min at 8000g. Filter-sterilize and store at 4°C.*

**Recipe 44: Electroporation Buffer**

Combine 500 ml of PBS (without Mg<sup>2+</sup> and Ca<sup>2+</sup>) with 5 ml of glucose 10% for a final concentration of 0.1%.

**Recipe 45: 10  $\mu$ M T3**

Dissolve 10  $\mu$ l of 1 mM T3 (Recipe 37) in 990  $\mu$ l of DMSO.

**Instructions**

**SRC2-2 Labeling**

SRC2-2 is a peptide derived from the p160 family of nuclear receptor coactivators. The SRC2-2 peptide was utilized for screening for inhibitors of TR, because it had the tightest binding to TR $\beta$  (0.44  $\mu$ M) of all the NR-box peptides investigated (31). Because the high-throughput screen is based on displacement of this coactivator from the purified NR (in this case TR LBD) using fluorescence polarization, the first step is to create a fluorescently tagged form of the coactivator (in this case SRC2-2) peptide.

1. Dissolve 5 mg of crude SRC2-2 peptide in 3 ml of DMF:PBS, pH 7.0 (1:1).
2. Dissolve 30 mg of 5-iodoacetamidofluorescein in 300  $\mu$ l of DMF.

3. Add fluorescein solution to peptide solution and stir at room temperature for 2 hours in the dark.
4. Add 100  $\mu$ l of ethanethiol to inactivate excess 5-iodoacetamidofluorescein, and continue stirring for 5 min.
5. Purify fluorescently labeled peptide by preparative RP-HPLC [gradient: 100% TFA in Water (Recipe 1) to 20% TFA in Water (Recipe 1) and 80% TFA in Acetonitrile (Recipe 2), linear gradient over 30 min; flow rate: 20 ml/min; total run time: 30 min; UV detection: 215 and 280 nm].
6. Check the purity of fractions by HPLC–ESMS [gradient: 100% TFA in Water (Recipe 1) to 20% TFA in Water (Recipe 1) and 80% TFA in MeOH (Recipe 3), linear gradient over 8 min; flow rate: 1 ml/min; run time: 10 min]. Analyze labeled peptide by photodiode array, total ion count, and expected mass ( $m/z$ ).
7. Evaporate the pure fraction using the Genevac evaporator  
*Note: Lyophilization may be used as an alternative method to dehydrate the samples.*
8. Dissolve each fraction in 1 ml of DMSO.
9. Dissolve 1  $\mu$ l of the DMSO solution in 1 ml of 20 mM Tris Buffer, pH 9.0 (Recipe 4).
10. Measure absorption at 492 nm with spectrometer.
11. Calculate concentration using the extinction coefficient  $78000 \text{ cm}^{-1} \text{ M}^{-1}$  and the formula below.  $A_\lambda = \epsilon \times c \times d$  ( $\epsilon = 78,000 \text{ cm}^{-1} \text{ M}^{-1}$ ,  $A_\lambda$  = measured absorbance,  $d$  = diameter of cell,  $M$  = mol/l)

### **Protein Expression and Purification of the Thyroid Receptor**

To perform the high-throughput screen and subsequent validation assays, purified NR or NR LBD are required. In this case, the following procedure, which is based on purification of histidine-tagged TR peptides using nickel columns or beads, can be used to purify the hTR $\alpha$  LBD, hTR $\beta$  LBD, or unliganded TR LBD. To produce unliganded protein, sonicate in Sonication Buffer (Recipe 13) lacking T3, wash in Talon Buffers (Recipes 15, 16, and 17) lacking T3, and reduce imidazole concentration of Talon Buffer 4 (Recipe 18) from 500 mM to 100 mM. We have also used the same procedure for purifying an hTR $\beta$  LBD C309A mutant (His<sub>6</sub>; residues T209 to D461) expressed in *E. coli* BL21 cells. However, to express and purify this protein, the bacteria must be grown at 18° to 20°C, instead of 22°C during the induction period.

*Note: Purification of the TR protein in the presence of T3 increased the yield dramatically, and in protein binding assays, we obtained more consistent  $K_d$  values. In the presence of T3, TR remained in solution at concentrations up to 145 mM. Several freeze-thaw cycles (up to five) did not alter the activity of the protein.*

#### **Transformation from purified super-coiled plasmid DNA**

1. Dissolve 35 g of LB agar in 1000 ml of deionized water.
2. Autoclave and allow to cool to 37°C, then add 1 ml of 1000  $\times$  Ampicillin (Recipe 19) and pour into sterile petri dishes until dish surface is completely covered. Leave plates at room temperature for 24 to 48 hours to dry.
3. Thaw *E. coli* BL21(DE3) strain and DNA stock, hTR $\beta$  LBD (His<sub>6</sub> T209-D461) and hTR $\alpha$  LBD (His<sub>6</sub> E148-V410), on ice.
4. Once thawed, add 1  $\mu$ l of DNA (20 to 40 ng/ml) to each tube of competent cells and spin briefly to mix.
5. Incubate 30 min on ice.
6. Heat shock at 42°C for 45 s and then incubate 2 min on ice.
7. Add 950  $\mu$ l of 1  $\times$  LB Broth (Recipe 20) to each tube and shake tubes at 37°C for 1 hour.
8. Label plates with cell type, protein, volume plated, and date and add 100 to 200  $\mu$ l on each plate and spread with glass beads (add 20 to 50 beads and spread by moving the plate).
9. Discard beads and incubate plates at 37°C overnight.

#### **Preculture and culture preparation**

1. Pick a single colony from each of the transformation plates and add to 50 ml of 1  $\times$  LB Broth (Recipe 20) with 1  $\times$  ampicillin diluted from 1000  $\times$  Ampicillin (Recipe 19).
2. Grow culture at 37°C for 4 to 6 hours while shaking.
3. Measure the optical density (OD) at absorbance 600 ( $A_{600}$ ) of 100  $\mu$ l of precultured bacteria diluted with 900  $\mu$ l of 1  $\times$  LB Broth (Recipe 20).

4. Calculate the volume of the preculture to add to the LB in Fernback flasks using the following formula:

$$1.5 / (\text{OD} \times 10) = \text{Volume (liters) of preculture to inoculate in 1 liter}$$

5. Add the appropriate amount of preculture cells to 1 liter of 2 × LB Broth (Recipe 21) in each Fernback flask and grow at 22°C for 14 to 16 hours (overnight) on an orbital shaker.

### **Induction**

1. Starting at 13 hours, measure the OD ( $A_{600}$ ) of 100 µl samples diluted with 900 µl of 1 × LB (Recipe 20).
2. For bacteria expressing hTRβ LBD, when OD ( $A_{600}$ ) reaches 0.6, induce protein expression using 1 ml of 0.5 M IPTG (Recipe 22) (final concentration 500 µM) for each liter and incubate at 22°C for about 4 hours on an orbital shaker. For bacteria expressing hTRα LBD, induce expression with IPTG when the OD ( $A_{600}$ ) reaches 1.2.
3. Transfer culture to 1-liter centrifugation bottles and spin at 8000g for 20 min.
4. Decant supernatant and transfer into 50-ml conical tubes.

*Note: Supernatant should be clear. If it is cloudy, the cells may have lysed or died. In that case, discard culture and start over again.*

5. Flash-freeze bacteria in liquid nitrogen and store at –80°C.

### **Protein purification**

1. Combine the stored cell pellets and resuspend in 20 ml of Sonication Buffer (Recipe 13) with 20 mg lysozyme per liter of original cell culture.
2. Sonicate on ice using until the suspension is no longer “goeey,” using the following parameters:

Duty cycle: 70; timer 12 min (3 min intervals); output control: 6

3. Centrifuge 1 hour at 4°C at 100,000g.
4. To a conical tube (50 ml) add Talon resin (0.5 to 0.75 ml per liter cell culture) and wash the resin two times with 15 ml of Talon Buffer 1 (Recipe 15).

*Note: All buffers for the purification are stored on ice. The wash and elution steps were carried out by resuspending the Talon resin in the conical tube, centrifuging it for 5 min at 4°C at 50g, and decanting the supernatant. It is very important that the resin remain in the bottom of the tube.*

5. Decant Talon Buffer 1 (Recipe 15) and add protein supernatant to Talon resin (40 ml of supernatant for each conical tube) and rotate gently for at least 1 hour at 4°C using the rotisserie shaker.
6. Pellet the resin by centrifuging for 5 min.
7. Wash the resin three times with 15 ml of Talon Buffer 2 (Recipe 16).
8. Wash the resin with 15 ml of Talon Buffer 3 (Recipe 17).
9. Elute with 5 × 3 ml of Talon Buffer 4 (Recipe 18).
10. Analyze samples of the eluted protein by SDS-PAGE using standard methods.
11. Pool fractions containing protein and dialyze overnight against 4 liters of Assay Buffer (Recipe 23).
12. Measured the protein concentration using a BCA assay (usually around 50 to 100 µM).
13. Measure protein functionality by a direct binding assay or store at –80°C in 1-ml aliquots.

### **Protein-Binding Assay, High-Throughput Screen, and Dose-Response Analysis**

The fitted binding curve for the binding assay not only provides the estimated  $K_d$ , but also the expected saturation at high and low concentrations of protein. If no saturation is detectable at higher concentrations, this indicates that protein is nonfunctional. We obtained the following binding constants ( $K_d$ ): hTRβ,  $K_d = 0.44 \mu\text{M}$ ; hTRα LBD,  $K_d = 0.17 \mu\text{M}$ ; hTRβ LBD (C309A),  $K_d = 0.17 \mu\text{M}$ .

### Protein-binding assay

*Note: This assay is conducted in quadruplicate.*

1. Concentrate protein to 50  $\mu$ M, using an Amicon centrifugal filter unit if necessary.
2. To 100  $\mu$ l of concentrated protein, add 1  $\mu$ l of 10 mM T3 (Recipe 9).
3. Transfer 50  $\mu$ l of this mixture into each of well A1 and A2 of a 96-well opaque plate.
4. Add 50  $\mu$ l of Assay Buffer (Recipe 23) to wells A2 through A12.
5. Create serial dilutions in wells A2 through A12 by sequentially transferring 50  $\mu$ l (50  $\mu$ l from A2 into A3, 50  $\mu$ l from A3 into A4, ... 50  $\mu$ l from A11 into A12).
6. Prepare 800  $\mu$ l of a 20 nM solution of the labeled SRC2-2 in Assay Buffer (Recipe 23).
7. Add 50  $\mu$ l of SRC2-2 (20 nM) into wells B1 through B12.
8. Transfer 10  $\mu$ l of each well of row A (96-well plate) into each well of rows A and B of a black 384-well plate with a 12-channel pipette.
9. Transfer 10  $\mu$ l of each well of row B (96-well plate) into each well of rows A and B of a black 384 well plate with a 12-channel pipette.

*Note: Total volume of 384 wells is 20 ml. Visually inspect each well for air bubbles. Careful pipetting and spinning the assay plate for 5 min at 400g can improve the standard deviation. Sometimes poking the well with a 10-ml pipette tip removes air bubbles.*

10. Equilibrate for 30 min.
11. Measure binding using fluorescence polarization (excitation  $\lambda$  485 nm, emission  $\lambda$  530 nm) with plate reader.

*Note: Fluorescence polarization may be read up to 8 hours after assay without significant loss of reproducibility.*

12. Analyze data using SigmaPlot 8.0 and obtain the  $K_d$  value by fitting the data to the following equation:

$$y = \min + (\max - \min) / (1 + (x/K_d)^{\text{Hill slope}})$$

### High-throughput screen

A library comprising 138,000 compounds (ChemRX, 28K; ChemDiv, 53K; ChemBridge, 24K; SPECS, 31K; Microsource, 2K) was screened in 384-well format in a single point format. The complete composition of this library is available from the BASC Web site ([www.ucsf.edu/basc](http://www.ucsf.edu/basc)). Compounds are screened for their ability to compete for coactivator binding to the TR in the presence of the T3 ligand.

*Note: The protocol for the liquid handling using the Multimek should be carefully developed before running the screen. Mixing by trituration (repeated aspirating and dispensing) can create air bubbles, especially when using air gaps in the automation protocol. Sufficient mixing should be investigated using a colored compound, such as fluorescein.*

1. Add 34  $\mu$ l of Assay Buffer (Recipe 23) containing 5.9% DMSO to each well, except columns 1, 2, 11 and 12, of an opaque 384-well plate using a WellMate.
2. Add 6  $\mu$ l of compound solutions (dissolved in 1 mM DMSO) using a Multimek equipped with a 96-channel head, and mix by trituration. (The concentration of compounds in these dilution plates is 150  $\mu$ M.)
3. Transfer 6  $\mu$ l from the dilution plates into 384-well black plates using a Multimek.
4. Add 24  $\mu$ l of Protein Cocktail (Recipe 24) using a WellMate. The final concentration of compound is 30  $\mu$ M with DMSO content of about 4%.

*Note: Visually inspect each well for air bubbles. Careful pipetting and spinning the assay plate for 5 min at 400g can improve the standard deviation. Sometimes, poking the well with a 10-ml pipette tip removes air bubbles.*

5. Add 30  $\mu$ l of Positive Control (Recipe 25) to wells A1, A2, B1, and B2 of each plate using a micropipettor (by hand).
6. Add 30  $\mu$ l of Negative Control (Recipe 26) to wells C1, C2, D1, and D2 of each plate using a micropipettor (by hand).
7. Incubate for 2 hours at room temperature.
8. Measure fluorescence polarization (excitation  $\lambda$  485 nm, emission  $\lambda$  530 nm) and fluorescence intensity with a plate reader.

- Analyze data using “Assay Explorer.”

*Note: The data may also be analyzed using ActivityBase (idbs, Guildford, Surrey, UK).*

### **Dose-response analysis**

*Note: This assay is conducted in quadruplicate.*

- Using a 96-well plate, prepare a serial dilution of compound (1000 to 0.48  $\mu\text{M}$  in DMSO) in wells A1 through A12.
- Add 90  $\mu\text{l}$  of Assay Buffer (Recipe 23) to wells B1 through B12.
- Transfer 10  $\mu\text{l}$  of row A to row B and mix by trituration.
- Add 50  $\mu\text{l}$  of Protein Cocktail (Recipe 24) to wells C1 through C12.
- Transfer 10  $\mu\text{l}$  of every well of row B (96 well plate) into each well of rows A and B (black 384 well plate) with a 12-channel pipette.
- Transfer 10  $\mu\text{l}$  of each well of row C (96 well plate) into each well of rows A and B (black 384 well plate) with a 12-channel pipette.

*Note: Total volume of 384 wells is 20 ml. Visually inspect each well for air bubbles. Careful pipetting and spinning the assay plate for 5 min at 400g can improve the standard deviation. Sometimes, poking the well with a 10-ml pipette tip removes air bubbles.*

- Add 20  $\mu\text{l}$  of Positive Control (Recipe 25) to wells C1 through C4.
- Add 20  $\mu\text{l}$  of Negative Control (Recipe 26) to wells C5 through C8.
- Incubate for 3 hours at room temperature.
- Measure inhibition using fluorescence polarization (excitation  $\lambda$  485 nm, emission  $\lambda$  530 nm) with an Analyst AD plate reader.
- Analyze data using SigmaPlot 8.0 and obtain the  $K_d$  value by fitting the data to the following equation:

$$y = \min + (\max - \min) / (1 + (x/K_d) \times \text{Hill slope})$$

The final compound concentrations are 50 to 0.024  $\mu\text{M}$ .

### **Hit Validation by Glutathione-S-Transferase Pull-Down Assay**

The GST pull-down assay fulfills two functions: (i) It represents a secondary assay to validate those hit compounds that were positive in the high-throughput screen for their ability to bind to the full-length TR; and (ii) it determines whether the small molecules can inhibit the interaction between full-length TR and full-length coactivator protein. Therefore, GST-TR protein was expressed in *E. coli* using the steps up to the preparation of the bacterial pellet described in “Protein expression and purification of the thyroid receptor,” above. Radiolabeled SRC2 full-length protein was obtained by using a TNT T7 quick coupled transcription/translation system.

#### **Transformation and preparation of bacterial pellet**

- Transform bacteria with the plasmid DNA that includes the full GST-TR $\beta$  construct and prepare a bacterial culture.
- Resuspend bacterial pellet on ice in TST Buffer (Recipe 27) (20 ml per liter of bacterial culture) and add 0.2 ml of 100 mM DTT (Recipe 7), 0.2 ml of 100 mM PMSF (Recipe 8), and 0.02 ml of Protease Inhibitor Cocktail (Recipe 28).
- Store pellet at  $-80^\circ\text{C}$ .

#### **Protein purification**

- Thaw pellet and add 10 mg of lysozyme per liter of bacteria culture.
- Incubate on ice for 15 min.
- Sonicate using the following parameters:  
Duty cycle: 70, timer 12 min (3 min intervals), output control: 6
- Reserve a 10- $\mu\text{l}$  aliquot to verify protein weight by SDS-PAGE.
- Centrifuge twice for 30 min each at 100,000g at  $4^\circ\text{C}$ , decanting supernatant between spins.

6. Prepare Glutathione Sepharose 4B beads (0.5 ml/liter of culture) by washing it three times with 10 ml of TST Buffer (Recipe 27).  
*Note: All buffers are stored on ice.*
7. Incubate the supernatant with beads and shake for 1 hour at 4°C using the rotisserie shaker.
8. Dispense beads and supernatant into a Poly-Prep column and wash twice with 5 ml of PBS containing 0.1% NP-40.  
*Note: Liquid will flow slowly through the column.*
9. Suspend the beads with 0.6 ml of IPAB Buffer (Recipe 33) in the Poly-Prep column and transfer into microcentrifuge tubes.
10. Add glycerol to the bead slurry to a final concentration of 20% and shake to mix. Total volume should be 1.6 ml for each liter of culture.
11. Take an aliquot of the suspension and measure protein concentration using BCA method.
12. Snap-freeze with liquid nitrogen and store at -20°C.

### **GST pull-down assay**

*Note: This part of the procedure should be performed in a cold room.*

1. Add 127.5 µl of PBB (Recipe 34) to each of eight microcentrifuge tubes.
2. Add 2 µl of DMSO to tube 1 (Control 1).
3. Add 1 µl of DMSO and 1 µl of 1.5 mM T3 (Recipe 35) (10 µM final concentration) to tube 2 (Control 2).
4. Prepare a serial dilution of hit compound (50 to 0.39 µM) in DMSO (final concentrations are 7.5 to 0.075 µM).
5. Add 1 µl of 1.5 mM T3 (Recipe 35) and 1 µl of hit compound of each concentration to tubes 3 through 8.
6. Add 10 µl of sepharose bead slurry corresponding to 3 µg of GST-TRβ fusion protein to tubes 2 through 8.
7. Perform in vitro translation reaction using 0.5µg SRC2 plasmid in the presence of <sup>35</sup>S-methionine according to manufacturer's instructions.

*Note: From this point on, precautions for handling radioactivity must be taken.*

8. Dilute 50 µl of in vitro translation reaction with 450 µl of PBB (Recipe 34).
9. Add 10 µl of diluted translation reaction to each tube.
10. Rock for 90 min at 4°C.
11. Spin in a microcentrifuge at 13,000 rpm for 10 to 15 s.
12. Remove 120 µl of supernatant with a pipette and discard supernatant properly as radioactive waste.  
*Note: Do not try to remove all of the supernatant; you may dislodge and remove the beads.*
13. Add 200 µl of IPAB Buffer (Recipe 33) to the beads.
14. Mix by inversion and microcentrifuge for 10 to 15 s.
15. Remove 200 µl of supernatant with a pipette and discard as radioactive waste.
16. Wash three more times with 200 µl of IPAB Buffer (Recipe 33), pelleting by pulsing in a microcentrifuge and removing supernatant carefully with a pipette.
17. After the last wash, remove as much supernatant as possible without disturbing the beads.

*Note: You may wish to use a narrow-tip pipette tip to avoid removing the beads.*

18. Dry the beads in a vacuum centrifuge (such as a CentriVap) for 5 to 10 min at "high."
19. Add 20 µl of NuPAGE loading buffer and denature at 70°C for 10 min.  
*Note: Take care to seal tubes or use cap locks to prevent caps from popping off during denaturation.*
20. Microcentrifuge at maximum speed for 3 min and remove 15 µl to analyze by SDS-PAGE (NuPAGE).
21. For input lane use 1 µl of diluted translation reaction diluted with 22 µl of NuPAGE loading buffer.
22. Run gel at 200 V.

23. Incubate the gel for 15 min in Gel Fixer (Recipe 36).
24. Scan gel with PhosphorImager.

*Note: Typhoon (GE) would be an alternative instrument.*

### **Hormone Displacement Assay**

This assay is used to validate that the hit compounds do not compete with T3 for binding to the TR. This assay is conducted in triplicate for T3 and hit compounds.

1. Produce full-length hTR $\beta$  using a TNT T7 quick-coupled transcription translation system according to the manufacturer's instructions.
2. In wells A1 through A5 of a 96-well plate, prepare a 1:10 dilution (1000 to 0.1  $\mu$ M) of T3 starting with 1 mM T3 (Recipe 37) in DMSO.
3. In wells B1 through B5, prepare a 1:10 dilution (1000 to 0.1  $\mu$ M) of hit compound in DMSO.
4. Add 50  $\mu$ l Hormone Assay Buffer (Recipe 38) to the wells of rows C through H, columns 1 through 5.
5. Transfer 1  $\mu$ l from each well of row A to the corresponding wells in rows C, D, and E and mix by trituration (A1 to C1, D1, E1; A2 to C2, D2, E2, ...and A5 to C5, D5, E5).
6. Transfer 1  $\mu$ l from each well of row B to the corresponding wells in rows F, G, and H and mix by trituration (B1 to F1, G1, H1; B2 to F2, G2, H2, ...and B5 to F5, G5, H5).
7. Add 50  $\mu$ l of Hormone Assay Cocktail (Recipe 41) to rows C through H and incubate 3 hours at room temperature with gentle shaking.

*Note: The Hormone Assay Cocktail contains  $^{125}$ I-T3, so take precautions appropriate to the use of gamma-emitting radioisotopes. Use lead shielding and proper disposal methods.*

8. Prepare 30 Poly-Prep columns by placing them in a column rack above the trough.
9. Gently stir 2 g of G25 Sephadex in 40 ml of Hormone Assay Buffer (Recipe 38) for 10 min.
10. Add 5 ml of the G25 Sephadex suspension to each column to obtain a 2-ml bed volume.
11. Store columns with a slight excess of Hormone Assay Buffer (Recipe 38).
12. Apply one reaction mixture to the top of each column and, using 3  $\times$  500  $\mu$ l of Hormone Assay Buffer (Recipe 38), elute directly into 7 ml scintillation vials.
13. Add 4 ml of microscintillation fluid to each vial.
14. Read vials in scintillation counter.
15. Analyze data using SigmaPlot 8.0 and obtain the  $K_d$  value by fitting the data to the following equation:

$$y = \min + (\max - \min) / (1 + (x/K_d) \times \text{Hill slope})$$

*Note: Normalize the calculated  $K_d$  for the compound by assuming a  $K_d$  of 0.081 nM for T3, which takes into account the variation of the actual concentration of radiolabeled thyroid hormone.*

### **Transcription Assay**

This assay tests whether the hit compounds can penetrate the cell membrane and inhibit TR activity in a cellular context. This procedure uses the human bone osteosarcoma epithelial cell line U2OS, which are transfected with a plasmid encoding TR $\beta$  and a reporter plasmid containing a synthetic TR response element (DR-4). DR-4 contains two copies of a direct repeat spaced by four nucleotides (AGGTCA-cagg-AGGTCA), and it is cloned immediately upstream of a minimal thymidine kinase promoter that is linked to the luciferase coding sequence. Cells should be grown in a 37°C, 5% CO<sub>2</sub> humidified incubator and handled using sterile technique in a laminar flow hood. The assay is conducted in triplicate.

1. Thaw 1 ml of U2OS starter culture at room temperature.
2. Add thawed cells to a 150-mm cell culture dish containing 25 ml of Growth Medium (Recipe 42).

3. Grow cells to a confluence of no more than 80% (usually within 2 days).
4. Remove growth medium and wash cells with 10 ml of PBS without  $\text{Ca}^{2+}$  and  $\text{Mg}^{2+}$ , prewarmed to 37°C.
5. Add 5 ml trypsin solution and incubate for 3 to 5 min at 37°C, 5%  $\text{CO}_2$ .
6. Add detached cells to 5 ml of Assay Medium (Recipe 43) and count the cells using a hemocytometer.
7. Pellet the cells by centrifugation (800g) and remove medium.
8. Resuspend the cells in appropriate amount of Electroporation Buffer (Recipe 44) to achieve  $2 \times 10^6$  cells per 0.5 ml.
9. Add 1.5  $\mu\text{l}$  of the TR $\beta$ -CMV plasmid (2.5  $\mu\text{g}$ ), 0.5  $\mu\text{l}$  of the pRL-CMV plasmid (2.5  $\mu\text{g}$ ), and 5  $\mu\text{l}$  of the DR-4 reporter plasmid (5  $\mu\text{g}$ ) into all microcentrifuge tubes, and add 0.5 ml of the buffer containing U2OS cells (step 8, above).
10. Mix gently and add to electroporation cuvettes.
11. Electroporate at a potential of 0.25 kV and capacity of 960 mF.
12. Thoroughly mix cells within the cuvette for 2 min.  
*Note: Thorough mixing is essential to ensure adequate and even resuspension of the cell pellet. Uneven resuspension can produce a low signal-to-noise ratio during luminance detection.*
13. Transfer cells into conical tube and dilute with Assay Medium (Recipe 43) to a concentration of 200,000 cells/ml.
14. Add 100  $\mu\text{l}$  of cell suspension to each well of a 96-well cell culture plate and incubate for 4 to 6 hours at 37°C, 5%  $\text{CO}_2$ .
15. In wells A1 through A12 of a 96 opaque well plate, prepare a serial dilution (10  $\mu\text{l}$ ) of hit compound (500 to 0.24  $\mu\text{M}$ ) in 10  $\mu\text{M}$  T3 (Recipe 45) solution.
16. Use wells B1 through B6 for controls: to wells B1 and B2, add 10  $\mu\text{l}$  of 10  $\mu\text{M}$  T3; to wells B3 and B4, add 10  $\mu\text{l}$  of DMSO; and to wells B5 and B6, add 10  $\mu\text{l}$  of hit compound (500  $\mu\text{M}$ ).
17. Using a 12-channel pipette, transfer 1  $\mu\text{l}$  from each well of row A (96 opaque well plate) to each well of rows A, B, and C of the cell culture plate.
18. Transfer 1  $\mu\text{l}$  from each well of B1 through B6 (96 opaque well plate) to the wells of row D of the cell culture plate.
19. Incubate for 16 hours at 37°C, 5%  $\text{CO}_2$ .
20. Remove the medium from the cell culture plates and wash the cells with 100  $\mu\text{l}$  of PBS without  $\text{Ca}^{2+}$  and  $\text{Mg}^{2+}$ .
21. Add 20  $\mu\text{l}$  of lysis buffer provided with Dual Luciferase Assay kit to each well and rock culture plate for 15 min at room temperature.
22. Add 100  $\mu\text{l}$  of the kit's Luciferase reagent and read luminance with plate reader.
23. Add 100  $\mu\text{l}$  of the kit's Stop & Glo reagent and read luminance again.
24. Analyze data using SigmaPlot 8.0 and normalize to basal expression (treatment with equal amounts of DMSO, but no T3) and fully induced expression (treatment with equal amounts of DMSO and T3).

### Related Techniques

There are two related high-throughput screening techniques. (i) Alfascreen is a heterogeneous assay that relies on hydrogel-coated donor and acceptor beads that are conjugated to interacting proteins. The beads come in close proximity when binding occurs and are excited by a laser, producing singlet oxygen that migrates from the donor bead to react with chemiluminescers on the acceptor bead. The chemiluminescers then activate fluorophores, emitting light at 520 to 620 nm. (ii) Förster resonance energy transfer (FRET) measures the energy transfer between two interacting fluorescently labeled proteins.

The fluorescence polarization assay has the advantage that it is a cost-efficient, reliable, and robust process that is broadly applicable to many protein-protein interactions. The secondary assays described herein are only a few examples of possible alternative assays that can be used to validate hit compounds.

Notes and Remarks

The described high-throughput screening method can be used to discover small molecules capable of inhibiting the interactions of nuclear receptors and their coactivators. The goal is to develop drugs for hormone-dependent diseases and research tools to investigate the functional changes in signaling by the targeted receptor and overall changes in transcriptional regulation in the cellular environment.

References

1. A. Aranda, A. Pascual, Nuclear hormone receptors and gene expression. *Physiol. Rev.* **81**, 1269–1304 (2001).
2. C. B. Harvey, G. R. Williams, Mechanism of thyroid hormone action. *Thyroid* **12**, 441–446 (2002).
3. H. E. Xu, M. H. Lambert, V. G. Montana, K. D. Plunket, L. B. Moore, J. L. Collins, J. A. Oplinger, S. A. Klierer, R. T. Gampe, Jr., D. D. McKee, J. T. Moore, T. M. Willson, Structural determinants of ligand binding selectivity between the peroxisome proliferator-activated receptors. *Proc. Natl. Acad. Sci. U.S.A.* **98**, 13919–13924 (2001).
4. P. M. Yen, Physiological and molecular basis of thyroid hormone action. *Physiol. Rev.* **81**, 1097–1142 (2001).
5. J. Malm, Thyroid hormone ligands and metabolic diseases. *Curr. Pharm. Des.* **10**, 3525–3532 (2004).
6. J. Zhang, M. A. Lazar, The mechanism of action of thyroid hormones. *Annu. Rev. Physiol.* **62**, 439–466 (2000).
7. G. E. Krassas, N. Pontikides, K. Loustis, G. Koliakos, T. Constantinidis, D. Panidis, Resistin levels in hyperthyroid patients before and after restoration of thyroid function: Relationship with body weight and body composition. *Eur. J. Endocrinol.* **153**, 217–221 (2005).
8. G. J. Grover, K. Mellstrom, J. Malm, Development of the thyroid hormone receptor beta-subtype agonist KB-141: A strategy for body weight reduction and lipid lowering with minimal cardiac side effects. *Cardiovasc. Drug Rev.* **23**, 133–148 (2005).
9. R. Sari, M. K. Balci, H. Altunbas, U. Karayalcin, The effect of body weight and weight loss on thyroid volume and function in obese women. *Clin. Endocrinol. (Oxford)* **59**, 258–262 (2003).
10. J. D. Baxter, P. Webb, G. Grover, T. S. Scanlan, Selective activation of thyroid hormone signaling pathways by GC-1: A new approach to controlling cholesterol and body weight. *Trends Endocrinol. Metab.* **15**, 154–157 (2004).
11. G. J. Grover, K. Mellstrom, L. Ye, J. Malm, Y. L. Li, L. G. Bladh, P. G. Sleph, M. A. Smith, R. George, B. Vennstrom, K. Mookhtiar, R. Horvath, J. Speelman, D. Egan, J. D. Baxter, Selective thyroid hormone receptor-beta activation: A strategy for reduction of weight, cholesterol, and lipoprotein (a) with reduced cardiovascular liability. *Proc. Natl. Acad. Sci. U.S.A.* **100**, 10067–10072 (2003).
12. D. J. Mangelsdorf, C. Thummel, M. Beato, P. Herrlich, G. Schutz, K. Umesono, B. Blumberg, P. Kastner, M. Mark, P. Chambon, R. M. Evans, The nuclear receptor superfamily: the 2nd decade. *Cell* **83**, 835–839 (1995).
13. J. M. Moore, R. K. Guy, Coregulator interactions with the thyroid hormone receptor. *Mol. Cell. Proteomics* **4**, 475–482 (2005).
14. P. Webb, N. H. Nguyen, G. Chiellini, H. A. I. Yoshihara, S. T. C. Lima, J. W. Apriletti, R. C. J. Ribeiro, A. Marimuthu, B. L. West, P. Goede, K. Mellstrom, S. Nilsson, P. J. Kushner, R. J. Fletterick, T. S. Scanlan, J. D. Baxter, Design of thyroid hormone receptor antagonists from first principles. *J. Steroid Biochem. Mol. Biol.* **83**, 59–73 (2002).
15. S. W. Dietrich, M. B. Bolger, P. A. Kollman, E. C. Jorgensen, Thyroxine analogs. 23. Quantitative structure-activity correlation studies of in vivo and in vitro thyromimetic activities. *J. Med. Chem.* **20**, 863–880 (1977).
16. D. Briel, D. Pohlars, M. Uhlig, S. Vieweg, G. H. Scholz, M. Thormann, H. J. Hofmann, 3-amino-5-phenoxythiophenes: Syntheses and structure-function studies of a novel class of inhibitors of cellular L-triiodothyronine uptake. *J. Med. Chem.* **42**, 1849–1854 (1999).
17. J. L. Stanton, E. Cahill, R. Dotson, J. Tan, H. C. Tomaselli, J. M. Wasvary, Z. F. Stephan, R. E. Steele, Synthesis and biological activity of phenoxyphenyl oxamic acid derivatives related to L-thyronine. *Bioorg. Med. Chem. Lett.* **10**, 1661–1663 (2000).
18. L. Ye, Y. L. Li, K. Mellstrom, C. Mellin, L. G. Bladh, K. Koehler, N. Garg, A. M. G. Collazo, C. Litten, B. Husman, K. Persson, J. Lunggren, G. Grover, P. G. Sleph, R. George, J. Malm, Thyroid receptor ligands. 1. Agonist ligands selective for the thyroid receptor beta(1). *J. Med. Chem.* **46**, 1580–1588 (2003).
19. R. L. Wagner, B. R. Huber, A. K. Shiau, A. Kelly, S. T. C. Lima, T. S. Scanlan, J. W. Apriletti, J. D. Baxter, B. L. West, R. J. Fletterick, Hormone selectivity in thyroid hormone receptors. *Mol. Endocrinol.* **15**, 398–410 (2001).
20. M. A. Lazar, Thyroid hormone receptors: multiple forms, multiple possibilities. *Endocr. Rev.* **14**, 184–193 (1993).
21. I. Klein, K. Ojamaa, Thyroid hormone and the cardiovascular system. *N. Engl. J. Med.* **344**, 501–509 (2001).
22. T. R. Geistlinger, R. K. Guy, An inhibitor of the interaction of thyroid hormone receptor beta and glucocorticoid interacting protein 1. *J. Am. Chem. Soc.* **123**, 1525–1526 (2001).
23. T. R. Geistlinger, R. K. Guy, Novel selective inhibitors of the interaction of individual nuclear hormone receptors with a mutually shared steroid receptor coactivator 2. *J. Am. Chem. Soc.* **125**, 6852–6853 (2003).
24. A. M. Leduc, J. O. Trent, J. L. Wittliff, K. S. Bramlett, S. L. Briggs, N. Y. Chirgadze, Y. Wang, T. P. Burris, A. F. Spatola, Helix-stabilized cyclic peptides as selective inhibitors of steroid receptor-coactivator interactions. *Proc. Natl. Acad. Sci. U.S.A.* **100**, 11273–11278 (2003).
25. A. K. Galande, K. S. Bramlett, T. P. Burris, J. L. Wittliff, A. F. Spatola, Thioether side chain cyclization for helical peptide formation: Inhibitors of estrogen receptor-coactivator interactions. *J. Pept. Res.* **63**, 297–302 (2004).
26. M. R. Arkin, J. A. Wells, Small-molecule inhibitors of protein-protein interactions: Progressing towards the dream. *Nat. Rev. Drug Discov.* **3**, 301–317 (2004).
27. T. Berg, Modulation of protein-protein interactions with small organic molecules. *Angew. Chem. Int. Ed. Engl.* **42**, 2462–2481 (2003).
28. P. L. Toogood, Inhibition of protein-protein association by small molecules: Approaches and progress. *J. Med. Chem.* **45**, 1543–1558 (2002).
29. M. H. A. Roehrl, J. Y. Wang, G. Wagner, A general framework for development and data analysis of competitive high-throughput screens for small-molecule inhibitors of protein: Protein interactions by fluorescence polarization. *Biochemistry* **43**, 16056–16066 (2004).
30. L. A. Arnold, E. Estébanez-Perpiñá, M. Togashi, N. Jouravel, A. Shelat, A. C. McReynolds, E. Mar, P. Nguyen, J. D. Baxter, R. J. Fletterick, P. Webb, R. K. Guy, Discovery of small molecule inhibitors of the interaction of the thyroid hormone receptor with transcriptional coregulators. *J. Biol. Chem.* **280**, 43048–43055 (2005).
31. J. M. Moore, S. J. Galicia, A. C. McReynolds, N. H. Nguyen, T. S. Scanlan, R. K. Guy, Quantitative proteomics of the thyroid hormone receptor-coregulator interactions. *J. Biol. Chem.* **279**, 27584–27590 (2004).

**Citation:** L. A. Arnold, E. Estébanez-Perpiñá, M. Togashi, A. Shelat, C. A. Ocasio, A. C. McReynolds, P. Nguyen, J. D. Baxter, R. J. Fletterick, P. Webb, R. K. Guy, A high-throughput screening method to identify small molecule inhibitors of thyroid hormone receptor coactivator binding. *Sci. STKE* **2006**, pl3 (2006).

# The Molecular Mechanisms of Coactivator Utilization in Ligand-dependent Transactivation by the Androgen Receptor\*<sup>§</sup>

Received for publication, June 23, 2004, and in revised form, November 2, 2004  
Published, JBC Papers in Press, November 24, 2004, DOI 10.1074/jbc.M407046200

Eva Estébanez-Perpiñá<sup>‡</sup>, Jamie M. R. Moore<sup>§</sup>, Ellena Mar<sup>‡</sup>, Edson Delgado-Rodriguez<sup>¶</sup>,  
Phuong Nguyen<sup>¶</sup>, John D. Baxter<sup>¶</sup>, Benjamin M. Buehrer<sup>\*\*‡‡</sup>, Paul Webb<sup>¶</sup>,  
Robert J. Fletterick<sup>‡</sup>, and R. Kiplin Guy<sup>§§</sup>

From the <sup>‡</sup>Department of Biochemistry and Biophysics, University of California, San Francisco, California 94143, the <sup>§</sup>Departments of Pharmaceutical Chemistry and Cellular and Molecular Pharmacology, University of California, San Francisco, California 94143, the <sup>¶</sup>Metabolic Research Unit and Diabetes Center, University of California, San Francisco, California 94143, and <sup>\*\*</sup>Karo Bio USA, Durham, North Carolina 27703

**Androgens drive sex differentiation, bone and muscle development, and promote growth of hormone-dependent cancers by binding the nuclear androgen receptor (AR), which recruits coactivators to responsive genes. Most nuclear receptors recruit steroid receptor coactivators (SRCs) to their ligand binding domain (LBD) using a leucine-rich motif (LXXLL). AR is believed to recruit unique coactivators to its LBD using an aromatic-rich motif (FXXLF) while recruiting SRCs to its N-terminal domain (NTD) through an alternate mechanism. Here, we report that the AR-LBD interacts with both FXXLF motifs and a subset of LXXLL motifs and that contacts with these LXXLL motifs are both necessary and sufficient for SRC-mediated AR regulation of transcription. Crystal structures of the activated AR in complex with both recruitment motifs reveal that side chains unique to the AR-LBD rearrange to bind either the bulky FXXLF motifs or the more compact LXXLL motifs and that AR utilizes subsidiary contacts with LXXLL flanking sequences to discriminate between LXXLL motifs.**

The cellular effects of the hormone 5- $\alpha$ -dihydrotestosterone (DHT)<sup>1</sup> are mediated by the androgen receptor (AR), a member of

\* This work was supported by the Prostate Cancer Foundation, by National Institutes of Health Grants DK58080 (to R. J. F. and R. K. G.) DK51281 (to J. D. B.), and CA8952 (to E. E.-P.) and by Department of Defense Grants DAMD17-01-1-0188 (to J. M. R. M.) and PC030607 (to P. W.). The costs of publication of this article were defrayed in part by the payment of page charges. This article must therefore be hereby marked "advertisement" in accordance with 18 U.S.C. Section 1734 solely to indicate this fact.

The atomic coordinates and structure factors (codes 1T63, 1T5Z, 1T65, and 1XJ7) have been deposited in the Protein Data Bank, Research Collaboratory for Structural Bioinformatics, Rutgers University, New Brunswick, NJ (<http://www.rcsb.org/>).

<sup>§</sup> The on-line version of this article (available at <http://www.jbc.org/>) contains supplemental Fig. S1.

<sup>¶</sup> Has proprietary interests in, and serves as a consultant and Deputy Director to, Karo Bio AB, which has commercial interests in this area of research.

<sup>‡‡</sup> Present address, Karo Bio AB, Halsovagen, S-141, 57 Huddinge, Sweden.

<sup>§§</sup> To whom correspondence should be addressed: Dept. of Pharmaceutical Chemistry, University of California, 600 16th St., San Francisco, CA 94143. Tel.: 415-502-7051; Fax: 415-514-0689; E-mail: [rguy@cgl.ucsf.edu](mailto:rguy@cgl.ucsf.edu).

<sup>1</sup> The abbreviations used are: DHT, 5- $\alpha$ -dihydrotestosterone; AR, androgen receptor; NR, nuclear receptor; Fmoc, N-(9-fluorenyl)methoxycarbonyl; SRC, steroid receptor coactivator; LBD, ligand binding domain; NTD, N-terminal domain; MMTV, mouse mammary tumor virus; LTR, long terminal repeat; GST, glutathione S-transferase; DBD, DNA

the nuclear hormone receptor superfamily (1). AR is absolutely required for normal male development, plays a variety of important roles in metabolism and homeostasis in adult men and women (2, 3), and is required for prostate cancer growth. Consequently, AR is a major target for pharmaceutical development and the recognized target for existing prostate cancer therapies, including androgen withdrawal and antiandrogens (1, 4–6). It is nonetheless desirable to obtain new antiandrogens that spare patients from harmful side-effects and inhibit AR action in secondary hormone-resistant prostate cancer, where AR action becomes sensitized to low levels of androgens or existing antiandrogens (6, 7). Improved understanding of AR signaling pathways will facilitate development of these compounds.

Like most nuclear receptors (NRs), AR activity depends on interactions with members of the steroid receptor coactivator (SRC) family (1, 8, 9). Several lines of evidence indicate that AR contacts with SRCs are important in prostate cancer. First, androgens promote SRC recruitment to the androgen-regulated prostate-specific antigen promoter, and this event is inhibited by the antiandrogen flutamide (10). Second, exogenous SRC2 (GRIP1/TIF2) promotes the androgen-dependent progression from the G<sub>1</sub> to S phase in LNCaP prostate tumor cells, in a manner that requires specific AR contact (10). Third, SRCs often become expressed at high levels in prostate cancers (5). Finally, AR contacts with SRCs mediate hormone-independent AR signaling in conditions that resemble secondary prostate cancer (11, 12). Thus, strategies to inhibit AR contacts with SRCs could be useful in blocking prostate cancer cell growth.

For many NRs, overall transcriptional activity stems mostly from the hormone-dependent activation function (AF-2) within the NRs ligand binding domain (LBD), and involves interaction between a conserved hydrophobic cleft on the surface of the LBD and short leucine-rich hydrophobic motifs (NR boxes, consensus LXXLL motif) reiterated within each SRC (13, 14). In contrast, current models of AR action suggest that AR activity stems from a potent hormone-independent activation function, AF-1, within the N-terminal domain (NTD) of the AR and emphasize the role of contacts between NTD and glutamine-rich sequences within the SRC C terminus in SRC recruitment (15–19). The AR-LBD is proposed to bind LXXLL motifs weakly and, instead, bind preferentially to aromatic-rich motifs that are found within the AR NTD (FQNLF and WHTLF) and AR-specific coactivators such as ARA70 (16, 20–23). The intramolecular interactions between the LBD and the

binding domain; CMV, cytomegalovirus; TR, thyroid receptor; AF, activation function.

NTD FQNLF motif promote formation of head to tail dimers (N-C interaction), which render the AF-2 surface unavailable for direct cofactor contacts (21). Together, the notion that AR AF-2 binds coactivators weakly, and the fact that it will be occluded by the N-C interaction, has led to the suggestion that AR AF-2 does not play an active role in SRC recruitment.

Nonetheless, several lines of evidence suggest that AR AF-2 can contribute directly to coactivator recruitment in some contexts. First, the N-C interaction is required for optimal AR activity at some promoters, including those of *probasin*, *prostate-specific antigen*, and *C3*, but not at others, including those of the *sex-limiting protein* and the mouse mammary tumor virus-long terminal repeats (MMTV-LTRs) (16). Thus, AF-2 may be available for coactivator contacts in some circumstances. Second, mutation of AR AF-2 recognition sequences within target coactivators inhibits AR coactivation (16, 19, 20). Thus, mutation of FXXLF motifs within AR-specific coactivators such as ARA70 blocks their ability to interact with AR and potentiate AF-2 activity. More surprisingly, given the prevailing notion that AR AF-2 contacts with LXXLL motifs are weak, mutation of all three SRC LXXLL motifs inhibits AR coactivation when SRCs are overexpressed, when AR NTD FQNLF and WHTLF motifs are mutated, or when AR acts at promoters such as the MMTV-LTR.

It is important to understand the overall significance of particular AR to coregulator contacts, and the mechanism of these interactions, to develop strategies to inhibit AR activity in prostate cancer. In this study, we examine AR AF-2 interactions with target coactivators. Our studies confirm that AR AF-2 binds FXXLF motifs, but also show that AR AF-2 binds a subset of SRC LXXLL motifs with higher affinity and, further, that the same LXXLL motifs are required to mediate AR AF-2 activity. Crystal structures of AR-LBD in complex with native FXXLF and LXXLL peptides reveal the structural basis for these unusual coactivator binding preferences and may suggest new approaches to drug design.

#### EXPERIMENTAL PROCEDURES

**Protein Expression and Purification**—AR-LBD (residues 663–919) was expressed in *Escherichia coli* and purified to homogeneity using a modified version of previously published protocols (24). Bacterial cell preparations were grown at ambient or lower temperatures to high optical density at 600 nm (>1.00) in 2× LB supplemented with DHT. AR-LBD protein was expressed by induction with isopropyl 1-thio-β-D-galactopyranoside for 14–16 h at 15 °C before harvest and cell lysis by freeze-thawing and mild sonication. Purification involved an initial affinity chromatography step using a glutathione-Sepharose column, followed by thrombin cleavage of the GST affinity tag. Finally cation exchange chromatography with Sepharose SP afforded the purified protein. Our procedures differ from published work in that we use Sepharose SP for the second purification step instead of Fractogel SO<sub>3</sub>, which does not retain AR in our experiments.

**Peptide Library Synthesis**—Coregulator peptides consisting of 20 amino acids with the general motif of CXXXXXXXXLXX(L/A)(L/A)XXXXXXXX were constructed, where C is cysteine, L is leucine, A is alanine, and X is any amino acid. The sequences of all the coregulator peptides were obtained from human isoform candidate genes (SRC1/AAC50305, SRC2/Q15596, SRC3/Q9Y6Q9, and ARA70/Q13772). The peptides were synthesized in parallel using standard Fmoc chemistry in 48-well synthesis blocks (FlexChem System, Robbins). Preloaded Wang (Novagen) resin was deprotected with 20% piperidine in dimethylformamide. The next amino acid was then coupled using 2-(1H-benzotriazole-1-yl)-1,1,3,3-tetramethyluronium hexafluorophosphate (2.38 eq. wt.), Fmoc-protected amino acid (2.5 eq. wt.), and diisopropylethylamine (5 eq. wt.) in anhydrous dimethylformamide. Coupling efficiency was monitored by the Kaiser test. Synthesis then proceeded through a cycle of deprotection and coupling steps until the peptides were completely synthesized. The completed peptides were cleaved from the resin with concomitant side-chain deprotection (81% trifluoroacetic acid, 5% phenol, 5% thioanisole, 2.5% ethanedithiol, 3% water, 2% dimethylsulfide, 1.5% ammonium iodide), and crude product was dried down using a SpeedVac (GeneVac). Reversed-phase

chromatography followed by mass spectrometry (matrix-assisted laser desorption ionization time-of-flight/electrospray ionization) was used to purify the peptides. The purified peptides were then lyophilized. A thiol-reactive fluorophore, 5-iodoacetamidofluorescein (Molecular Probes), was then coupled to the N-terminal cysteine following the manufacturer's protocol. Labeled peptide was isolated using reversed-phase chromatography and mass spectrometry. Peptides were quantified using UV spectroscopy. Purity was assessed using liquid chromatography/mass spectrometry.

**Peptide Binding Assay**—Using a BiomekFX in the Center for Advanced Technology, AR-LBD was serially diluted from 100 μM to 0.002 μM in binding buffer (50 mM sodium phosphate, 150 mM NaCl, pH 7.2, 1 mM dithiothreitol, 1 mM EDTA, 0.01% Nonidet P-40, 10% glycerol) containing 150 μM ligand (dihydroxytestosterone) in 96-well plates. Then 10 μl of diluted protein was added to 10 μl of fluorescent coregulator peptide (20 nM) in 384-well plates yielding final protein concentrations of 50–0.001 μM and 10 nM fluorescent peptide concentration. The samples were allowed to equilibrate for 30 min. Binding was then measured using fluorescence polarization (excitation λ, 485 nm; emission λ, 530 nm) on an Analyst AD plate reader (Molecular Devices). Two independent experiments were assayed for each state in quadruplicate. Data were analyzed using SigmaPlot 8.0 (SPSS, Chicago, IL), and the *K<sub>d</sub>* values were obtained by fitting data to the equation,  $y = \min + (\max - \min) / (1 + (x/K_d)^{\wedge} \text{Hillslope})$ .

**GST Pull-down Assays**—Full-length SRC-2 (amino acids 1–1462) and AR NTD-DBD (amino acids 1–660) was expressed in a coupled transcription/translation system (TnT, Promega). AR-LBD (amino acids 646–919), or AR-LBD mutants, were expressed in *E. coli* strain BL21 as a GST fusion protein and attached to glutathione beads according to the manufacturer's protocol (Amersham Biosciences). Binding assays were performed by mixing glutathione-linked Sepharose beads containing 4 μg of GST fusion protein (estimated by Coomassie Plus protein assay reagent, Pierce) with 2 μl of <sup>35</sup>S-labeled SRC-2 or AR NTD-DBD in 20 mM HEPES, 150 mM KCl, 25 mM MgCl<sub>2</sub>, 10% glycerol, 1 mM dithiothreitol, 0.2 mM phenylmethylsulfonyl fluoride, 20 μg/ml bovine serum albumin, and protease inhibitors containing to a final volume of 150 μl. The bead mix was shaken at 4 °C for 1.5 h, washed three times in 200 μl of binding buffer. The bound proteins were resuspended in SDS-PAGE loading buffer, separated by using 10% SDS-polyacrylamide gel electrophoresis, and visualized by autoradiography.

**Cell Culture and Transfection Assays**—HeLa, DU145, and CV-1 cells were maintained in Dulbecco's modified Eagle's medium H-21 4.5 g/liter glucose, containing 10% steroid depleted fetal bovine serum (Invitrogen), 2 mM glutamine, 50 units/ml penicillin, and 50 mg/ml streptomycin. For transfection, cells were collected and resuspended in Dulbecco's phosphate-buffered saline (0.5 ml/4.5 × 10<sup>7</sup> cells) containing 0.1% dextrose, and typically 4 μg of luciferase reporter plasmid, 1 μg of AR expression vector or empty vector control, and 2 μg of pCMV-β-galactosidase. Cells were electroporated at 240 V and 960 microfarads, transferred to fresh media, and plated into 12-well plates. After incubation for 24 h at 37 °C with androgen or vehicle, cells were collected, and pellets were lysed by addition of 150 μl of 100 mM Tris-HCl, pH 7.8, containing 0.1% Triton X-100.

For transfections with full-length AR, the reporter gene utilized the Mouse Mammary Tumor Virus promoter fused to luciferase. For transfections with *GAL-AR-LBD*, *GAL-TR LBD*, and *GAL-CBP* fusions, the reporter contained five *GAL4* response elements upstream of a minimal promoter. LUC and β-galactosidase activities were measured using the Luciferase Assay System (Promega) and Galacto-Light Plus β-galactosidase reporter gene assay system (Applied Biosystems), according to the manufacturer's instructions.

**Crystallization, Structure Determination, and Refinement**—The complexes of SRC2–2, SRC2–3, SRC3–2, and ARA70 peptides and AR-LBD were prepared by mixing at 0 °C for 2 h, with variable ratios of peptide (3–10 mM) and protein (at about 4.5 mg/ml). Crystals were obtained by vapor diffusion methods (sitting-drop technique) using crystal screens from Hampton. The protein-peptide complex solution was mixed with the reservoir solution (0.8 M sodium citrate, 0.1 M Tris, pH 7.5 or pH 8.0), and concentrated against 300 μl of the reservoir. Crystals appeared after 1 day and grew to maximal dimensions after 4 days. After 4 days these crystals started to crack, so new crystallization trials were necessary to find additives that would stabilize the crystals. 0.3 μl of either 2.0 M NaCl, 1.0 M LiCl<sub>2</sub>, or 0.1 M EDTA were added to a 1-μl protein plus a –1-μl reservoir drop to stabilize AR-LBD crystals at room temperature.

Crystals for either AR-DHT or AR-DHT-peptide were transferred to a new drop containing 10% (v/v) of glycerol for cryoprotection. The crystals were then flash-cooled using liquid nitrogen and measured

TABLE I  
 Statistics for data collection and refinement

	AR-SRC2-3	AR-SRC2-2 (non-helical)	AR-SRC3 (RAC3)	AR-ARA70
Molecules/asymmetric unit	1	1	1	1
Space group	P2 <sub>1</sub> 2 <sub>1</sub> 2 <sub>1</sub>			
Cell constants a/b/c (Å)	54.49/67.37/70.52	55.60/67.58/69.32	53.06/66.83/71.07	55.68/66.42/68.25
Resolution (Å)	2.07	1.66	2.7	2.3
Reflections measured	393,765	511,617	375,686	458,173
Unique reflections	16,416	35,221	17,753	13,713
Overall completeness (%)	97.2	91.7	90	92.8
Outermost shell completeness (%)	94.3	88.0	83.8	85.2
R merge (%) <sup>a</sup>	4.4	6	5.5	5
Reflections used refinement	15,915	32,260	6,151	10,881
Resolution range (Å)	24–2.07	25–1.66	25–2.7	24–2.3
R factor (%) <sup>b</sup>	19.8	21.1	25.3	22.8
R free (%) <sup>c</sup>	23.2	24.8	31.5	25.8
Number of water molecules	160	361	100	106
Matthews coefficient	2.157	2.116	2.100	2.104
Solvent content (%)	43	42	41.5	40
Ramachandran plot most favored (%)	93	92	82	92
Ramachandran plot allowed (%)	7	7	17	8

<sup>a</sup> R merge (%) =  $\sum_{hkl} |I| - I / \sum_{hkl} |I|$ .

<sup>b</sup> R factor (%) =  $\sum_{hkl} |F_o| - |F_c| / \sum_{hkl} |F_o|$ .

<sup>c</sup> The R free set contained 5% of total data.

using the synchrotron radiation at the 8.3.1 beam line at the Advanced Light Source (Berkeley). Crystals containing SRC2-3, SRC2-2, and SRC3-2 diffracted to 2.07, 1.66, and 2.7 Å, respectively. Cocrystals of ARA70 peptide with AR-LBD were also grown, and a complete data set was obtained at 2.3 Å resolution. All the crystals belong to space group P2<sub>1</sub>2<sub>1</sub>2<sub>1</sub> (orthorhombic) and contain one molecule per asymmetric unit.

The diffraction data were integrated and scaled using the computer program ELVES ([ucxray.berkeley.edu/~jamesh/elves/](http://ucxray.berkeley.edu/~jamesh/elves/)) (25). Molecular replacement solutions for all AR-LBD peptide structures were obtained using rotation and translation functions from Crystallography & NMR Systems (CNS, [cns.csb.yale.edu/v1.1/](http://cns.csb.yale.edu/v1.1/)) (26).

The first electron maps calculated after the rigid body refinement that followed the molecular replacement displayed clear electron density for the peptides. During the improvement of the protein model, the Fourier maps revealed better electron density for more flanking residues of the peptides. The electron density for the peptide was always modeled as a short  $\alpha$ -helix. However, refinement of the SRC2-2 peptide as an  $\alpha$ -helix was unsuccessful as such peptide does not adopt such helical conformation on the AR-LBD AF2 surface. Further SRC2-2 model building and refinement were not pursued as an  $\alpha$ -helix. A composite omit map not including the peptides was calculated in the last steps of refinement for overcoming phase bias for each one of the complexes. This map was calculated omitting 5% of the total model allowing a better tracing of the peptide and permitted to visualize more residues that were not visible in the  $2F_o - F_c$  map. Model building was done using the program QUANTA (Accelrys Software, [www.accelrys.com/quanta/](http://www.accelrys.com/quanta/)) monitored using the free R factor. Calculation of the electron density maps and crystallographic refinement was performed with CNS using the target parameters of Engh and Huber (27). Several cycles of model building, conjugate gradient minimization, and simulated annealing using CNS resulted in structures with good stereochemistry. A Ramachandran plot shows that most of the residues fall into the most favored or additionally favored regions. The statistics for data collection and refinement of each one of the data sets can be found in Table I.

The structures have been deposited with the Protein Data Bank (PDB) and assigned the following ID numbers: AR-DHT-SRC2-3, PDB 1T63, RCSB RCSB022358; AR-DHT-ARA70, PDB 1T5Z, RCSB RCSB022354; AR-DHT-SRC2-2, PDB 1T65, RCSB RCSB022360; and AR-DHT-SRC3-2, PDB 1XJ7, RCSB RCSB030414.

## RESULTS

**AR AF-2 Binds SRC-2 NR Boxes 1 and 3 with High Affinity**—To understand the unusual spectrum of AR AF-2 coactivator interactions, we measured binding of the AR-LBD to a library composed of NR boxes from known coactivating proteins, including both SRCs and AR specific coactivators (Fig. 1A). Such peptides are known to bind to other NRs with equal affinity to the full-length coactivator (28). AR-LBD interacted to varying degrees with all of the peptides containing an

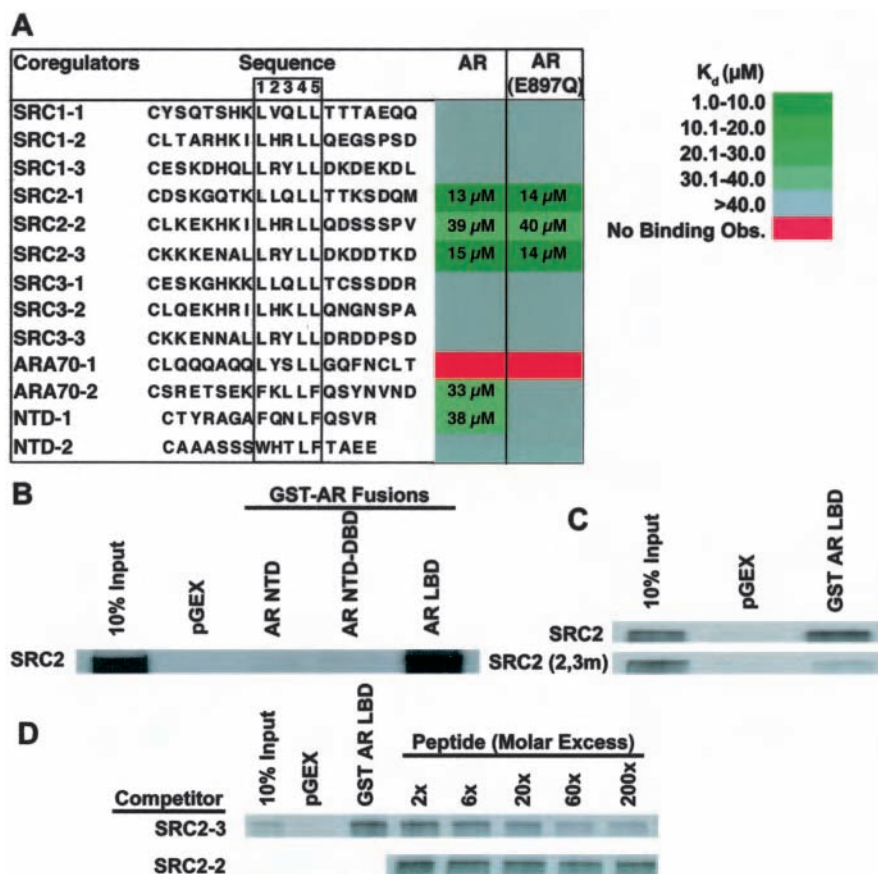
LXXLL motif tested except the first NR box of ARA70. As expected, AR-LBD interacted with FXXLF sequences present in ARA70 and the AR NTD (21, 29) fairly strongly with measurable dissociation constants of  $33 \pm 3.3$  and  $38 \pm 3.8 \mu\text{M}$ , respectively. Surprisingly, AR also recognized a subset of NR boxes from the SRC family (30). Specifically, peptides of the first (SRC2-1,  $K_d = 13 \pm 2.1 \mu\text{M}$ ) and third (SRC2-3,  $K_d = 15 \pm 1.2 \mu\text{M}$ ) NR boxes of SRC-2 (GRIP1/TiF-2/N-CoA-2) bound strongly to AR, followed in affinity by FXXLF motifs. The second NR box of SRC3 (RAC3/pCIP/p300/CBP-interacting protein) was also recruited to AR ( $K_d = 39 \pm 5 \mu\text{M}$ ). The remaining NR boxes from SRC-1, SRC-2, and NTD weakly interacted with AR either nonspecifically or with binding affinities above the assay range ( $>40 \mu\text{M}$ ). Control experiments with the same sequences in which LXXLL or FXXLF had been converted to LXXAA or FXXAA revealed the binding was dependent upon the intact triad of hydrophobic amino acids (not shown). This substitution has been shown previously to abolish interactions with NR (31).

Pull-down experiments confirmed that the AR-LBD bound SRC2 strongly, as opposed to the AR NTD or NTD-DBD (Fig. 1B). Furthermore, AR-LBD interactions with SRC2 were inhibited by mutation of SRC2 boxes 2 and 3 (Fig. 1C), or by increasing concentrations of SRC2-3 peptide (Fig. 1D). Thus, AR-LBD binds FXXLF motifs but also binds a subset of classic NR box peptides with comparable or higher affinities. Moreover, the preference of AR for individual LXXLL motifs is different from that observed with other NRs, such as the estrogen receptor and thyroid receptors (TRs), which bind box 2 in each of the three SRCs with high affinity (28, 32–34).

**AR-dependent Transactivation Requires SRC2 Boxes 1 and 3**—Next, we examined the ability of SRC2 to coactivate isolated AR AF-2 and requirements for individual LXXLL motifs in this effect. As expected, a fusion protein containing the AR-LBD (amino acids 646–919) linked to the yeast GAL4 DNA binding function conferred androgen-dependent transcriptional activity on a GAL4-responsive reporter in several cell types, and simultaneous expression of SRC2 strongly enhanced AR AF-2 activity (Fig. 2A). Overall, AR AF-2 activity was more potent than that of AR AF-1 in HeLa and DU145, particularly in the presence of SRC2, and about 20–30% as potent as that induced by TR and estrogen receptor  $\alpha$  LBDs, which bind a wider range of SRCs (see supplemental material). As expected from prior results, AF-1 dominates signaling in CV-1 cells, the effects of

FIG. 1. The androgen receptor-ligand binding domain (AR-LBD) binds a subset of steroid receptor coactivator (SRC) nuclear receptor interaction motifs (NR boxes).

A, sequences of relevant NR boxes and relative equilibrium affinities of these NR boxes for binding to AR-LBD and a mutant AR-LBD (E897Q) in which one charge clamp residue has been neutralized. The binding affinities were determined using fluorescence polarization with fluorescently labeled NR box peptides. The coregulator peptides are listed in the left column where SRC1-1, SRC1-2, and SRC1-3 represent the first, second, and third NR boxes in SRC1, respectively. Each color represents a unique  $K_d$  range as defined by the legend in the bottom right-hand corner. For coregulator peptides that displayed saturated binding curves with AR, the actual  $K_d$  values are listed. The gray color represents conditions where some interaction of coregulator peptides with AR was observed, however, saturating binding curves were not achieved in the protein concentration range studied. B, pull down of SRC2 by GST fusions of AR domains. C, effects of mutation of NR boxes of SRC2 on the pull down by the GST fusion of the AR-LBD. SRC2 (2,3m) indicates the SRC2 protein where NR boxes 2 and 3 have been mutated from LXXLL to LXXAA. D, competition for binding of SRC2 by NR box peptides during a pull down of SRC2 by the GST fusion of the AR-LBD.



AF-1 and AF-2 are balanced in DU145 cells, and AF-2 dominates in HeLa cells (35, 36). Thus, our results are consistent with the notion that AR AF-2 is potent (35, 36) and contradict the notion that AR AF-2 has little or no intrinsic activity.

Mutation of individual SRC-2 NR boxes to LXXAA reveals a requirement for boxes 1 and 3 to provide full AR AF-2 activity, both in HeLa (Supplemental Fig. S1) and in DU145 cells (Fig. 2B). In contrast, NR box 2 of SRC2 is required to mediate TR $\beta$  AF-2 in HeLa (Supplemental Fig. S1), consistent with our own determinations of the affinity of SRC2 NR boxes for TR $\beta$  and with previous results (8, 28). Moreover, each mutant SRC showed equivalent ability to enhance activity of CBP AD2, which binds the SRCs at a distinct locus and in a manner that is independent of NR boxes (Supplemental Fig. S1) (8). Thus, the NR box mutations that reduce AR transactivation do not affect other elements of SRC2 activity.

NR boxes also played a role in the ability of SRC2 to coactivate full-length AR (Fig. 2C). For these experiments, we utilized an MMTV-LTR-driven reporter, because the N-C interaction is dispensable for optimal AR activity at this promoter, and HeLa cells, because AR AF-2 activity is relatively strong in this cell type. Here, SRC-2 enhancement of AR signaling was lessened when the NR boxes were mutated (17–19, 37). In particular, mutation of the third NR box (SRC2-3) abrogated SRC-2 action (see Fig. 4). Thus, there is exact congruence between the affinity of particular NR boxes for AR and their requirement for transactivation in the context of the isolated AR-LBD and full-length AR.

**X-Ray Structures of AR-LBD in Complex with Coregulator Peptides Reveal the Atomic Basis for AR Selective Binding to SRC2 NR Boxes and ARA70**—To determine how AR binds aromatic-rich coactivator domains and a particular subset of SRC NR boxes, we obtained crystal structures of the AR-LBD in complex with ARA70-2, SRC2-2, SRC2-3, and SRC3-2. As expected by analogy with other NR AF-2s, SRC2-3, SRC3-2,

and ARA70 peptides bind as a short  $\alpha$ -helix into the L-shaped hydrophobic cleft normally utilized by coactivators. On the contrary, the low affinity peptide SRC2-2 was seen to bind to AR-LBD AF through an energetically non-favorable conformation that could not be modeled as an  $\alpha$ -helix. Comparison of the structures also reveals features that explain the ability of the AR AF-2 to bind to both LXXLL and FXXLF motifs.

The AR-LBD crystal structure in complex with the SRC2-3 peptide KENALLRYLLDKDD (14-mer) has been solved to 2.07 Å resolution. Thirteen residues of this peptide are clearly defined in the electron density, and the interaction buries 1322 Å<sup>2</sup> of predominantly hydrophobic surface area from both molecules. Our structure shows that SRC2-3 hydrophobic motif binds in nearly the same manner as previously stated in other NRs with LXXLL p160 coactivator motifs (32, 38–40). The residues located N-terminally from the first Leu residue (residue +1) are termed -1, -2, and so on, whereas the residues C-terminal from Leu+1, are termed +2, +3, etc. The core hydrophobic motif of the peptide (residues +1 to +5) forms a short  $\alpha$ -helix that binds in the groove formed by helices 3, 4, 5, and 12. The LBD interacts primarily with the hydrophobic face of the SRC2-3 peptide  $\alpha$ -helix formed by the side chains of the three LXXLL motif leucines (Leu-923, Leu-926, and Leu-927). The side chain of Leu-923 is embedded within the groove and forms van der Waals contacts with the side chains of Val-716, Met-734, and Asn-738. The side chain of Leu-927 is also isolated within the groove and makes van der Waals contacts with the side chains of Gln-733 and Met-734. The side chain of the second NR box 3 leucine (Leu-926), makes van der Waals contacts with the side chains of Val-716 and Met-894. The LBD residues implicated in hydrophobic contacts with the peptide are valines 716, 730, and 901, methionines 734 and 894, glutamines 733 and 738, Ile-898, and the non-polar parts of Asp-731 and Glu-893 and Glu-897.

The main-chain carbonyl groups of residues Leu-927, Asp-

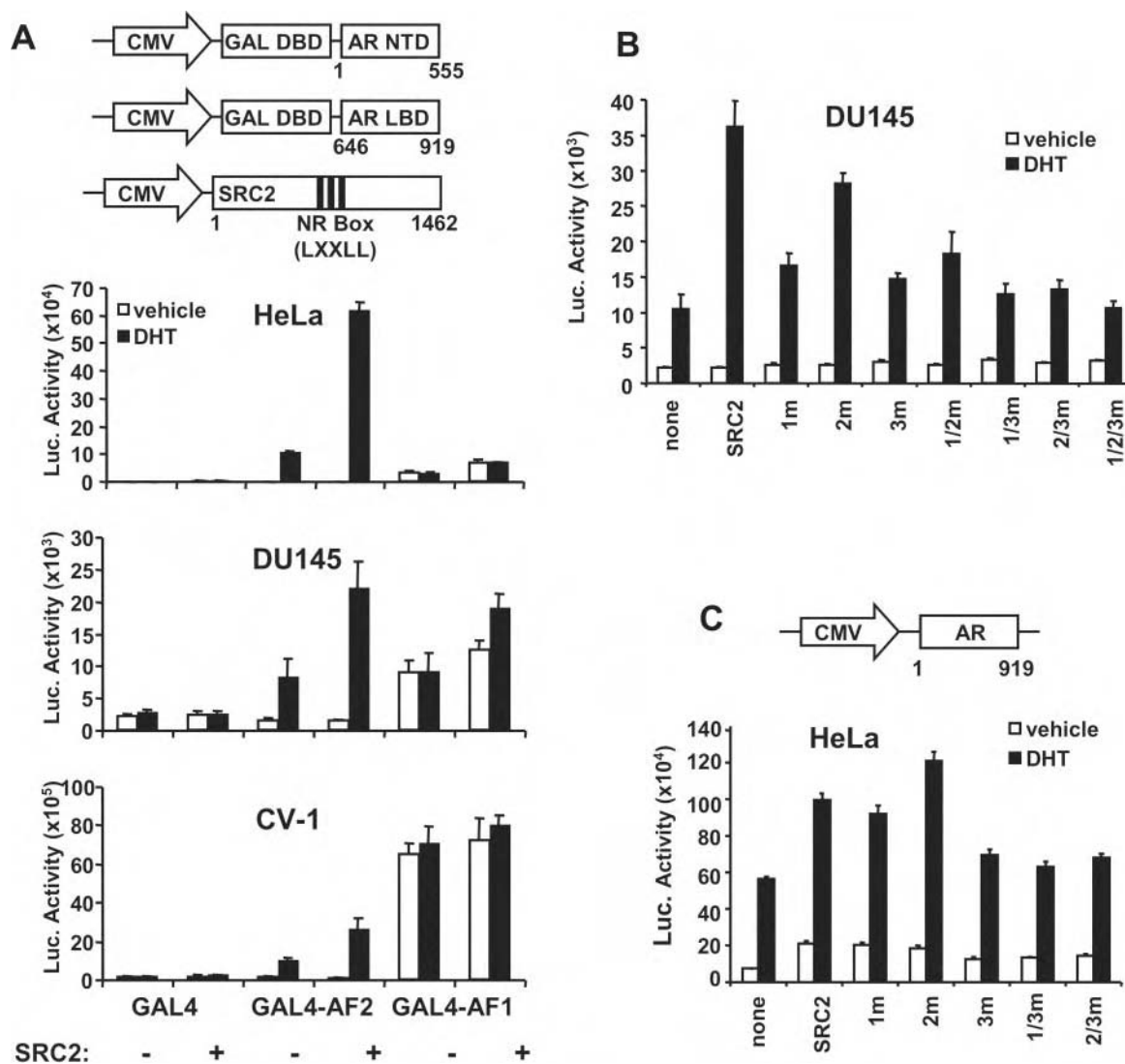


**FIG. 2. Transcriptional activation by AR, AR-NTD, and AR-LBD constructs and the enhancement of activation by SRC constructs.** A, transcriptional activation of a GAL4-luciferase reporter construct by fusions of GAL4 DNA binding domain with AR-NTD AF-1 or LBD AF-2 domains in three cell lines. In all cell lines, AR-LBD induces signaling in response to DHT, and this effect is enhanced by expression of SRC2. The level of AR-NTD-driven expression varies from cell line to cell line but remains constant in the presence or absence of both DHT and SRC2. B, the effects of mutation of SRC2 NR boxes 1 through 3 upon signaling by GAL4-AR-LBD constructs from a GAL-driven luciferase reporter. Mutations of SRC2-1 and SRC2-3 both significantly reduce potentiation of transactivation by AR. These mutational effects correlate with the observed relative affinities of the NR boxes for the receptor. C, activation of transcription at an MMTV-luciferase reporter by full-length AR and the effects of coexpression of SRC2 and mutants. Mutation of SRC2-3 significantly reduces potentiation of transactivation by AR.

930 and Asp-931 from the SRC2-3 peptide also interact with Lys-720, which is highly conserved in NRs and comprises the upper part of a charge clamp that stabilizes the  $\alpha$ -helical NR box peptide conformation. However, contrary to predictions made on the basis of mutagenic analysis of AR surface residues (30), and comparisons with a glucocorticoid receptor/SRC2-3 structure (39), the SRC2-3 peptide does not form any hydrogen bonds to the second highly conserved charge clamp residue, Glu-897 on Helix 12. Instead, the peptide engages in hydrophobic contacts with Glu-897, and the distance to the three unpaired amide NH of the peptide helix is 5 Å, so electrostatic stabilization is possible. The peptide also engages in hydrogen bonding to seven water molecules in its vicinity. Residue Asp-928 located at position +6 adopts two different conformations. However, neither Asp-928 (+6) nor Arg-924 (+2) interact with charged residues on the AR surface that comprise a second charge clamp, again contrary to predictions made on the basis of a glucocorticoid receptor/SRC2-3 structure (39). Nonetheless, the SRC2-3 peptide displays clear electron density in the current structure for five residues N-terminal to the core hydro-

phobic motif and for four more residues C-terminal to the same motif, therefore displaying significantly greater electron density than any other NR box peptide in complex with a NR LBD to date.

The AR-LBD crystal structure in complex with the SRC3-2 peptide HKKLLQLLT (9-mer) has been solved to 2.7 Å resolution. All nine residues of this peptide are clearly defined in the electron density, and the interaction buries 1052 Å<sup>2</sup> of predominantly hydrophobic surface area from both molecules. Our structure shows that SRC3-2 hydrophobic motif binds in nearly the same manner as previously stated for SRC2-3. The LBD residues implicated in hydrophobic contacts with the peptide are valines 716 and 730, methionines 734 and 894, Ile-898, and the non-polar parts of Glu-897 and Lys-720, unexpectedly. SRC3-2 peptide is shorter C-terminally than SRC2-3 and does not make any hydrogen bonds with Lys-720. Surprisingly, another basic residue, Arg-726 adopts in this complex the C-terminal capping role stabilizing the peptide  $\alpha$ -helix. This polar interaction is not present in the other peptide-AR-LBD complexes described in this report. This crystal structure shows

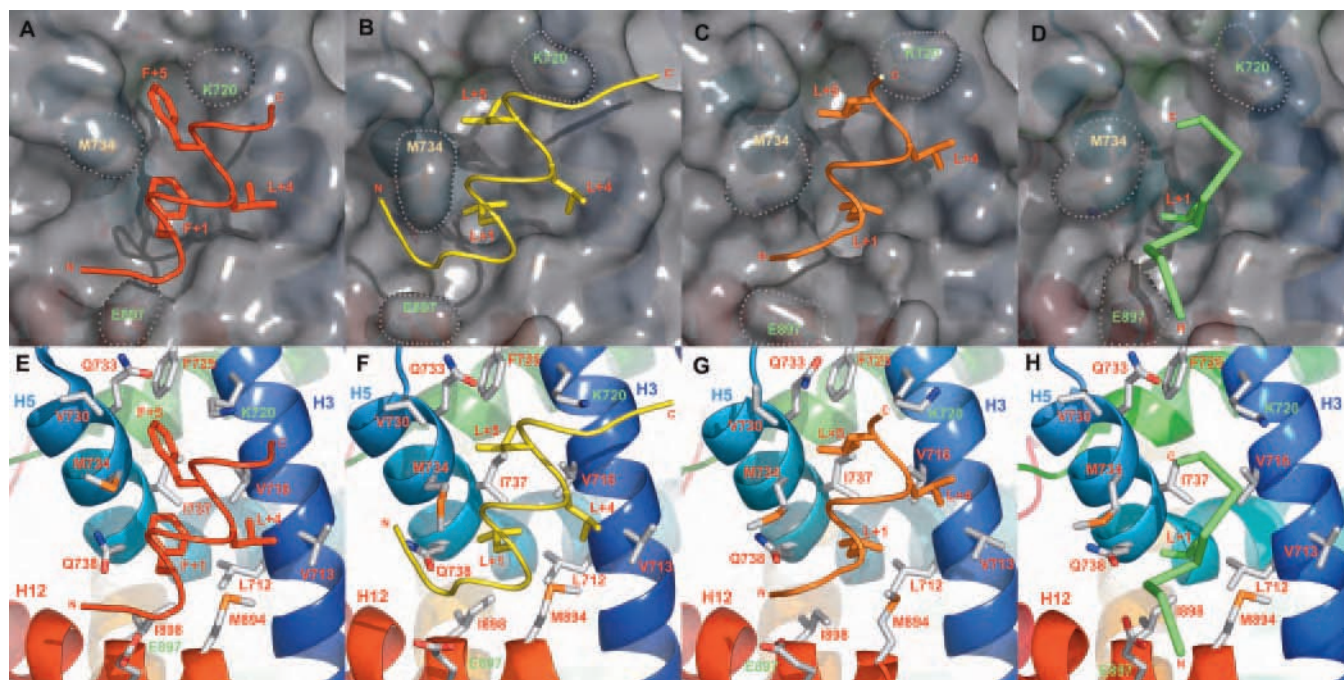


**FIG. 3. Associations of the AR-LBD with coactivator domains determined by x-ray crystallography (A–H).** Close-up views of the interaction between ARA70, SRC2-3, SRC2-2, and SRC3-2 peptides with AR-LBD AF2. The nuclear receptor AF-2 transactivation function is ascribed to a surface-exposed hydrophobic cleft comprising residues from helices 3 (H3, dark blue), 5 (H5, pale blue), and 12 (H12, red), as can be clearly seen in the bottom figures (E–H). A–H, the helix backbone of peptides from ARA70 (RETSEKFKLLFQSYN) (left, red), SRC2-3 (KENALLRYLLDKDD) (middle left, yellow), and SRC3-2 (HKKLLQLLT) (middle right, orange) are shown, and the non-helical SRC2-2 peptide backbone (KHKILHRLQLDSS) (right, green) can be seen. AR-LBD is represented by a solid semi-transparent surface (gray) in the top figures (A–D). The side chains of the motif hydrophobic residues Phe+1/Leu+1, Leu+4, and Phe+5/Leu+5 of the peptides are shown as stick models. Helix 12, with its Glu-897 side chain, stabilizes the N terminus of the ARA70 peptide, but not those of the SRC peptides. On H3, the side chain of Lys-720 is shown capping the C terminus of ARA70 and SRC2-3 peptides (E and F). B, the side chains of the AR-LBD residues contacting the peptides are depicted as stick models. ARA70: The triad compressed by the Phe aromatic side chains and Val-716 and Val-730, Met-734, Ile-737, and the hydrophobic segment of Glu-893. The Leu side chains of SRC2-3 and SRC3-2 fit loosely into a flat hydrophobic pocket comprising the side chains of three valines, 716, 730, and 901, methionines 734 and 894, glutamines 733 and 738, Asp-731, and Glu-897. The accommodation of the bulkier Phe residues of ARA70 is accompanied by the rearrangements of Met-734, Glu-897, and Lys-720 predominantly (indicated by gray dots on the surface representation of AR). D and H, SRC2-2 does not bind to AR-LBD AF2 in an helical conformation, and, apart from Leu+1, the rest of the peptide cannot be superimposed to the other SRC peptides shown in this report. All the figures were generated with Pymol (42).

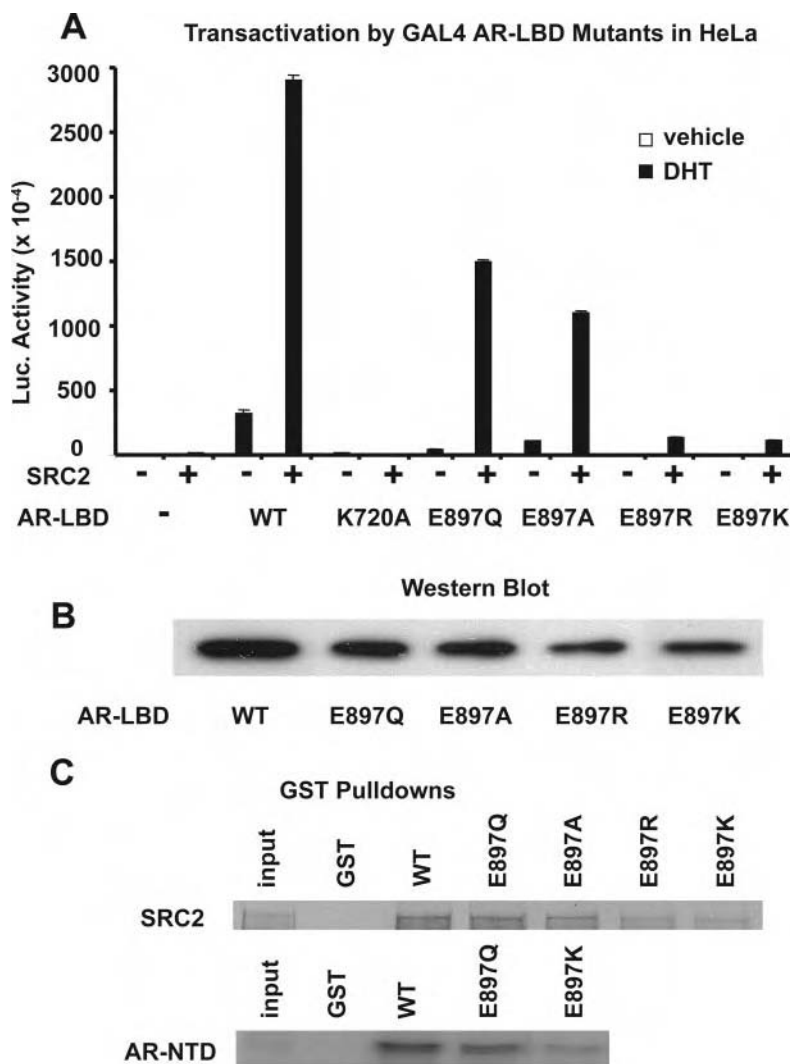
traceable electron density for six residues located at the protein N terminus that correspond to some residues of the hinge region of AR, and this is the first time that such residues are visible in an electron density. Those residues are in a random coiled-coil conformation.

The AR-LBD complex with the SRC2-2 peptide comprises the following sequence, KHKILHRLQLDSS (13-mer). Despite the fact that the crystal of SRC2-2 diffracted to 1.66 Å, the electron density that accounts for the peptide was more difficult to interpret and discontinuous suggesting that its affinity for AR-LBD is weak. It was surprising to state that SRC2-2 adopts two different conformations. The first was very similar to the SRC2-3 peptide and was modeled as a short  $\alpha$ -helix. However, a second conformation, more similar to a coiled-coil, could be interpreted and refined (referred as the non-canonical conformation). In the SRC2-3-like conformation, interpretable electron density starts at the first leucine of the SRC2-2 peptide and finishes at Gln-928. Building this peptide from the box 3 conformation leaves only Leu-923 correctly placed within the weak electron density, His-924 bulges out of the density, and only the main chain returns to the electron density for Arg-925, Leu-926, Leu-927, and Gln-928. On the other hand, if NR box 2 is built and refined as a random coil, interpretable and continuous electron density starts at residue His-920 until Leu-926. From all these residues, only Leu-923 is completely defined, and for the rest of the six residues only the main chain is defined in the electron density, leaving the side chains unseen. NR box 2 in Box3-like conformation buries 850 Å<sup>2</sup> of predomi-

nantly hydrophobic surface area, whereas NR box 2 in random coil conformation buries 792 Å<sup>2</sup> of predominantly hydrophobic surface area from both molecules.

In the Box 3-like conformation, the side chain of Leu-923 is embedded within the groove and forms van der Waals contacts with the side chains of Leu-712, Asn-738, Met-894, and Ile-898. The side chain of Leu-927 makes van der Waals contacts with the side chain of Met-734. The side chain of the second NR box 2 leucine (Leu-926), makes van der Waals contacts with the side chain of Val-716. The LBD residues implicated in hydrophobic contacts with the peptide are Val-716, methionines 734 and 894, Gln-738, Ile-898, and the non-polar part of Glu-893. The residue Leu-926 interacts with Lys-720, through its main chain carbonyl group. In the non-canonical conformation, Leu-926 also interacts with Lys-720, through its main chain carbonyl group. NR box 2 peptide does not form any hydrogen bonds to the second highly conserved charge clamp residues, Glu-897, in either conformation. However, His-920 could be bonded to Glu-893. Except for three N-terminal residues that are disordered, the position and interactions of the ARA70 FXXLF peptide with the AR surface more closely recapitulate the binding mode observed in structures of ternary complexes of SRC LXXLL motifs with hormone-bound NR LBDs (Fig. 3, A and C) (32, 38–40). The triad of aromatic side chains (FXXLF) that forms the hydrophobic face of the coactivator helix fits tightly into a deep narrow pocket. In addition, charged residues at either end of the cleft, Glu-897 and Lys-720, cap the helix (the “charge clamp”). The fully engaged interaction is

**FIG. 4. Role of the binding pocket and charge clamp residues of the AR-LBD AF-2 in interaction with cofactors and potentiation of transcriptional activation by a GAL4-AR-LBD construct.** A, removing the charge at Lys-720 or reversing the charge at Glu-897 (the positive and negative ends of the "charge clamp" that stabilizes helix dipole for the NR box) markedly reduces the potentiation of transcriptional activation by GAL AR-LBD by SRC2 in HeLa cells. However, neutralization of the charge at Glu-897 has modest effects on transcriptional activation. B, Western blot demonstrating that all Glu-897 mutants are expressed at similar levels in HeLa cells during the transactivation experiments. C, as expected from the peptide binding data (Fig. 1A), neutralization of charge at Glu-897 has no discernable effect upon the interaction of SRC2 as measured by GST Pull-down. Similarly, there is a modest reduction in binding of AR NTD by E897Q. However, reversal of charge (E897K) strongly reduces binding of both SRC2 and AR NTD.



manifested in the tight binding of this coactivator and its strong transactivation.

**The AR-LBD Charge Clamp Plays Coregulator Selective Roles in Transactivation and Binding**—One unexpected feature of our crystal structures is that the two residues that comprise the canonical AR-LBD charge clamp (Lys-720 on helix 3 and Glu-897 on helix 12) interact differently with FXXLF and LXXLL peptide backbones. Although previous studies suggested that Glu-897 was absolutely required for SRC binding, our structures revealed that Glu-897 is fully engaged with the carbonyl backbone of the FXXLF peptide, but not that of the LXXLL peptide. Similar arrangements were also observed in crystals of the AR-LBD in complex with artificial FXXLF and LXXLL peptides derived from phage display (41).

To understand the apparent discrepancy between the reported requirement for Glu-897 in AR activity and its lack of contact with the LXXLL motif of SRC2-3 in the crystal structure, we examined the effects of a series of charge clamp mutations on isolated AR AF-2 activity *in vivo* (Fig. 4A) and coregulator binding *in vitro* (Fig. 1A). As expected, a mutation within the upper charge clamp residue (Lys-720 → Ala) inhibited AR AF-2 activity (Fig. 4A) and prevented the recruitment of SRC2 (Fig. 4C). The reversal of the normal negative charge at Glu-897 by introduction of a positive charge (Glu-897 → Lys and Glu-897 → Arg) had the same effect, probably due to repulsion of the charged NR box (30, 35). However, AR-LBDs bearing mutations that neutralized or lessened electrostatic potential at Glu-897 (Glu-897 → Ala and Glu-897 → Gln)

retained significant AF-2 activity, especially in the presence of SRC2 (Fig. 4A) (9). These same mutants had no discernable effects upon recruitment of SRC2 (Fig. 4C) and a modest effect on recruitment of the AR NTD. This is in keeping with the effects of the Glu-897 → Gln mutation on NR box peptide recruitment (Fig. 1A). Western blotting of cell extracts confirmed that these differences in transcriptional activity were not related to differential expression of the AR-LBD mutants. Thus, the lower charge clamp residue (Glu-897) is dispensable for SRC-2 binding but required for ARA70 binding, exactly paralleling the requirement for this residue observed in both of our crystal structures.

#### DISCUSSION

In this report, we examined the binding of AR AF-2 to a range of target motifs within potential AR coactivators, confirmed the functional consequence of these interactions, and determined how AR AF-2 binds selectively to particular motifs. Our results confirm that AR AF-2 recognizes FXXLF motifs derived from the AR NTD and ARA70 with moderate affinity (<40 μM) but also show that AR binds some LXXLL motifs, particularly SRC2-1 and SRC2-3, with higher affinity (<10 μM). The discovery that AR AF-2 binds strongly to selected LXXLL motifs is surprising, but several lines of evidence confirm the importance of these interactions. Thus, bacterially expressed AR-LBD binds SRC2 strongly, as compared with TRβ AF-2 and AR AF-1, and these interactions are dependent upon NR boxes. Moreover, isolated AR AF-2 activates tran-

scription relatively strongly and does so in a manner that is potentiated by SRC2 and dependent upon SRC2-1 and SRC2-3. Finally, SRC2 LXXLL motifs were required for coactivation of full-length AR; at least at the MMTV promoter. Thus, AR AF-2 binds FXXLF motifs, but can also make important contacts with a subset of coregulator LXXLL motifs. AR therefore has the potential to activate transcription in an analogous manner to other NRs.

To understand the unusual selectivity of AR AF-2 for target coactivator motifs, we solved the structures of the AR-LBD in complex with an FXXLF motif derived from ARA70 and both high affinity (SRC2-3) and low affinity (SRC2-2) AR interacting motifs. Our structures indicate that the ARA70 FXXLF motif occupies a similar position to those of other coregulator NR box peptides in complex with LBDs of other NRs. Comparisons of each of the ternary complexes with each other, and with our own structures of AR in the absence of an associated peptide (not shown), reveal a striking rearrangement of the AF-2 surface that explains the ability of AR to accommodate the bulky hydrophobic side chains of the FXXLF motifs. Movements of Lys-720, Met-734, and Glu-897 create the deeper pockets and enhanced electrostatics allowing the binding of the ARA70 peptide (see Fig. 3). Similar rearrangements were also observed in crystals of AR-LBD in complex with artificial FXXLF and LXXLL peptides derived from phage display (41). Of these residues, Met-734 is relatively unique among the NR superfamily, and only conserved at an equivalent position within the glucocorticoid receptor LBD. Thus, the presence of Met-734 probably explains the unique capacity of the AR AF-2 surface to bind accommodate motifs with bulky hydrophobic side chains.

Crystal structures of AR-LBD in complex with SRC2-3 and SRC2-3 suggest an alternate explanation for the ability of AR AF-2 to discriminate between different LXXLL motifs. The SRC2-3 and SRC2-2 LXXLL motifs, by contrast to the ARA70 FXXLF motif and a variety of NR box peptides in complex with a variety of NR LBDs, are translated by about 2 Å in the cleft, toward helix 3. Overall, this unusual positioning disrupts the electrostatic stabilization characteristic of most NR/NR box interactions, likely explaining reduced AR binding to most LXXLL motifs. However, for SRC2-3, the high degree of negative charge in the four residues following the motif (sequence DKDD) interacts with positively charged patches on the receptor surface. In fact, these portions of the structure are better ordered than in all previous NR-coactivator complexes and are not visible in AR-LBD structures with the SRC2-2 peptide, which binds the AR-LBD with lower affinity. This influence offsets suboptimal electrostatics and explains the selective binding of AR AF-2 to SRC2-3. Thus, AR discriminates between cofactor NR box motifs by making auxiliary contacts outside of the core LXXLL motif. Interestingly, the ARA70 peptide is also relatively well ordered, about 12 of 15 amino acids are visible in our crystal structure. Although it has been previously suggested that NR LBDs may discriminate between target motifs by contacting residues that flank the hydrophobic LXXLL core (28, 31), our studies provide the first description of a structural basis for this effect.

AR AF-2 has the potential to participate in transcriptional activation in several ways, but the relative importance of different modes of AR AF-2 action are not yet clear. The N-C interaction is required for optimal AR action at a variety of androgen-regulated promoters, including those of prostate-specific genes such as *PSA* and *probasin*, suggesting that AF-2 mediates intramolecular interactions in these contexts. We predict that AR AF-2 could participate in coactivator binding in several contexts, including in the presence AR specific coactivators that contain FXXLF motifs, in conditions of SRC2 over-

expression, and at promoters that resemble the MMTV-LTR. The requirement for AR AF-2 in growth of prostate cancer cells has not been rigorously addressed, but it is interesting to note that SRC2 enhancement of the androgen-dependent G<sub>1</sub> to S transition in LNCaP prostate tumor cells is dependent upon the integrity of the SRC2 NR box region (which binds AF-2) and independent of the SRC2 C terminus (which binds AR AF-1) (10). Perhaps AR AF-2 contacts with SRC LXXLL motifs will prove to be relevant for cell cycle progression.

In conclusion, AR has a potent AF-2 that drives the cell's expression program by binding FXXLF motifs and selected LXXLL motifs. The receptor uses the same general coactivator binding mechanisms as other NRs, by providing a dimorphic cleft that facilitates interaction with aromatic amino acids in addition to leucines. The ability of the AR surface to rearrange to interact with FXXLF motifs is unique among transcription factors and represents a gain of function relative to other structurally defined interactions in the family. Most NRs are unable to accommodate bulky side chains in the binding domains of the coactivators, and the dyadic recognition of AR has enabled development of more complex control mechanisms involving the NTD and the use of specialized subsets of coactivators. Most importantly, the new function *does not* come at the cost of a loss of ability to interact productively with SRCs. AR AF-2 interactions with SRCs are likely to be physiologically relevant, particularly in certain forms of prostate cancer.

**Acknowledgments**—We thank Eugene Hur, Luke M. Rice, Elena Sablin, and Maia Vinogradova for useful discussions and James Holton, Corie Ralston, and Advanced Light Source beamline staff for assistance in data collection and processing.

#### REFERENCES

- Lee, H. J., and Chang, C. (2003) *Cell Mol. Life Sci.* **60**, 1613–1622
- Liu, P. Y., Death, A. K., and Handelsman, D. J. (2003) *Endocr. Rev.* **24**, 313–340
- Legros, J. J., Charlier, C., Bouillon, G., and Plomteux, G. (2003) *Ann. Endocrinol. (Paris)* **64**, 136
- Gregory, C. W., He, B., Johnson, R. T., Ford, O. H., Mohler, J. L., French, F. S., and Wilson, E. M. (2001) *Cancer Res.* **61**, 4315–4319
- Culig, Z., Klocker, H., Bartsch, G., and Hobisch, A. (2002) *Endocr. Relat. Cancer* **9**, 155–170
- Santos, A. F., Huang, H., and Tindall, D. J. (2004) *Steroids* **69**, 79–85
- Balk, S. P. (2002) *Urology* **60**, 132–138; discussion 138–139
- Ding, X. F., Anderson, C. M., Ma, H., Hong, H., Uht, R. M., Kushner, P. J., and Stallcup, M. R. (1998) *Mol. Endocrinol.* **12**, 302–313
- Berrevoets, C. A., Doesburg, P., Steketee, K., Trapman, J., and Brinkmann, A. O. (1998) *Mol. Endocrinol.* **12**, 1172–1183
- Shang, Y., Myers, M., and Brown, M. (2002) *Mol. Cell* **9**, 601–610
- Gregory, C. W., Fei, X., Ponguta, L. A., He, B., Bill, H. M., French, F. S., and Wilson, E. M. (2004) *J. Biol. Chem.* **279**, 7119–7130
- Blaszczek, N., Masri, B. A., Mawji, N. R., Ueda, T., McAlinden, G., Duncan, C. P., Bruchovsky, N., Schweikert, H. U., Schnabel, D., Jones, E. C., and Sadar, M. D. (2004) *Clin. Cancer Res.* **10**, 1860–1869
- Needham, M., Raines, S., McPheat, J., Stacey, C., Ellston, J., Hoare, S., and Parker, M. (2000) *J. Steroid Biochem. Mol. Biol.* **72**, 35–46
- Leo, C., and Chen, J. D. (2000) *Gene (Amst.)* **245**, 1–11
- Alen, P., Claessens, F., Schoenmakers, E., Swinnen, J. V., Verhoeven, G., Rombauts, W., and Peeters, B. (1999) *Mol. Endocrinol.* **13**, 117–128
- He, B., Lee, L. W., Minges, J. T., and Wilson, E. M. (2002) *J. Biol. Chem.* **277**, 25631–25639
- Ma, H., Hong, H., Huang, S. M., Irvine, R. A., Webb, P., Kushner, P. J., Coetzee, G. A., and Stallcup, M. R. (1999) *Mol. Cell. Biol.* **19**, 6164–6173
- Christiaens, V., Bevan, C. L., Callewaert, L., Haelens, A., Verrijdt, G., Rombauts, W., and Claessens, F. (2002) *J. Biol. Chem.* **277**, 49230–49237
- Powell, S. M., Christiaens, V., Voulgaraki, D., Waxman, J., Claessens, F., and Bevan, C. L. (2004) *Endocr. Relat. Cancer* **11**, 117–130
- He, B., Minges, J. T., Lee, L. W., and Wilson, E. M. (2002) *J. Biol. Chem.* **277**, 10226–10235
- He, B., and Wilson, E. M. (2002) *Mol. Genet. Metab.* **75**, 293–298
- Zhou, Z. X., He, B., Hall, S. H., Wilson, E. M., and French, F. S. (2002) *Mol. Endocrinol.* **16**, 287–300
- He, B., Kempainen, J. A., and Wilson, E. M. (2000) *J. Biol. Chem.* **275**, 22986–22994
- Matias, P. M., Donner, P., Coelho, R., Thomaz, M., Peixoto, C., Macedo, S., Otto, N., Joschko, S., Scholz, P., Wegg, A., Basler, S., Schafer, M., Egner, U., and Carrondo, M. A. (2000) *J. Biol. Chem.* **275**, 26164–26171
- Holton, J., and Alber, T. (2004) *Proc. Natl. Acad. Sci. U. S. A.* **101**, 1537–1542
- Brunger, A. T., Adams, P. D., and Rice, L. M. (1998) *Curr. Opin. Struct. Biol.* **8**, 606–611
- Engh, R. A., and Huber, R. (1991) *Acta Crystallogr. Sect. A* **47**, 392–400
- Darimont, B. D., Wagner, R. L., Apriletti, J. W., Stallcup, M. R., Kushner, P. J.,

- Baxter, J. D., Fletterick, R. J., and Yamamoto, K. R. (1998) *Genes Dev.* **12**, 3343–3356
29. Bourguet, W., Andry, V., Iltis, C., Klaholz, B., Potier, N., Van Dorsselaer, A., Chambon, P., Gronemeyer, H., and Moras, D. (2000) *Protein Expression Purif.* **19**, 284–288
30. He, B., and Wilson, E. M. (2003) *Mol. Cell. Biol.* **23**, 2135–2150
31. McInerney, E. M., Rose, D. W., Flynn, S. E., Westin, S., Mullen, T. M., Krones, A., Inostroza, J., Torchia, J., Nolte, R. T., Assa-Munt, N., Milburn, M. V., Glass, C. K., and Rosenfeld, M. G. (1998) *Genes Dev.* **12**, 3357–3368
32. Shiau, A. K., Barstad, D., Loria, P. M., Cheng, L., Kushner, P. J., Agard, D. A., and Greene, G. L. (1998) *Cell* **95**, 927–937
33. Ribeiro, R. C., Apriletti, J. W., West, B. L., Wagner, R. L., Fletterick, R. J., Schaufele, F., and Baxter, J. D. (1995) *Ann. N. Y. Acad. Sci.* **758**, 366–389
34. Moore, J. M., Galicia, S. J., McReynolds, A. C., Nguyen, N. H., Scanlan, T. S., and Guy, R. K. (2004) *J. Biol. Chem.* **279**, 27584–27590
35. Slagsvold, T., Kraus, I., Bentzen, T., Palvimo, J., and Saatcioglu, F. (2000) *Mol. Endocrinol.* **14**, 1603–1617
36. Wang, Q., Lu, J., and Yong, E. L. (2001) *J. Biol. Chem.* **276**, 7493–7499
37. Bevan, C. L., Hoare, S., Claessens, F., Heery, D. M., and Parker, M. G. (1999) *Mol. Cell. Biol.* **19**, 8383–8392
38. Shiau, A. K., Barstad, D., Radek, J. T., Meyers, M. J., Nettles, K. W., Katzenellenbogen, B. S., Katzenellenbogen, J. A., Agard, D. A., and Greene, G. L. (2002) *Nat. Struct. Biol.* **9**, 359–364
39. Bledsoe, R. K., Montana, V. G., Stanley, T. B., Delves, C. J., Apolito, C. J., McKee, D. D., Consler, T. G., Parks, D. J., Stewart, E. L., Willson, T. M., Lambert, M. H., Moore, J. T., Pearce, K. H., and Xu, H. E. (2002) *Cell* **110**, 93–105
40. Pike, J. W., Yamamoto, H., and Shevde, N. K. (2002) *Adv. Ren. Replace Ther.* **9**, 168–174
41. Hur, E., Pfaff, S. J., Payne, E. S., Gron, H., Buehrer, B. M., and Fletterick, R. J. (2004) *PLoS Biol.* **2**, E274
42. DeLano, W. L. (2002) *Pymol*, DeLano Scientific, San Carlos, CA

# Discovery of Small Molecule Inhibitors of the Interaction of the Thyroid Hormone Receptor with Transcriptional Coregulators\*

Received for publication, June 20, 2005, and in revised form, October 18, 2005. Published, JBC Papers in Press, October 31, 2005, DOI 10.1074/jbc.M506693200

Leggy A. Arnold<sup>‡</sup>, Eva Estébanez-Perpiñá<sup>§1</sup>, Marie Togashi<sup>¶1</sup>, Natalia Jouravel<sup>§</sup>, Anang Shelat<sup>‡</sup>,  
 Andrea C. McReynolds<sup>‡</sup>, Ellena Mar<sup>§</sup>, Phuong Nguyen<sup>¶</sup>, John D. Baxter<sup>¶</sup>, Robert J. Fletterick<sup>§</sup>,  
 Paul Webb<sup>¶</sup>, and R. Kiplin Guy<sup>¶||2</sup>

From the <sup>‡</sup>Department of Pharmaceutical Chemistry, <sup>||</sup>Department of Molecular and Cellular Pharmacology, <sup>§</sup>Department of Biochemistry and Biophysics, <sup>¶</sup>Diabetes Center and Department of Medicine, University of California, San Francisco, California 94143

Thyroid hormone (3,5,3'-triiodo-L-thyronine, T3) is an endocrine hormone that exerts homeostatic regulation of basal metabolic rate, heart rate and contractility, fat deposition, and other phenomena (1, 2). T3 binds to the thyroid hormone receptors (TRs) and controls their regulation of transcription of target genes. The binding of TRs to thyroid hormone induces a conformational change in TRs that regulates the composition of the transcriptional regulatory complex. Recruitment of the correct coregulators (CoR) is important for successful gene regulation. In principle, inhibition of the TR-CoR interaction can have a direct influence on gene transcription in the presence of thyroid hormones. Herein we report a high throughput screen for small molecules capable of inhibiting TR coactivator interactions. One class of inhibitors identified in this screen was aromatic  $\beta$ -aminoketones, which exhibited IC<sub>50</sub> values of  $\sim 2 \mu\text{M}$ . These compounds can undergo a deamination, generating unsaturated ketones capable of reacting with nucleophilic amino acids. Several experiments confirm the hypothesis that these inhibitors are covalently bound to TR. Optimization of these compounds produced leads that inhibited the TR-CoR interaction *in vitro* with potency of  $\sim 0.6 \mu\text{M}$  and thyroid signaling in cellular systems. These are the first small molecules irreversibly inhibiting the coactivator binding of a nuclear receptor and suppressing its transcriptional activity.

Thyroid hormone receptors (TRs)<sup>3</sup> regulate development, growth, and metabolism (1, 2). The TRs are nuclear receptors (NR), part of a superfamily whose members function as hormone-activated transcription factors (3). The majority of thyroid hormone responses are induced by regulation of transcription by the thyroid hormone T3 (4). Two genes, THRA and THRB encode the two protein isoforms TR $\alpha$  and TR $\beta$ , which yield four distinct subtypes by alternative splicing (5). Several functional domains of TRs have been identified: a ligand-indepen-

dent transactivation domain (AF-1) on the amino terminus, a central DNA binding domain, a ligand binding domain (LBD), and a carboxyl-terminal ligand dependent activation function (AF-2) (6). TR binds specific sequences of DNA in the 5'-flanking regions of T3-responsive genes, known as thyroid response elements, most often as a heterodimer with the retinoid X receptor (7). Both unliganded and liganded TRs can bind thyroid response elements and regulate genes under their control. The unliganded TR complex can recruit a nuclear receptor corepressor (NCoR) or a silencing mediator of retinoic acid to silence basal transcription (8). In the presence of T3, TRs undergo a conformational change with the result that the composition of the coregulator complex can change with strong effects on transcriptional regulation. Several coactivator proteins have been identified (9). The best studied group of coactivators is the p160 or steroid receptor coactivator (SRC) proteins (7) including SRC1 (10), SRC2 (11, 12), and SRC3 (13). Another group of ligand-dependent-interacting proteins include the thyroid hormone receptor activating protein (TRAP) (14), peroxisome proliferator-activated receptor- $\gamma$  coactivator-1 (PGC-1) (15), and the thyroid hormone receptor binding protein (TRBP) (16). Additionally, quantitative *in vitro* binding assays (17) have shown strong interactions between TR and the coregulators p300 (18), androgen receptor activator (ARA70) (19), receptor interacting protein 140 (RIP140) (20), dosage-sensitive sex reversal-adrenal hypoplasia congenital critical region of the X chromosome gene (DAX1) (21), and the small heterodimer partner (SHP) (22).

The coregulators mentioned have in common that they have variable numbers of highly conserved LXXLL motifs; termed NR-boxes, in their nuclear receptor interacting domain (NID). The NR boxes are both necessary and sufficient for the interaction between CoR and TR. The coactivator binding site of TR LBD is formed by 16 residues from four helices (H3, H4, H5, and H12) (23). Scanning surface mutagenesis revealed that only six residues (Val<sup>284</sup>, Lys<sup>288</sup>, Ile<sup>302</sup>, Lys<sup>306</sup>, Leu<sup>454</sup>, and Glu<sup>457</sup>) are crucial for coactivator binding (24). This feature makes the AF-2 domain an ideal target for inhibitor development.

Several inhibitors of this interaction have been reported. The first reported inhibitors were macrolactam-constrained SRC2 NR box peptides (25). A combinatorial approach discovered novel  $\alpha$ -helical peptomimetics that could selectively inhibit the interaction between coactivators and TR or the estrogen receptor (ER), with selectivity between ER isoforms ER $\alpha$  and ER $\beta$  (26). A similar approach, using disulfide bridges to constrain peptides, resulted in selective ER $\alpha$  coactivator inhibitor with a  $K_d$  of 25 nM (27, 28). A report identifying a small molecule capable of inhibiting the interaction of a NR and its coactivator was published recently (29). These pyrimidine-based scaffolds showed affinities between 30 and 50  $\mu\text{M}$  but did not inhibit NR signaling in cell culture or

\* This work was supported by the Howard Hughes Medical Institute Research Resources Program Grant 76296-549901, Grants DK58080 and DK61648 from the National Institutes of Health, the Sandler Research Foundation, and a UCSF Prostate Cancer SPORE Research Fellowship. The costs of publication of this article were defrayed in part by the payment of page charges. This article must therefore be hereby marked "advertisement" in accordance with 18 U.S.C. Section 1734 solely to indicate this fact.

<sup>1</sup> Both authors contributed equally to this work.

<sup>2</sup> To whom correspondence should be addressed: Dept. of Chemical Biology in Therapeutics, St. Jude Children's Research Hospital, Memphis, TN 38105. Tel.: 901-495-5714; Fax: 901-495-5715; E-mail: kip.guy@stjude.org.

<sup>3</sup> The abbreviations used are: TR, thyroid hormone receptor; NR, nuclear receptors; T3, 3,5,3'-triiodo-L-thyronine, thyroid hormone; CoA, coactivator; CoR, coregulator; LBD, ligand binding domain; SRC, steroid receptor coactivator; NID, nuclear receptor interacting domain; ER, estrogen receptor; HTS, high throughput screening.

*in vivo* models. To date, none of these inhibitors may be used to regulate NR signaling in cellular systems.

All functional TR modulators known today are analogs of the T3 itself (30–33). These small molecule derivatives show selectivity toward different isoforms of TR resulting in tissue specific activities (34). GC-1, a TR $\beta$  selective agonist shows interesting properties *in vivo* and could be crystallized with TR LBD (35–40). The first functional T3 antagonist was NH-3, which inhibits thyroid hormone function in both cell culture and whole animal-based assays (41).

High throughput screening (HTS) together with computational screening and fragment discovery are current methods for discovering lead compounds for manipulation of protein function. Although such methods have been applied to discovery of small molecule inhibitors of protein-protein interactions (42), only a limited number of successes have been reported (43, 44). One of the most robust and sensitive HTS methods for studying protein-protein interactions is the competitive fluorescence polarization assay (45). Herein, we present the first HTS using an *in vitro* fluorescence polarization assay to measure the ability of small molecules to inhibit the interaction between the TR $\beta$  LBD and its coactivator, SRC2. This screen revealed a number of hits for inhibitors of the TR-CoR interaction. One particular class of compounds has been examined carefully, and its mechanism of inhibition has been investigated. The resulting lead compounds are potent and selective inhibitors of both the TR-CoR interaction *in vitro* and thyroid hormone signaling in cellular systems. They have potential both as drug candidates and useful biochemical tools for study of the role of the interaction of TR and its coregulators.

## EXPERIMENTAL PROCEDURES

**Labeled Peptides**—Peptide SRC2-2 (CLKEKHKILHRLQLDSSSPV) labeled with 5-iodoacetamidofluorescein (Molecular Probes) was kindly provided by Jamie M. R. Moore (probe) (17);  $\alpha$ -helical proteomimetics **3** (positive control) and **11** (negative control) were kindly provided by Timothy R. Geistlinger (26).

**Vector**—hTR $\beta$  LBD (His<sub>6</sub>, T209-D461) was cloned into the BamHI and HindIII restriction sites downstream of the hexahistidine tag of the expression vector pET DUET-1 (Novagen). The replacement of C309 for A in the hTR $\beta$  LBD construct was performed with the QuikChange XL site-directed mutagenesis kit (Stratagene). The sequence of both constructs was verified by DNA sequencing (Elim Biopharmaceuticals, Inc., Hayward, CA).

**Protein Expression and Purification**—hTR $\beta$  LBD (His<sub>6</sub>; residues T209-D461) was expressed in BL21(DE3) (Invitrogen) (10  $\times$  1L culture) at 20  $^{\circ}$ C, 0.5 mM isopropyl-1-thio- $\beta$ -D-galactopyranoside added at  $A_{600} = 0.6$  (17). When the  $A_{600}$  reached 4, cells were harvested, resuspended in 20 ml of buffer/1 liter of culture (20 mM Tris, 300 mM NaCl, 0.025% Tween 20, 0.10 mM phenylmethylsulfonyl fluoride, 10 mg of lysozyme, pH 7.5), incubated for 30 min on ice, and then sonicated for 3  $\times$  3 min on ice. The lysed cells were centrifuged at 100,000  $\times g$  for 1 h, and the supernatant was loaded onto Talon resin (20 ml, Clontech). Protein was eluted with 500 mM imidazole (3  $\times$  5 ml) plus ligand (3,3',5-triiodo-L-thyronine (Sigma)). Protein purity (>90%) was assessed by SDS-PAGE and high pressure size exclusion chromatography, and protein concentration was measured by the Bradford protein assay. The protein was dialyzed overnight against assay buffer (3  $\times$  4 liters, 50 mM sodium phosphate, 150 mM NaCl, pH 7.2, 1 mM dithiothreitol, 1 mM EDTA, 0.01% Nonidet P-40, 10% glycerol). The protein functionality was determined by a direct binding assay of SRC2-2 (see Fig. 3A) giving a  $K_d$  for SRC2-2 of 0.44  $\mu$ M, agreeing with prior results. hTR $\alpha$  LBD (His<sub>6</sub>; residues Glu<sup>148</sup>-Val<sup>410</sup>) was expressed using the same procedure as hTR $\beta$

with the exception that 0.5 mM isopropyl-1-thio- $\beta$ -D-galactopyranoside was added at  $A_{600} = 1.2$ . Unliganded protein was eluted with 100 mM imidazole. Purity assessment and buffer exchange were carried out as described. The functionality was determined in a direct binding assay (see Fig. 3A) giving a  $K_d$  for SRC2-2 of 0.17  $\mu$ M, agreeing with prior results. hTR $\beta$  LBD C309A (His<sub>6</sub>; residues Thr<sup>209</sup>-Asp<sup>461</sup>) was expressed in BL21 cells (Stratagene) at 18–20  $^{\circ}$ C by using the pET DUET1-hTR $\beta$  LBD (41). General procedures were as described above. The functionality was determined in a direct binding assay (see Fig. 3A) giving a  $K_d$  for SRC2-2 of 0.17  $\mu$ M.

**Direct Binding Assay**—The protein was serially diluted from 70 to 0.002  $\mu$ M in binding buffer (50 mM sodium phosphate, 150 mM NaCl, pH 7.2, 1 mM dithiothreitol, 1 mM EDTA, 0.01% Nonidet P-40, 10% glycerol) containing 1  $\mu$ M ligand T3 in 96-well plates (17). Then 10  $\mu$ l of diluted protein was added to 10  $\mu$ l of labeled SRC2-2 (20 nM) in 384-well plates yielding final protein concentrations of 35–0.001  $\mu$ M and 10 nM fluorescent peptide concentration. The samples were allowed to equilibrate for 30 min. Binding was then measured using fluorescence polarization (excitation  $\lambda$  485 nm, emission  $\lambda$  530 nm) on an Analyst AD plate reader (Molecular Devices). Two independent experiments, each in quadruplicate, were carried out for each state. Data were analyzed using SigmaPlot 8.0 (SPSS, Chicago, IL), and the  $K_d$  values were obtained by fitting data to the following equation ( $y = \min + (\max - \min)/1 + (x/K_d)$ Hill slope).

**Screening Procedure**—The small molecule screen was carried out at the Bay Area Screening Center (BASC) at the California Institute for Quantitative Biology (QB3). A library comprised of 138,000 compounds (ChemRX, 28,000; ChemDiv, 53,000; ChemBridge, 24,000; SPECS, 31,000; Microsource, 2,000) was screened in 384-well format. The complete composition of this library is available from the BASC website (ucsf.edu/basc). First, 384-well dilution plates (costar 3702) were prepared by addition of 34  $\mu$ l of dilution buffer (20 mM Tris-HCl, 100 mM NaCl, pH 7.2, 1 mM dithiothreitol, 1 mM EDTA, 0.01% Nonidet P-40, 10% glycerol, 5.9% Me<sub>2</sub>SO) to each well by using a WellMate (Matrix) followed by addition of 6  $\mu$ l compound solutions (1 mM compound in dimethyl sulfoxide (Me<sub>2</sub>SO)) using a Multimek (Beckman) equipped with a 96-channel head and mixing by subsequent aspiration and dispensing. Second, 5  $\mu$ l from the dilution plates were transferred to 384-well assay plates (Costar 3710) using a Multimek followed by the addition of 24  $\mu$ l of protein mixture (20 mM Tris-HCl, 100 mM NaCl, pH 7.2, 1 mM dithiothreitol, 1 mM EDTA, 0.01% Nonidet P-40, 10% glycerol, 1  $\mu$ M TR $\beta$  LBD, 1  $\mu$ M T3, 0.025  $\mu$ M labeled SRC2-2 using a WellMate. The final concentration of compound was 30  $\mu$ M with 4% Me<sub>2</sub>SO content. Each plate was monitored by the addition of a positive control **3** and negative control **11**. After an incubation time of 2 h the binding was measured using fluorescence polarization (excitation  $\lambda$  485 nm, emission  $\lambda$  530 nm) on an Analyst AD plate reader (Molecular Devices). Additionally the fluorescence intensity was measured. All data relevant to the project (plate and compound information, screening data, annotation info, etc.) was deposited directly into a MySQL data base (v. 4.1.7). Data were manipulated and analyzed using protocols written in Pipeline Pilot 4.5.1 (Scitegic, Inc). Our protocols automated the process of joining experimental data to compound information, flagging suspicious plates based on low Z-factors, extracting compounds with statistically significant activity, and annotating hits with additional information (*i.e.* chemical similarity to known bioactive compounds, known genotoxic/cytotoxic molecules, or available compounds, and profiles from ADME models).

**Dose-response Experiments**—The small molecules were serially diluted from 1000 to 4.88  $\mu$ M in Me<sub>2</sub>SO into a 96-well plate (Costar

3365). 10  $\mu\text{l}$  of each concentration was transferred into 100  $\mu\text{l}$  of binding buffer (20 mM Tris-HCl, 100 mM NaCl, pH 7.2, 1 mM dithiothreitol, 1 mM EDTA, 0.01% Nonidet P-40, 10% glycerol) and mixed by subsequent aspiration and dispensing. Then 10  $\mu\text{l}$  of diluted compound was added to 10  $\mu\text{l}$  of protein mixture (20 mM Tris-HCl, 100 mM NaCl, pH 7.2, 1 mM dithiothreitol, 1 mM EDTA, 0.01% Nonidet P-40, 10% glycerol, 2  $\mu\text{M}$  TR $\beta$  LBD, 2  $\mu\text{M}$  T3, 0.02  $\mu\text{M}$  labeled SRC2-2 in 384-well plates yielding final compound concentration of 50–0.024  $\mu\text{M}$ . The samples were allowed to equilibrate for 3 h. Binding was then measured using fluorescence polarization (excitation  $\lambda$  485 nm, emission  $\lambda$  530 nm) on an Analyst AD (Molecular Devices). Two independent experiments, in quadruplicate, were carried out for each compound. Data were analyzed using SigmaPlot 8.0, and the  $K_d$  values were obtained by fitting data to the following equation ( $y = \min + (\max - \min)/1 + (x/K_d)$ Hill slope).

**Thyroid Hormone Competition Binding Assay**—Full-length hTR $\beta$  was produced using a TNT T7 quick-coupled transcription translation system (Promega). Competition assays for binding of unlabeled T3 and L1 were performed using 1 nM [ $^{125}\text{I}$ ]T3 in gel filtration binding assay as described (46).

**Binding Assay with L8 and L9**—TR $\beta$  or TR $\beta$  C309A (5  $\mu\text{M}$ ) and T3 (20  $\mu\text{M}$ ) were incubated in binding buffer (100  $\mu\text{M}$ ) with different concentrations L8 and L9, respectively. After 3 h at room temperature an aliquot of 20  $\mu\text{M}$  was treated with a denaturing buffer (10  $\mu\text{M}$ ), boiled for 2 min, and separated using 10% SDS-polyacrylamide gel electrophoresis and visualized by a fluorescence spectrometer.

**Pull-down Assays**—GST fusions to the thyroid hormone receptor (full-length) were expressed in *Escherichia coli* BL21. Cultures were grown to  $A_{600}$  1.2–1.5 at 22  $^{\circ}\text{C}$  and induced with 0.5 mM isopropyl-D-thiogalactoside for 4 h. The cultures were centrifuged (1000  $\times g$ ), and bacterial pellets were resuspended in 20 mM Hepes, pH 7.9, 80 mM KCl, 6 mM MgCl<sub>2</sub>, 1 mM DTT, 1 mM ATP, 0.2 mM phenylmethylsulfonyl fluoride, and protease inhibitors and sonicated. Debris was pelleted by centrifugation (100,000  $\times g$ ). The supernatant was incubated with glutathione-Sepharose 4B beads (Amersham Biosciences) and washed as previously described. Protein preparations were stored at  $-20^{\circ}\text{C}$  in 20% glycerol until use. [ $^{35}\text{S}$ ]methionine-labeled SRC2 was produced by using coupled *in vitro* transcription-translation (TNT kit, Promega). The binding reactions were carried out on ice in a volume of 150  $\mu\text{l}$  composed of 137.5  $\mu\text{l}$  of protein-binding buffer along with 10  $\mu\text{l}$  of GST-bead slurry corresponding to 3  $\mu\text{g}$  of fusion protein, 1  $\mu\text{l}$  of *in vitro* translated protein, and 1.5  $\mu\text{l}$  of ligand or vehicle. The protein-binding buffer composed of 20  $\mu\text{l}$  of A-150 (20 mM Hepes, 150 mM KCl, 10 mM, MgCl<sub>2</sub>, 1% glycerol) and 2  $\mu\text{l}$  each of phosphate-buffered saline supplemented with 1% Triton X-100 and 1% Nonidet P-40. Phenylmethylsulfonyl fluoride, dithiothreitol, bovine serum albumin, and protease inhibitor mixture (Novagen) was freshly prepared. The mix was incubated at 4  $^{\circ}\text{C}$  with gentle agitation; the beads were pelleted, washed four times with protein-binding buffer containing no bovine serum albumin, and dried under vacuum for 20 min. The sample was taken up in SDS-PAGE loading buffer and then subjected to SDS-PAGE and autoradiography.

**Transient Transfection Assays**—Human bone osteosarcoma epithelial cells (U2OS) cells (Cell Culture Facility, UCSF) were grown to  $\sim 80\%$  confluency in Dulbecco's modified Eagle's/H-21, 4.5 g/liter glucose medium containing 10% newborn calf serum (heat-inactivated), 2 mM glutamine, 50 units/ml penicillin, and 50  $\mu\text{g}/\text{ml}$  streptomycin. Cells ( $\sim 1.5 \times 10^6$ ) were collected and resuspended in 0.5 ml of electroporation buffer (Dulbecco's phosphate-buffered saline containing 0.1% glucose, 10 mg/ml bioprene). 5  $\mu\text{g}$  of a TR expression vector (full-length hTR $\beta$ -CMV) and 1.5  $\mu\text{g}$  of a reporter plasmid contained a synthetic TR

response element (DR-4) containing two copies of a direct repeat spaced by four nucleotides (AGGTCAcaggAGGTCA) cloned immediately upstream of a minimal ( $-32/+45$ ) thymidine kinase promoter linked to luciferase coding sequence (35). Cells were electroporated using a Bio-Rad gene pulser at 350 V and 960 microfarads, pooled in growth medium (DME H-21 with 10% charcoal-treated, hormone-stripped, newborn bovine serum), and plated in 96-well dishes. After a 3-h incubation compounds were added to the cell culture medium as Me<sub>2</sub>SO solutions so as to yield a final Me<sub>2</sub>SO concentration of 1%. After additional 18 h of incubation, cells were harvested and assayed for luciferase activity using the Promega dual luciferase kit (Promega) and an Analyst AD (Molecular Devices). Data were analyzed using SigmaPlot 8.0, and the IC values were obtained by fitting data to the following equation ( $y = \min + (\max - \min)/1 + (x/K_d)$ Hill slope).

## RESULTS

The high-throughput screen was carried out using a 384-well plate format. A total of 300 compounds as single points together with quadruple positive and quadruple negative controls were dispensed in each 384-well plate followed by the addition of TR $\beta$  LBD and the labeled SRC2-2 peptide. The SRC2-2 peptide was utilized because it had the tightest binding (0.44  $\mu\text{M}$ ) of all the NR box peptides investigated (17). After incubation for 2 h the fluorescence polarization and fluorescence intensity was measured. From the 138,000 compounds screened 27 hit compounds inhibited the interaction between TR $\beta$  LBD and the SRC2-2 coactivator peptide with at least 50% efficacy at a concentration of 30  $\mu\text{M}$  and had a fluorescence intensity variation of less than 10%. The structures of these hits, along with the percent inhibitions at 30  $\mu\text{M}$  are shown in Fig. 1. The molecules are divided into six groups depending on their chemical properties. Group A represents electrophilic molecules with a medium sized alkyl substituent. Based on our results at least two of them are irreversible inhibitors of the TR-CoA interaction.

All hits shown in Fig. 1 were evaluated by performing a dose to the response of inhibition study over a range of compound concentrations of 0.024–30  $\mu\text{M}$  to allow the calculation of the IC<sub>50</sub> values. Only two compounds (Fig. 2B, L1 and L2) had IC<sub>50</sub> values less than 10  $\mu\text{M}$  (C, entries 1 and 2), with a clear saturation at a higher concentration (A). These were designated validated hits. The remaining compounds were all sufficiently weak in potency to call their validity into question. This represents an overall hit rate of 0.00145%.

Both of the validated hits are  $\beta$ -aminoketones. These compounds are better known as Mannich bases, first synthesized in the 19th century and systematically studied by Carl Mannich in the beginning of last century (47). Several biological activities have been discovered for this compound class including anticancer, antimicrobial, and cytotoxic activities (48). These activities have been attributed to the liberation of  $\alpha,\beta$ -unsaturated ketones by internal elimination of the amino group. Although this reaction proceeds very slowly under physiological pH in water it has been reported that protein surfaces are able to catalyze this reaction very efficiently (49). Such soft electrophiles, termed Michael addition acceptors, can alkylate protein nucleophiles such as cysteine, tyrosine, and serine. Because of the strong nucleophilicity of organic sulfides, cysteine residues are the most reactive toward this class of Michael acceptors.

To investigate the probability that a similar mechanism underlay inhibition of coactivator binding to the TR $\beta$  LBD we tested the unsaturated ketone L3 (Fig. 2B). Interestingly, it showed a similar inhibitory ability of the coactivator recruitment suggesting that indeed the liberated unsaturated ketone L3 is the active species for compounds L1 and L2 (Fig. 2C, entry 3). To determine whether the binding is based on the

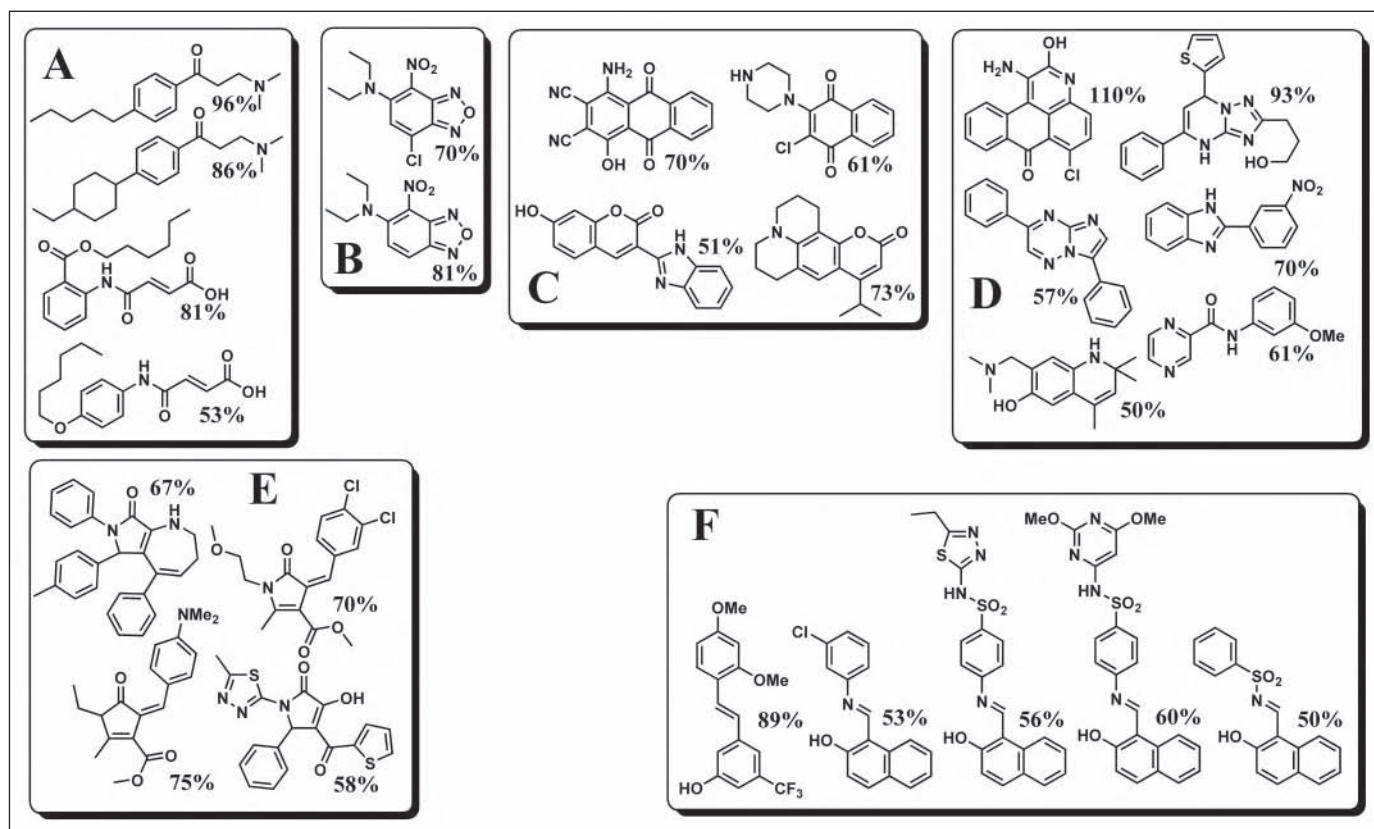


FIGURE 1. Hit structures from HTS for inhibitors of the interaction of hTR $\beta$  and SRC2-2. Structures of hits are shown, grouped by chemotype, and annotated with the percent inhibition of SRC2-2 binding at 30  $\mu$ M concentration of compound; A, electrophilic molecules with alkyl substituents; B, 7-nitrobenz-2-oxa-1,3-diazole derivatives; C, quinone and coumarin derivatives; D, N-heterocycles; E, highly substituted pyrrolidone derivatives; F, stilbene derivatives.

electrophilic nature of the molecule **L3** and not on steric effects, a saturated ketone **L4** was tested. This compound exhibited no competitive ability in the polarization assay (Fig. 2C, entry 4). Subsequently we investigated the importance of the alkyl substituent. Compound **L5**, with an elongated alkyl chain and compound **L6**, with no substituent, both failed to compete with SRC2-2 for binding to the TR $\beta$  LBD (Fig. 2C, entries 5 and 6). Taken together, these results argue for a receptor templated covalent inactivation mechanism.

To ascertain some details of the deamination reaction presumably producing **L3**, several compounds with different alkyl nitrogen substituents that should possess different propensities for elimination were synthesized and investigated in the coactivator binding assay with no significant change in the IC<sub>50</sub> values.<sup>4</sup> Point mutations of the charged amino acids Lys<sup>306</sup> and Glu<sup>457</sup> of the TR $\beta$  LBD diminish the binding of SRC2 (24). This property prevented using these mutants in the competitive coactivator binding assay to investigate whether the deamination reaction of **L1** takes place at the coactivator binding pocket of TR $\beta$  LBD or elsewhere on the TR $\beta$  protein surface.

A thyroid hormone binding assay in the presence of **L3** was conducted to rule out the possibility that the small molecule is competing with T3, which would also result in the release of the labeled coactivator in case of an antagonistic behavior (46). No competition of **L3** with the hormonal ligand was detected in a range of 0.1–10  $\mu$ M **L3** using [<sup>125</sup>I]T3 (Fig. 2D).

The probability of the formation of a covalent bond between **L1** and TR $\beta$  LBD was investigated by several independent methods. We synthesized Bodipy<sup>®</sup>-labeled compounds **L8** and **L9** (Fig. 2E). To prove that

such acrylate analogs have similar activity as compound **L3**, we first investigated the activity of a 4-alkyl-substituted aromatic acrylate **L7** (Fig. 2B). This compound showed a similar activity in the competition assay as the unsaturated ketone **L3** (Fig. 2C, entry 7).

Compound **L8** was incubated in different concentrations (10, 5, and 1  $\mu$ M) with TR $\beta$  LBD (5  $\mu$ M) in the presence of T3 (20  $\mu$ M). Separation by a SDS-polyacrylamide gel showed a strong fluorescent band corresponding to TR $\beta$  LBD-**L8** (Fig. 2F, lanes 7–9). In contrast, incubation with **L9** resulted in no detectable band under the same conditions (Fig. 2F, lanes 4–6).

Mass spectroscopy is used extensively to detect modified biomolecules like labeled proteins. We observed different MS spectra for the **L1** treated and untreated TR $\beta$  LBD (Fig. 2G). The difference of 200–250 *m/z* indicates that a covalent adduct is formed and that of one molecule of TR $\beta$  LBD reacts with one molecule of compound **L1**. The exact difference would be theoretically 217 *m/z*, well within the experimental error of the method.

The formation of a covalent bond between the **L1** and TR $\beta$  LBD implies that the binding is irreversible. In general irreversible inhibitors show a significant time dependence, which varies with their concentration. Therefore a competition assay with **L1** in the presence of TR $\beta$  LBD and fluorescent coactivator peptide was followed in time (Fig. 2H). At a high concentration (50  $\mu$ M) **L1** almost instantly inhibited binding of SRC2-2 to the TR $\beta$  LBD coactivator site. A time dependence of inhibition over 4 h was discovered with concentrations of **L1** between 25 and 1.5  $\mu$ M. At 0.33  $\mu$ M **L1**, no significant inhibition was observed. This indicates that the inhibition is time dependent and requires a stoichiometric amount of **L1**, to the limits of accuracy of the determination of protein concentration.

<sup>4</sup> L. A. Arnold, unpublished results.

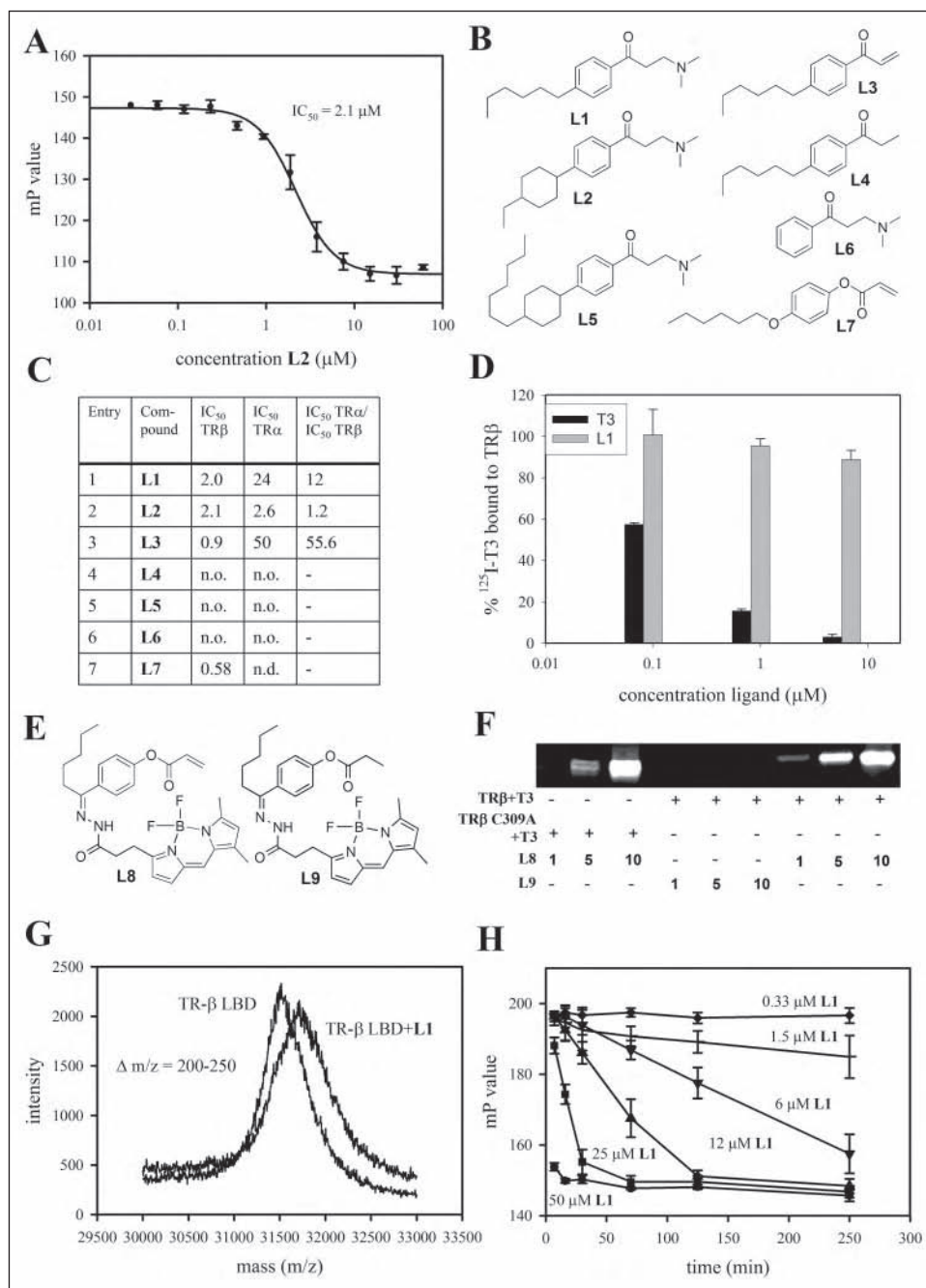


FIGURE 2. Activities and structures of inhibitors.

**A**, competitive fluorescence polarization assay of **L2** in the presence of TR $\beta$  LBD ( $1 \mu\text{M}$ ), T3 ( $1 \mu\text{M}$ ), and fluorescence labeled SRC2-2 peptide ( $10 \text{ nM}$ ). The data were recorded after 4 h, and the  $\text{IC}_{50}$  is extracted by fitting to the equation ( $y = \text{min} + (\text{max} - \text{min}) / (1 + (x/K_d)^{\text{Hill slope}})$ ). **B**, small molecule analogs of **L1** synthesized to test mechanistic hypotheses. **C**, summary of  $\text{IC}_{50}$  values of compounds **L1–L7** for TR $\alpha$  and TR $\beta$ . Additionally the ratio (selectivity) between TR $\alpha$  LBD and TR $\beta$  LBD are given for compound **L1–L3**. *n.o.*, none observed; *n.d.*, none detected. **D**, competition ligand binding of **L1** in the presence of  $1 \text{ nM}$  [ $^{125}\text{I}$ ]T3 and full-length TR $\beta$  in a gel filtration binding assay. **E**, structure of labeled small molecules. **F**, fluorescent image of a 10% SDS-polyacrylamide gel showing labeled small molecules covalent bound to TR $\beta$ . Lanes 1–3, TR $\beta$  C309A and **L8**; 4–6, TR $\beta$  and **L9**; 7–9, TR $\beta$  and **L8**. **G**, matrix-assisted laser desorption ionization-mass spectrometry spectra of untreated TR $\beta$  LBD and TR $\beta$  LBD treated with **L1**. **H**, time dependence of inhibition of TR $\beta$  LBD coactivator binding by **L1** at different concentrations; competitive fluorescence polarization assay was followed over time.

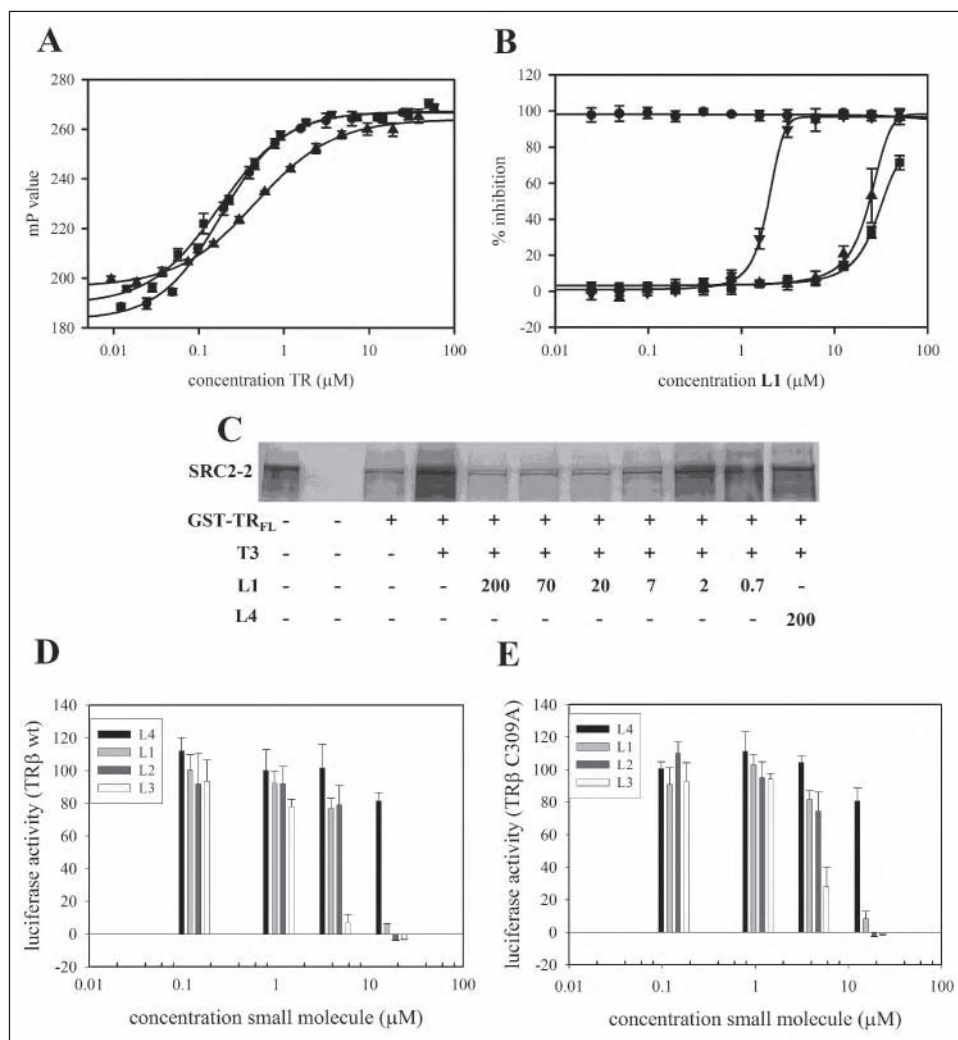
For **L1** to inhibit coactivator binding to TR $\beta$  LBD there must be accessible nucleophilic residues at the coactivator binding site. The LBD of TR $\beta$  has seven cysteine residues. Most of them are exposed on the surface of the protein. There are three cysteine residues near the coactivator binding site. One is freely exposed at the surface (Cys $^{298}$ ) and a pair of two adjoining cysteine residues (Cys $^{308}$  and Cys $^{309}$ ) is buried deeply in the binding pocket (Fig. 4A) (23). These cysteines are a unique feature of the TR coactivator binding pocket relative to other NR. Based upon our expectation of binding mode for the compounds, we hypothesized that Cys $^{309}$  was the most likely to be involved in the alkylation reaction.

To test the hypothesis that Cys $^{309}$  was forming the covalent adduct with **L1**, we prepared a C309A TR $\beta$  LBD mutant. The mutant was fully functional with respect to SRC2-2 binding in the presence of T3 measured by a direct binding assay ( $K_d = 0.17 \mu\text{M}$ ), in comparison to the wild

type TR $\beta$  LBD ( $K_d = 0.44 \mu\text{M}$ ) (Fig. 3A). Using this mutant in a competition binding assay showed that the  $\text{IC}_{50}$  value of **L1** was increased by more than 50-fold suggesting that Cys $^{309}$  plays a crucial role in the inhibition of the coactivator recruitment of wild type TR $\beta$  by **L1** (Fig. 3B). This hypothesis was supported by the fact that the labeling of TR $\beta$  C309A, employing **L8**, was significantly less efficient in comparison to the wild type (Fig. 2F, lanes 1–3).

The ability of **L1** to compete with intact coactivator SRC2, containing all three SRC2 NR boxes, was tested using a semiquantitative glutathione *S*-transferase assay (Fig. 3C). Control experiments indicated that the SRC2 bound to full-length hTR $\beta$  in the presence of T3 (Fig. 3C, lane 4) and failed to bind in the absence of T3 (lane 3). This interaction was blocked by **L1** at concentrations between 200 and  $7 \mu\text{M}$  (Fig. 3C, lanes 5–8). At lower concentrations (2– $0.7 \mu\text{M}$ , Fig. 3C, lanes 9 and 10) no inhibition was observed. The control experiment with compound **L4**

**FIGURE 3. Detailed mechanistic studies of inhibitors.** A, direct binding assay of labeled SRC2-2 peptide to hTR $\alpha$  LBD, hTR $\beta$  LBD, and hTR $\beta$  LBD (C309A). The protein was serially diluted and treated with 1  $\mu$ M ligand T3 and 0.01  $\mu$ M of fluorescent SRC2-2. The binding was measured after 30 min using fluorescence polarization. The  $K_d$  values were obtained by fitting data to the following equation ( $y = \min + (\max - \min)/1 + (x/K_d)$  Hill slope).  $\bullet$ , TR $\alpha$  LBD = 0.17  $\mu$ M;  $\blacktriangle$ , TR $\beta$  LBD = 0.46  $\mu$ M;  $\blacksquare$ , TR $\beta$  LBD (C309A) = 0.17  $\mu$ M. B, competition polarization assay with labeled SRC2-2 peptide (10 nM), L1, and TR (1  $\mu$ M). L1 was serially diluted and equilibrated with all components for 4 h prior to analysis.  $\bullet$ , TR $\alpha$  LBD, no T3;  $\blacktriangle$ , TR $\alpha$  LBD with T3;  $\blacktriangledown$ , TR $\beta$  LBD with T3;  $\blacksquare$ , TR $\beta$  LBD (C309A) with T3. C, autoradiogram of 10% SDS-polyacrylamide gel showing products of *in vitro* binding reactions between  $^{35}$ S-labeled SRC2 and GST fusion to full-length TR $\beta$ . Lane 1, 10% input labeled SRC2; 2, GST control; 3, no T3 hormone,  $^{35}$ S-labeled SRC2 binding is ligand-dependent; 4, no L1 inhibitor, maximal binding of  $^{35}$ S-labeled SRC2 to hTR $\beta$  in the presence of T3 (10  $\mu$ M); 5–10, different concentrations of L1 in the presence of T3; 11, L4, no inhibition. D, inhibition of expression of a thyroid response element-driven luciferase reporter enzyme by L1–L4 at different concentrations in the presence of a constant, fully inducing, concentration of T3. U2OS cells were transfected with a TR $\beta$  expression vector. The data are normalized to basal expression (treatment with equal amounts of Me $_2$ SO, but no T3) and fully induced expression (treatment with equal amounts of Me $_2$ SO and T3). E, inhibition of expression of a thyroid response element-driven luciferase reporter enzyme by L1–L4 at different concentrations in the presence of a constant, fully inducing, concentration of T3. U2OS cells were cotransfected with a TR $\beta$  C309A expression vector. The data are normalized to basal expression (treatment with equal amounts of Me $_2$ SO, but no T3) and fully induced expression (treatment with equal amounts of Me $_2$ SO and T3).



showed no inhibition at 200  $\mu$ M (Fig. 3C, lane 10). Thus, the inhibition of interaction of full-length hTR $\beta$  and SRC2 by L1 exhibited dose dependence, similar to the peptide binding studies described above.

The specificity of L1 inhibition of SRC2 binding was examined with respect to both TR isoforms, TR $\alpha$  and TR $\beta$ . Both isoforms were used under the same conditions in a competition polarization assay. L1 competes with SRC2 for binding to TR $\alpha$  with 12-fold lower apparent affinity giving an IC $_{50}$  of 24  $\mu$ M (Fig. 2C, entry 1). In the absence of T3 no SRC2 is recruited (Fig. 3B). For L3 this difference was even higher with 50-fold decrease in affinity for TR $\alpha$  (Fig. 2C, entry 3). Surprisingly L2 showed similar affinities for both TR $\alpha$  and TR $\beta$ , 2.6 and 2.1  $\mu$ M, respectively (Fig. 2C, entry 2). As expected compounds L4, L5, and L6 showed no binding to either isoform (Fig. 2C, entries 4–6).

To examine the influence of L1–L4 on transcriptional transactivation of a consensus thyroid response element, U2OS cells were cotransfected with an expression vector TR $\beta$ 1 and a thyroid response element-driven luciferase reporter plasmid. After incubation for 18 h the luciferase activity was determined for cells exposed to a fixed concentration of T3 and different concentrations of compounds L1–L4 (Fig. 3D). The compounds L1–L3 showed full inhibition of transcription at 17  $\mu$ M. L4, used as a control, had almost no influence on the luciferase activity in comparison to Me $_2$ SO alone. Minor inhibition of transcription was observed at 4  $\mu$ M applying L1 and L2. L3 in contrast fully suppressed transcription at concentration of 4  $\mu$ M and had minor effects at 1  $\mu$ M.

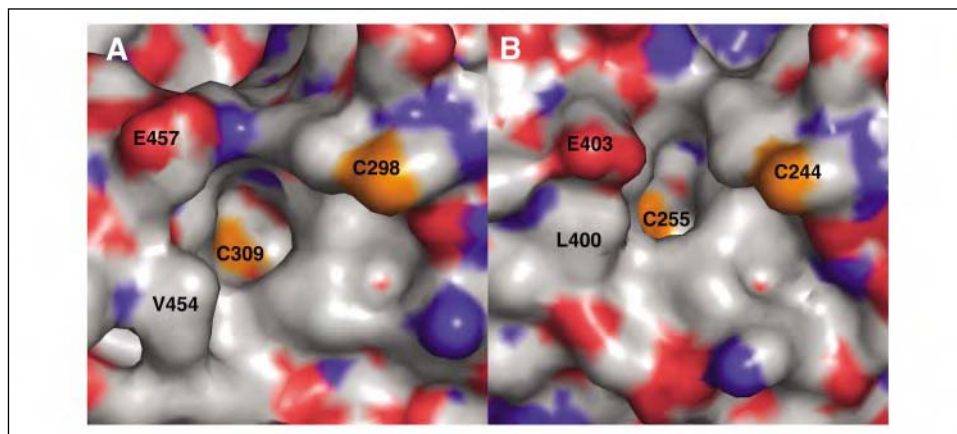
At the concentrations measured, the inhibition of transcription using an expression vector TR $\beta$  C309A was similar for L1 and L2 in comparison to the wild type TR $\beta$  (Fig. 3E). Major differences were observed for L3 showing no inhibition at 1  $\mu$ M and only moderate potency at 4  $\mu$ M. The viability of the cells was monitored with no significant cell death taking place in any experiment at these concentrations.

## DISCUSSION

A HTS of small molecules was successfully applied to find a hit that led to the first cell active modulators of nuclear hormone receptor coactivator interactions. The screen was based on the ability of liganded TR to recruit coregulator proteins capable of enhancing transcriptional regulation. We evaluated small molecules capable of inhibiting this protein-protein interaction by using fluorescence polarization with a peptide probe representing the coregulator. During the initial screen we identified 27 hit compounds showing an inhibition of more than 50% at a concentration of 30  $\mu$ M. The study of the dose response of inhibition of these 27 compounds revealed two validated hits with an IC $_{50}$  value of less than 10  $\mu$ M. The overall hit rate of 0.00145% is unusually low for a target-based HTS campaign. We hypothesize that this is because of the absence of molecules with the correct chemotypes in a library whose construction was biased toward current philosophy of “drug-like” character for enzymatic and cell surface receptor targets.

The two validated hit compounds L1 and L2, with IC $_{50}$  values of 2.0 and 2.1  $\mu$ M, respectively, are  $\beta$ -aminoketones. The biological activities

**FIGURE 4. Surface display of TR coactivator binding pocket.** A, TR $\beta$ ; B, TR $\alpha$ . The TR LBD coactivator binding site is represented by a solid surface indicating in gray the hydrophobic residues, in blue the positively charged residues, in red the negatively charged residues, and in yellow the cysteines. The thyroid receptor AF-2 transactivation function is a surface exposed hydrophobic cleft comprised of residues from helices 3, 5, and 12. Some of these residues important for coactivator binding are labeled in both TR $\beta$  and TR $\alpha$ . Both are depicted in identical orientation.



of this class of compounds have been attributed to the fact that they can liberate a corresponding unsaturated ketone capable of alkylating biological nucleophiles. A binding study with the corresponding unsaturated ketone **L3** showed an  $IC_{50}$  value of  $0.9 \mu\text{M}$ . This result suggests that the unsaturated ketone is the active species. To exclude the possibility that steric properties of **L3** are important for inhibition we tested saturated compound **L4**. This compound was not able to inhibit the TR $\beta$ -CoA binding.

We hypothesize that the deamination reaction producing the active **L3** *in situ* is catalyzed on the protein surface because of the unlikelihood of an intramolecular mechanism at physiological pH. The small variation of  $IC_{50}$  values based on aminoketones with different alkyl nitrogen substituents suggests a hydrophobic and fairly rigid catalytic site. However, direct investigation of the most likely catalytic residues of the TR $\beta$  coactivator binding domain is prevented because these residues are necessary for binding of the coactivator.

The electrophilic functionality of the active inhibitor species **L3** has been found to be an essential property of the TR antagonists suggesting that the inhibition is based on the alkylation of nucleophilic residues forming the TR $\beta$ -CoA interface. Binding studies with compounds **L5** and **L6** showed no inhibition, concluding that a medium-sized hydrophobic group at the 4 position of the aromatic  $\beta$ -aminoketones is necessary for interaction. Taken together, these studies strongly imply that the active species of inhibitors are actually  $\alpha,\beta$ -unsaturated ketones acting as direct alkylators of nucleophilic residues on the surface of the thyroid receptor. This is supported by the fact that the natural ligand T3 is not released by the addition of **L1**, which implies that the conformation of TR $\beta$  is not altered in the presence of **L1**.

Covalent inhibitors have several unique properties. 1) They produce an adduct with the target that has increased molecular weight. This feature can be used to permanently label the corresponding binding partner; 2) they require stoichiometric, but not largely superstoichiometric amounts of inhibitor for full activity, and 3) they exhibit strong time dependence when acting in modest excess relative to the target concentration. After the treatment of TR $\beta$  LBD with **L1** we could detect a new species with a 200–250  $m/z$  higher mass. We assigned this mass to TR $\beta$ -**L1** proving that TR $\beta$  is selectively alkylated by one equivalent of **L1**. In addition we followed the inhibition of TR $\beta$ -CoA by **L1** in time. A significant time dependence of inhibition was found between **L1** concentrations of 25 and  $1.5 \mu\text{M}$  when interacted with TR at a concentration of  $1 \mu\text{M}$ . The time dependence altered with the **L1** concentration suggesting an irreversible inhibition. A covalent complex was formed when TR $\beta$  was treated with fluorescently labeled analog **L8**, in contrast to the inactive compound **L9**, lacking the electrophilic properties of **L8**, which did not. In summary, the detection of the mono-alkylated TR $\beta$ ,

its time-dependent formation, and the fact that TR $\beta$  could be covalently labeled with a fluorescent inhibitor supports the postulated mechanism that **L1** forms the unsaturated ketone **L3**, alkylating irreversibly one of the residues of TR $\beta$  LBD.

Based upon the expected chemical reactivity of **L1**, as predicted by frontier molecular orbital theory, we would expect that **L1** is most likely to react with a solvent-exposed cysteine residue. The fact that we observe a single alkylation event is exceptional because there are seven cysteine residues present in TR $\beta$  LBD. Most of cysteine residues are exposed to the surface of the protein. We hypothesized that the selectivity might be driven by a preassociation event that positions the antibonding orbital of the electrophile **L1** near a nucleophilic cysteine. The coactivator binding site has three cysteine residues (Fig. 4, Cys<sup>308</sup>, Cys<sup>309</sup>, and Cys<sup>298</sup>). Of these, Cys<sup>309</sup> seemed most likely to be reacting with **L1** based upon our expected mode of binding. To support this hypothesis three independent experiments were carried out in systems where cysteine residue Cys<sup>309</sup> was replaced by an alanine: 1) competitive coactivator binding studies using TR $\beta$  C309A revealed that **L1** had a 50-fold reduced  $IC_{50}$  value in comparison with the wild type TR $\beta$ ; 2) direct labeling of TR $\beta$  C309A using **L8** was less efficient in comparison with the wild type; and 3) inhibition of transfection by **L3** using U2OS cells cotransfected by a TR $\beta$  C309A expression vector was significantly reduced in comparison with the wild type. Although a direct comparison with C308A and C298A clones is missing, we think that Cys<sup>309</sup> is the most likely target for **L1**. Cys<sup>309</sup> is exposed in a defined hydrophobic pocket capable of activation through nearby charged residues. The residues forming the coactivator binding surface of TR $\alpha$  and TR $\beta$  LBD are identical (Fig. 4). Although crystal structures of the binding pockets of the two isoforms of TR (TR $\alpha$  LBD and TR $\beta$  LBD) are very similar, there are distinct differences in the region immediately surrounding the pocket. We think that these differences in the hydrophobic relief are the reason for the significant differences in  $IC_{50}$  values for **L1** and **L3** for TR $\alpha$  and TR $\beta$  LBD. The decrease in affinity for TR $\alpha$  was 12-fold for **L1** and 50-fold for **L3**. On the other hand, **L2** showed the same affinity for both isoforms. This selectivity is very important for future studies targeting specific tissues with differently expressed levels of TR $\alpha$  and TR $\beta$ .

The ability to inhibit a protein-peptide interaction does not guarantee that the same inhibitor will block the interaction of the full-length proteins. In this case, **L1** fully inhibited the interaction of full-length SRC2, containing three NR boxes, and full-length TR $\beta$ . A concentration of  $7 \mu\text{M}$  **L1** was sufficient for blocking this receptor-coactivator interaction. The fact that the potency of **L1** in this semiquantitative glutathione *S*-transferase assay matched that in the protein-peptide interaction increased the likelihood that **L1** would block this interaction between the full-length transcription factors in a cellular environment.

A reporter gene transfection assay, carried out in cultured U2OS cells, showed indeed that compounds **L1**, **L2**, and **L3** were able to reduce transcriptional activation to basal levels. **L3** showed highly increased potency in comparison to **L1** and **L2** with almost full inhibition of transcription at 4  $\mu\text{M}$ . We concluded that **L3** can penetrate the cell membrane and is transported to the nucleus. Furthermore it can inhibit coregulator recruitment and has a direct impact on the transcriptional activity of TR $\beta$ .

In summary, we report that small molecules are able to inhibit the interaction between the liganded thyroid hormone receptor and its coactivator SRC2. To our knowledge this is the first irreversible inhibitor of the nuclear receptor coregulator binding that has been reported. Molecules like **L1** are a new class of TR antagonist, active in the presence of T3 but silencing its hormone-induced signaling. They open the door to understand the coupling of multiple thyroid hormone-regulated signaling events and the potential for treatment of hyperthyroidism using approaches that do not affect thyroid hormone levels. Compounds **L1** and **L3** exhibit exceptional TR $\beta$  selectivities making them potentially useful for the study of tissue selective thyroid activities. We are currently investigating the effects of these compounds in cell-based assays and *in vivo* studies.

*Acknowledgments*—The HTS was carried out in the Bay Area Screening Center (QB3/UCSF) with support from UCSF and the Sandler Research Foundation. We thank J. Williams, M. Uehara-Bingen, B. Wolff, and L. Hicks for their help with the HTS and C. Ocasio for assistance in cell culture and the TH competition assay.

## REFERENCES

- Yen, P. M. (2001) *Physiol. Rev.* **81**, 1097–1142
- Malm, J. (2004) *Curr. Pharm. Des.* **10**, 3525–3532
- Aranda, A., and Pascual, A. (2001) *Physiol. Rev.* **81**, 1269–1304
- Harvey, C. B., and Williams, G. R. (2002) *Thyroid* **12**, 441–446
- Williams, G. R. (2000) *Mol. Cell. Biol.* **20**, 8329–8342
- Mangelsdorf, D. J., Thummel, C., Beato, M., Herrlich, P., Schutz, G., Umesono, K., Blumberg, B., Kastner, P., Mark, M., Chambon, P., and Evans, R. M. (1995) *Cell* **83**, 835–839
- Xu, J. M., and Li, Q. T. (2003) *Mol. Endocrinol.* **17**, 1681–1692
- Hu, X., and Lazar, M. A. (2000) *Trends Endocrinol. Metab.* **11**, 6–10
- Moore, J. M. R., and Guy, R. K. (2005) *Mol. Cell. Proteomics* **4**, 475–482
- Onate, S. A., Tsai, S. Y., Tsai, M. J., and Omalley, B. W. (1995) *Science* **270**, 1354–1357
- Voegel, J. J., Heine, M. J. S., Zechel, C., Chambon, P., and Gronemeyer, H. (1996) *EMBO J.* **15**, 3667–3675
- Hong, H., Kohli, K., Garabedian, M. J., and Stallcup, M. R. (1997) *Mol. Cell. Biol.* **17**, 2735–2744
- Suen, C. S., Berrodin, T. J., Mastroeni, R., Cheskis, B. J., Lyttle, C. R., and Frail, D. E. (1998) *J. Biol. Chem.* **273**, 27645–27653
- Ito, M., and Roeder, R. G. (2001) *Trends Endocrinol. Metab.* **12**, 127–134
- Puigserver, P., Wu, Z. D., Park, C. W., Graves, R., Wright, M., and Spiegelman, B. M. (1998) *Cell* **92**, 829–839
- Ko, L., Cardona, G. R., and Chin, W. W. (2000) *Proc. Natl. Acad. Sci. U. S. A.* **97**, 6212–6217
- Moore, J. M. R., Galicia, S. J., McReynolds, A. C., Nguyen, N. H., Scanlan, T. S., and Guy, R. K. (2004) *J. Biol. Chem.* **279**, 27584–27590
- Kalkhoven, E. (2004) *Biochem. Pharmacol.* **68**, 1145–1155
- Heinlein, C. A., Ting, H. J., Yeh, S. Y., and Chang, C. S. (1999) *J. Biol. Chem.* **274**, 16147–16152
- Treuter, E., Albrektsen, T., Johansson, L., Leers, J., and Gustafsson, J. A. (1998) *Mol. Endocrinol.* **12**, 864–881
- Zhang, H., Thomsen, J. S., Johansson, L., Gustafsson, J. A., and Treuter, E. (2000) *J. Biol. Chem.* **275**, 39855–39859
- Seol, W., Choi, H. S., and Moore, D. D. (1996) *Science* **272**, 1336–1339
- Darimont, B. D., Wagner, R. L., Apriletti, J. W., Stallcup, M. R., Kushner, P. J., Baxter, J. D., Fletterick, R. J., and Yamamoto, K. R. (1998) *Genes Dev.* **12**, 3343–3356
- Feng, W. J., Ribeiro, R. C. J., Wagner, R. L., Nguyen, H., Apriletti, J. W., Fletterick, R. J., Baxter, J. D., Kushner, P. J., and West, B. L. (1998) *Science* **280**, 1747–1749
- Geistlinger, T. R., and Guy, R. K. (2001) *J. Am. Chem. Soc.* **123**, 1525–1526
- Geistlinger, T. R., and Guy, R. K. (2003) *J. Am. Chem. Soc.* **125**, 6852–6853
- Leduc, A. M., Trent, J. O., Wittliff, J. L., Bramlett, K. S., Briggs, S. L., Chirgadze, N. Y., Wang, Y., Burris, T. P., and Spatola, A. F. (2003) *Proc. Natl. Acad. Sci. U. S. A.* **100**, 11273–11278
- Galande, A. K., Bramlett, K. S., Burris, T. P., Wittliff, J. L., and Spatola, A. F. (2004) *J. Peptide Res.* **63**, 297–302
- Rodriguez, A. L., Tamrazi, A., Collins, M. L., and Katzenellenbogen, J. A. (2004) *J. Med. Chem.* **47**, 600–611
- Dietrich, S. W., Bolger, M. B., Kollman, P. A., and Jorgensen, E. C. (1977) *J. Med. Chem.* **20**, 863–880
- Briel, D., Pohlers, D., Uhlig, M., Vieweg, S., Scholz, G. H., Thormann, M., and Hofmann, H. J. (1999) *J. Med. Chem.* **42**, 1849–1854
- Stanton, J. L., Cahill, E., Dotson, R., Tan, J., Tomaselli, H. C., Wasvary, J. M., Stephan, Z. F., and Steele, R. E. (2000) *Bioorg. Med. Chem. Lett.* **10**, 1661–1663
- Ye, L., Li, Y. L., Mellstrom, K., Mellin, C., Bladh, L. G., Koehler, K., Garg, N., Collazo, A. M. G., Litten, C., Husman, B., Persson, K., Ljunggren, J., Grover, G., Sleph, P. G., George, R., and Malm, J. (2003) *J. Med. Chem.* **46**, 1580–1588
- Webb, P., Nguyen, N. H., Chiellini, G., Yoshihara, H. A. I., Lima, S. T. C., Apriletti, J. W., Ribeiro, R. C. J., Marimuthu, A., West, B. L., Goede, P., Mellstrom, K., Nilsson, S., Kushner, P. J., Fletterick, R. J., Scanlan, T. S., and Baxter, J. D. (2002) *J. Steroid Biochem. Mol. Biol.* **83**, 59–73
- Chiellini, G., Apriletti, J. W., Yoshihara, H. A., Baxter, J. D., Ribeiro, R. C. J., and Scanlan, T. S. (1998) *Chem. Biol.* **5**, 299–306
- Mishra, M. K., Wilson, F. E., Scanlan, T. S., and Chiellini, G. (2004) *J. Comp. Physiol. B* **174**, 471–479
- Grover, G. J., Egan, D. M., Sleph, P. G., Beehler, B. C., Chiellini, G., Nguyen, N. H., Baxter, J. D., and Scanlan, T. S. (2004) *Endocrinology* **145**, 1656–1661
- Freitas, F. R. S., Moriscot, A. S., Jorgetti, V., Soares, A. G., Passarelli, M., Scanlan, T. S., Brent, G. A., Bianco, A. C., and Gouveia, C. H. A. (2003) *Am. J. Physiol.* **285**, E1135–E1141
- Manzano, J., Morte, B., Scanlan, T. S., and Bernal, J. (2003) *Endocrinology* **144**, 5480–5487
- Trost, S. U., Swanson, E., Gloss, B., Wang-Iverson, D. B., Zhang, H. J., Volodarsky, T., Grover, G. J., Baxter, J. D., Chiellini, G., Scanlan, T. S., and Dillmann, W. H. (2000) *Endocrinology* **141**, 3057–3064
- Wagner, R. L., Huber, B. R., Shiau, A. K., Kelly, A., Lima, S. T. C., Scanlan, T. S., Apriletti, J. W., Baxter, J. D., West, B. L., and Fletterick, R. J. (2001) *J. Mol. Endocrinol.* **15**, 398–410
- Arkin, M. R., and Wells, J. A. (2004) *Nat. Rev. Drug Discov.* **3**, 301–317
- Berg, T. (2003) *Angew. Chem. Int. Ed. Engl.* **42**, 2462–2481
- Toogood, P. L. (2002) *J. Med. Chem.* **45**, 1543–1558
- Roehrl, M. H. A., Wang, J. Y., and Wagner, G. (2004) *Biochemistry* **43**, 16056–16066
- Apriletti, J. W., Baxter, J. D., Lau, K. H., and West, B. L. (1995) *Protein Express. Purif.* **6**, 363–370
- Arend, M., Westermann, B., and Risch, N. (1998) *Angew. Chem. Int. Ed. Engl.* **37**, 1045–1070
- Gul, H. I., Gul, M., Vepsalainen, J., Erciyas, E., and Hanninen, O. (2003) *Biol. Pharm. Bull.* **26**, 631–637
- Davioud-Charvet, E., McLeish, M. J., Veine, D. M., Giegel, D., Arscott, L. D., Andriacopulo, A. D., Becker, K., Muller, S., Schirmer, R. H., Williams, C. H., and Kenyon, G. L. (2003) *Biochemistry* **42**, 13319–13330